Influence of canopy structure
on light interception and productivity
of greenhouse cucumber

Dipl.-Ing. agr. Dirk Wiechers

geboren am 28.05.1978 in Hannover

2011

Referent: Prof. Dr. sc. agr. Hartmut Stützel

Korreferent: Prof. Dr. sc. agr. Henning Kage

Tag der Promotion: 29.07.2011

Abstract

Greenhouse cucumber (*Cucumis sativus* L.) production systems are characterized by a near to optimal level of control and supply of environmental factors like temperature, CO_2, water and nutrients. However, due to the spatial inhomogeneity in these canopies the interception of light is often suboptimal for productivity. The aim was to obtain a better quantitative understanding of this limitation. Dynamical plant models are an appropriate tool, as they incorporate morphological and physiological adaptations of plants to their environment. To account the adaptations a precise simulation of the light distribution on organ level is essential. In the first instance, a static three-dimensional (3D) plant model was combined with a mock-up of the surrounding canopy and a 3D radiosity based light distribution model. The results showed that simulations of leaf level photosynthetically active radiation (PAR) were suitable under different canopy architectures to derive light-induced physiological responses on organ level.

To analyze yield formation, L-Cucumber, a functional-structural plant model (FSPM) of greenhouse cucumber, was extended with detailed models of leaf photosynthesis and fruit dry matter partitioning. For the model of photosynthesis a combination of a stomatal conductance model and a biochemical model of photosynthesis was parameterized. Model performance was evaluated under various canopy conditions. L-Cucumber provided the possibility to account for spatial gradients of environmental factors induced by the spatial structure of the canopy, which are necessary for an accurate estimation of yield formation.

In greenhouse cucumber growth imbalances between individual fruits are common. These imbalances can be related to differences in fruit growth duration until reaching harvest size, and fruit abortion. For both traits environmental factors as well as canopy architecture play a key role for their differentiation. Additionally, events that a fruit reaches its harvestable size before or simultaneously with a fruit set prior could be observed. Introducing dominance and abortion events into the assimilate partitioning of L-Cucumber allowed simulating the typical fruit growth traits of cucumber fruits. In conclusion, the current implementation of L-Cucumber could serve as a basis to analyze the impact of canopy architecture and environmental factors on productivity for cucumber greenhouse production.

Kurzfassung

Produktionsysteme für Gewächshausgurken (*Cucumis sativus* L.) sind durch eine nahezu optimale Steuerung und Versorgung der Umweltfaktoren Temperatur, CO_2, Wasser und Nährstoffen gekennzeichnet. Wohingegen, die räumliche Inhomogenität der Lichtverteilung häufig suboptimal für eine hohe Produktivität ist. Um ein quantitatives Verständnis dieser Limitierung zu erlangen, sind dynamische Pflanzenmodelle, welche es erlauben, morphologische und physiologische Anpassungen der Pflanze an ihre Umwelt zu integrieren eine gutes Instrument. Dazu wurde ein statisches drei-dimensionales (3D) Pflanzenmodell mit einem Modell des umgebenen Bestandes und einem 3D Radiosität-basierten Lichtverteilungsmodell kombiniert. Die Ergebnisse zeigten, daß das Modell in der Lage war, photosynthetisch aktive Strahlung auf Blattebene in unterschiedlichen Beständen zu simulieren, was es ermöglicht, lichtabhängige Reaktionen auf Blattebene zu beschreiben.

Um die Ertragsbildung zu analysieren, wurde L-Cucumber, ein funktionell-strukturelles Pflanzenmodell (FSPM) für Gewächshausgurken, um detallierte Modelle der Einzelblattphotosynthese und Fruchttrockenmassenverteilung erweitert. Für die Photosynthese wurde ein kombiniertes Modell, bestehend aus einem Modell für stomatären Widerstand und einem biochemischen Photosynthesemodell parametrisiert. Die detallierte räumliche Darstellung der Pflanzen und des Bestandes ermöglichte es L-Cucumber räumliche Unterschiede von Umweltfaktoren unter verschiedenen Bestandesbedingungen zu berücksichtigen, was für eine genaue Bestimmung der Ertragsbildung sehr wichtig ist.

Bei Gewächshausgurken treten häufig Ungleichgewichte im Wachstum zwischen einzelnen Früchten auf. Diese lassen sich auf Unterschiede in der Wachstumsdauer der Früchte bis zur Ernte und dem Abwurf von Früchten zurückführen. In beiden Fällen beeinflussen sowohl Umweltfaktoren als auch die Bestandesarchitektur deren Ausprägung. Zusätzlich treten Fälle auf, in denen eine Frucht ihre Erntegröße vor einer älteren Frucht erreicht. Durch die Einführung von Dominanz und Abwurf in die Assimilatverteilung von L-Cucumber konnten typische Charakteristika des Fruchtwachstums bei Gurken simuliert werden. Folglich, kann die aktuelle Implementierung von L-Cucumber als Basis benutzt werden, um Einflüsse von Bestandesarchitekturen und Umweltfaktoren auf die Produktivität von Gewächshausgurken zu analysieren.

Contents

List of tables

List of figures

Abbrevations

Γ*	CO2 compensation point	
	in the absence of dark respiration	(μmol mol^{-1})
3D	three-dimensional	
A	actual rate of photosynthesis	(μmol CO$_2$ m^{-2} s^{-1})
A$_c$	Rubisco limited assimilation rate	(μmol CO$_2$ m^{-2} s^{-1})
A$_F$(t)	share of assimilates partitioned to fruits on a given day	(g dw d^{-1})
A$_j$	RuBP regeneration-limited assimilation rate	(μmol CO$_2$ m^{-2} s^{-1})
A$_n$	net rate of photosynthesis	(μmol CO$_2$ m^{-2} s^{-1})
A$_T$	abortion threshold	
b	minimum stomatal conductance	(mol H$_2$O m^{-2} s^{-1})
bias	mean deviation	
BWB model	Ball, Woodrow and Berry model	
	of stomatal conductance	
C$_c$	CO$_2$ concentration in the chloroplast	(μmol mol^{-1})
C$_i$	CO$_2$ concentration in the substomatal cavities	(μmol mol^{-1})
C$_{itr25}$	transition between A$_c$ and A$_j$	(μmol CO$_2$ m^{-2} s^{-1})
C$_s$	CO2 partial pressure at the leaf surface	(μbar)
D$_T$	dominance threshold	
D$_{TMF}$(t)	total maximum demand of all fruits on day t	(g dw d^{-1})
dw	dry weight	
FSPM	functional-structural plant model	

g_i	internal conductance	(μmol mol^{-1})
g_s	stomatal conductance	(mol H$_2$O m^{-2} s^{-1})
h_s	relative humidity at leaf surface	
I1	isometric canopy with 1 plant per m²	
I2	isometric canopy with 2 plant per m²	
J_{max}	rate of electron transport	(μmol CO$_2$ m^{-2} s^{-1})
J_{max25}	rate of electron transport at 25°C	(μmol CO$_2$ m^{-2} s^{-1})
k	intensity of photosynthetically active radiation extinction	
Kc	kinetic constant of Rubisco to CO$_2$	(μmol mol^{-1})
Km	Michaelis-Menten kinetic constant	
Ko	kinetic constant of Rubisco to O$_2$	(mmol mol^{-1})
L-System	Lindenmayer system	
LAI	leaf area index	
LED	light emmiting diode	
$L_{F,i}(t)$	fruit length of an individual fruit on a given day	(cm)
m	empirical parameter for sensitivity of the stomatal conductance	
niPAR	normalized incident PAR	
Pa	atmospheric pressure	(kPa)
PAR	photosynthetically active radiation	
PAR_0	PAR at top of the plant	
QTL	quantitative trait loci	
R1	row canopy with 1 plant per m²	

Chapter 1

General introduction

Background

Greenhouse cucumbers (*Cucumis sativus* L.) are usually cultivated in intensively managed production systems. Their growth habit is indeterminate crops, like tomato or pepper. Typically, these crops are pruned, have a strong monopodial growth of plants and are grown in distinct rows structures, i.e. they produce spatially discontinuous canopies. Yield is clearly influenced by plant arrangement and plant density (Kahlen, 2007). The yield formation of these crops, which constantly initiate new fruits, is also highly alternated by the non-uniform growth of individual fruits (Wubs *et al.*, 2009b; Schapendonk and Brouwer, 1984; Heuvelink, 1996). Furthermore, canopy architecture influences the quality of the harvested fruits (Klieber *et al.*, 1993). Considering the environmental factors affecting plant growth in greenhouse production systems characterized by the spatial discontinuous distribution of plants, reveals that the availability and distribution of light can be seen as the major limiting growth factor (Warren Wilson *et al.*, 1992). Whereas, the supply and control of nutrients, water, temperature, relative humidity and CO_2 in these systems is normally controlled close to the optimum.

Obtaining a quantitative understanding of yield formation processes under these conditions requires an integrated description of spatial distribution of resources and the growth and developmental processes of the plant. Mechanistic models of plants can be used to achieve a quantitative understanding of these processes (Vos *et al.*, 2007). The initial focus of plant models was to integrate physiological knowledge without an explicit description of the plant structure. More recently, models which focused on a detailed description of the plant morphology have been developed (de Reffye *et al.*, 1998). However, to use models to analyze processes of the plant growth and development, it is necessary to combine both approaches as only models which account for interactions between function and structure are capable to simulate variations of environmental and crop management (Prusinkiewicz *et al.*, 1997). These requirements are accomplished by so called functional-structural plant

models (FSPM) (Vos *et al.*, 2010). FSPM combine the approaches of physiological models with information of the three-dimensional (3D) plant and canopy structure for the dynamic representation of plant growth and development. This combination allows representing interactions between plant physiology, morphology and environment (Chelle, 2005; Kahlen and Stützel, 2011). In this thesis essential sub models describing the processes of plant growth and development (grey shaded part, Figure 1.1) for an extension of L-Cucumber (Kahlen *et al.*, 2008) a FSPM for the greenhouse cucumber were examined and parameterized. The interrelations between light and canopy structure were evaluated for the radiation transfer sub model, followed by analysis of the impact of canopy structure on the productivity of the photosynthesis sub model and the influence of the dry matter partitioning sub model on yield formation.
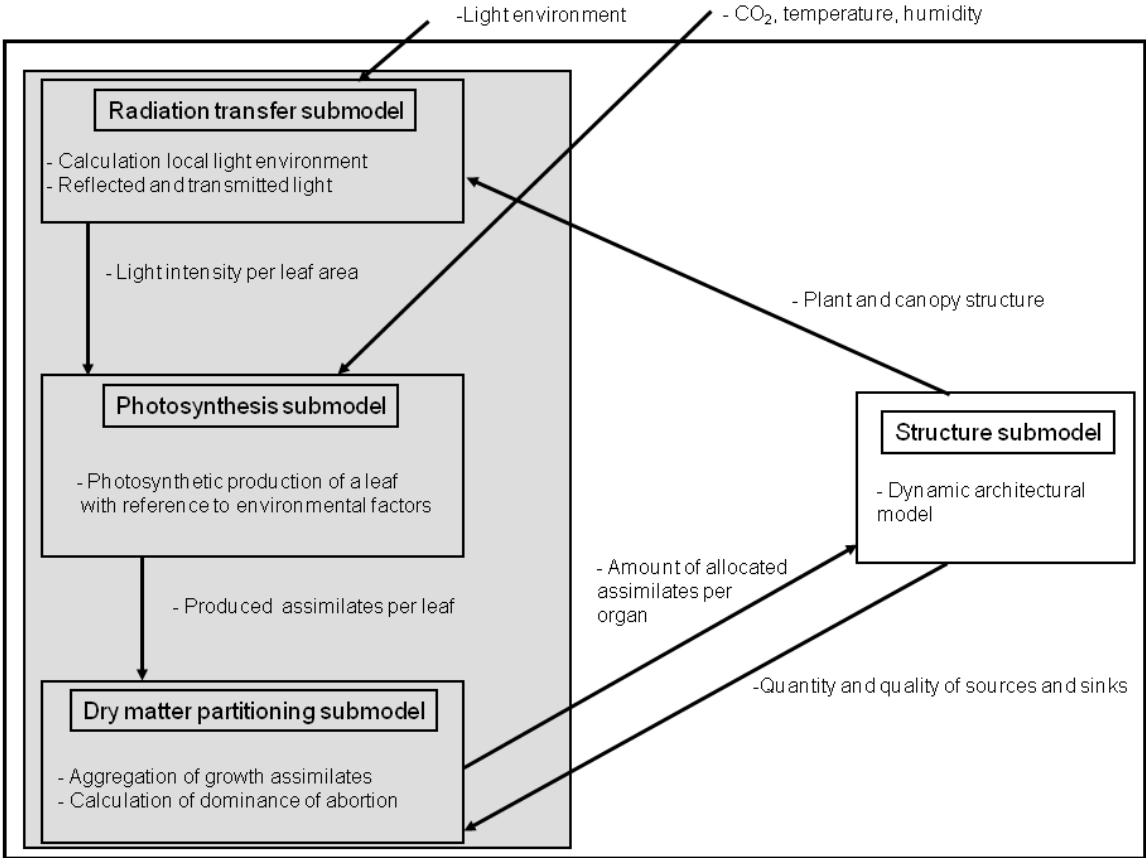
Figure 1.1 Basic structure of L-Cucumber. Grey shaded part on the left-hand side describes the parts examined in this thesis

Structural plant models

Static virtual plant models allow describing the plant morphology for a fixed time and the 3D structure is commonly represented by polygons. In order to describe the 3D morphological growth and development of plants *in silico* concepts have been developed which decompose the plant into elementary modules which are interconnected (Vos *et al.*, 2010). Different programming formalisms have been developed, e.g L-Systems (Kniemeyer and Kurth, 2008; Prusinkiewicz *et al.*, 1997) or Greenlab (Yan *et al.*, 2004) to describe the structural development of plants. In L-Systems a plant is described by interconnected modules, for example, leaves, fruits and petioles (Prusinkiewicz *et al.*, 1997). By using modules, the approach accounts for the repetitive structure of plants. The development of a plant is refined by productions or rewriting rules which are applied to a "string", a linear, one-dimensional data structure. Whereas, the symbols of the string are either describe different features like branching or graphical interpretations. This formalism allows describing the 3D development of a plant constrained by the local availability of resources. Recourses like assimilates, water, nutrients or hormones can be supplied over a transport system within the plant, or depend on physiological processes, like photosynthesis which in turn depends on the conditions of the local environment (Fourcaud *et al.*, 2008).

Radiation transfer models

The detailed 3D plant structure, based on geometric primitives, given by the L-System, offers the possibility to calculate the light environment for individual organs (Vos *et al.*, 2010). Besides Monte Carlo ray tracing based models (e.g. Cieslak *et al.*, 2008), a radiosity based approach was developed to simulate the radiation transfer within plant canopies (Chelle *et al.*, 1998). Using appropriate leaf optical properties and aggregating multiple 3D plants into a scene allows creating a mock-up of a canopy, which is able to estimate the incident light of individual leaves. Changing the distances of plants within and between rows, allows simulating changes in the radiation transfer for different canopy architectures.

Photosynthesis model

The level of detail provided by the structural plant models allows calculating of the photosynthesis of individual leaves. This is of particular advantage for a precise prediction of assimilate production, as photosynthesis is highly dependent on the availability of light (Chenu *et al.*, 2005). The model of leaf photosynthesis developed by Farquhar and coworkers (Farquhar *et al.*, 1980) describes the rate of photosynthesis based on the underlying biochemical processes. This offers the opportunity to describe the influences of multiple environmental factors, like CO_2, light, temperature or relative humidity, on the actual rate of photosynthesis. The model is extendable with other processes affecting photosynthesis, like stomatal conductance (Kim and Lieth, 2003). The ability to account for changes of multiple environmental factors and the possibility to extend the model makes this model well suited to represent photosynthesis in 3D plant models.

Dry matter partitioning model

Besides a precise estimation of assimilate production the simulation of plant growth and development requires an accurate representation of the allocation of assimilates among the different plant parts (Marcelis, 1993d). The detailed consideration of individual organs involves representing the partitioning of dry matter on this level. Several approaches have been developed to simulate partitioning (Marcelis, 1993d). A commonly implemented approach used in FSPM models is based on the source-sink relations in the plant (Vos *et al.*, 2010). Sources of assimilates are the photosynthetically active organs, mainly the leaves, whereas sinks are all organs which require assimilates for growth and development. If the demands of the sinks exceeds the supply produced by the sources, a limitation of assimilates occur. Under these conditions the growth of individual organs can be altered, thus the partitioning of assimilates among the organs changes. Cucumbers are a good example to study these effects, as they show clear changes in the growth of individual fruits, like dominant fruit growth and abortion of fruits (Marcelis, 1994).

Objectives

The aim of the thesis was to study the effects of different cucumber canopy architectures on light interception, photosynthesis and dry matter partitioning. A 3D FSPM approach was used to be able to analyze the interactions between morphological and physiological properties of the plants. The objectives of the study were divided into three chapters:

- Evaluation of a radiosity based light model for different spatial discontinuous greenhouse cucumber canopies, based on static 3D plant models derived from digitized plants (Chapter 2).
- Analysis of the influence of different canopy architecture and environmental conditions on the dry matter production for a FSPM which includes leaf-level photosynthesis (Chapter 3).
- Evaluation of different dry matter partitioning models including effects of dominance and fruit abortion on the simulation of individual fruit growth (Chapter 4).

Chapter 2

Evaluation of a radiosity based light model for greenhouse cucumber canopies

Dirk Wiechers, Katrin Kahlen, Hartmut Stützel

Abstract

Light distribution is a key factor of developmental and growth processes, and strongly depends on the foliage distribution which is affected, e.g., by the arrangement of the plants in the canopy. The precise simulation of the light distribution on organ level is an essential component for dynamical plant models which incorporate structural and physiological adaptions of plants to their environment. Combinations of static 3D plant models with 3D light models are used for analyzing the complex light distribution on leaf level *in silico*, but detailed measurements for evaluation of simulation results are almost non-existent. This study addressed the evaluation of a model on a high level of detail using individual leaf based light measurements in canopies of cucumber (*Cucumis sativus* L.).We combined a static 3D plant model derived from digitized plants on an individual organ scale with a mock-up of the surrounding canopy and a 3D radiosity based light distribution model. Variations of plant density and spacing were analyzed to cover a range of canopy architectures. An exclusion of components of the light environment by applying a shading encasement followed by a successive uncovering allowed investigating the scene under increasing levels of complexity. The combined 3D plant-light distribution approach allowed determining the interaction of the light directions and the canopy architecture as well as differences in the accuracy of the simulations. Depending on canopy architecture and shading treatment, the light distributions covered a range from exponentially shaped vertical gradients in encased

treatments to nearly flat light profiles in non encased conditions. In conclusion, simulations of leaf level PAR based on combinations of detailed 3D surfaced-based plant and light distribution models are suitable to derive light-induced physiological responses on organ level.

Introduction

A key environmental factor driving dry matter production and development of crops is the available quantity and quality of light (Chenu et al., 2005; Escobar-Gutiérrez et al., 2009). The optimal foliage distribution for maximum interception of light is of special interest in protected environments where factors like temperature, CO_2 concentration, vapor pressure deficit, supply of nutrients and water can be controlled at economically optimal levels (Warren Wilson et al., 1992). Light distribution within a greenhouse is affected by the sources of light, the supporting structure of the house and its optical properties as well as the structure and optical properties of the canopy (Aikman, 1989; Hovi-Pekkanen and Tahvonen, 2008). Canopy structure is influenced by intrinsic architectural traits of plants and canopy management practice such as vertical training systems, pruning and rows cropping. Variations in canopy structure cause changes in plant morphological and biochemical responses and influence the environmental conditions of the plant, finally affecting productivity, yield and quality of the harvested organ (Louarn et al., 2008). For example, shelf life quality of the harvested fruits of cucumber is influenced by training systems (Klieber et al., 1993) and an increase of yield can be obtained in an isometrically arranged canopy compared to row cultivation using an identical training system (Kahlen, 2007). These findings indicate that cucumber crops provide a good example for a discontinuous canopy structure, which is interacting with the light environment.

Detailed descriptions of measurements of light distribution for such canopies are rare in literature. Vertical profiles of photosynthetically active radiation (PAR) in tomato canopies indicated that a closer plant spacing increased the intercepted PAR by the canopy (Papadopoulos and Ormrod, 1988). Measurements of the light interception on perpendicular transects across the row for cucumber and tomato showed that the assumption to treat the light interception within a row crop as uniform is an oversimplification (Warren Wilson et al., 1992).For Eggplants, an approach to partition leaf area into classes of leaf mass per unit leaf area and to relate them to measurements of daily light interception on leaf level indicated that the method can be used in regularly spaced crops of genetically uniform plants (Rosati et al., 2001).

Since it is difficult to directly measure the amount of intercepted light by a plant, computational methods to estimate light propagation in a canopy have been developed

(Chenu et al., 2008). Commonly used models of crop light interception based on Lambert-Beer's law (Monsi and Saeki, 2005) assume the canopy as a random distribution of elements in space attenuating the light in the vertical direction of the crop. On canopy level, a simple approach for modeling the light propagation for a row canopy was introduced by Thornley et al. (1992) who split the total amount of light into the fractions of the three Cartesian directions. In combination with a model of photosynthesis, the model accounted for 85% of the variance of the measured canopy net photosynthetic rates. A further derivate of the Lambert-Beer's law model is the mixed model approach, developed for patchy canopies. This method subdivides the canopy into discrete homogeneous volumes and applies the Lambert-Beer's law only to volumes containing canopy components (e.g. Röhrig et al., 1999; Sinoquet et al., 2001). In non-uniform canopy structures, this is useful to represent the spatial distribution of the crop, but lacks to explicitly represent the individual plant organs (Chenu et al., 2008).

In order to describe plant architecture on a higher level of detail, surface based plant models describing the three-dimensional (3D) structure of the plant with explicit consideration of the individual organ surfaces have been developed (for overview see: Vos et al., 2007). Different light models customized to calculate the light environment of virtual 3D plant models are available (e.g. Chelle and Andrieu, 1998; Mech and Prusinkiewicz, 1996). Moreover, functional-structural plant models (FSPM) simulating dynamical plant systems based on light interception have been developed (for overview see: Vos et al., 2010). 3D models designed to simulate plant development need a precise description of their environment and the plant's interaction with it, introduced as phylloclimate, to be able to accurately represent responses of biological processes (Chelle, 2005).

Several studies have been published using static architectural models to derive light distribution and spectral composition within canopies (e.g. Chelle et al., 2007; Combes et al., 2008; Drouet and Kiniry, 2008). These studies used different levels of detail and spectral bands for the simulation of canopy light distribution. However, none of these models has been evaluated with measurements on the phylloclimate level.

The aim of the present study was to analyze the light distribution of different heterogeneous canopy structures using a combination of a surface based plant model with a 3D light model and to evaluate the simulated light distributions with organ based measurements of PAR.

The specific objectives were (1) the investigation of the influence of the plant density and spacing on the light distribution within the canopy, (2) to identify the impact of the light directions on the complexity of the light environment and (3) to evaluate the accuracy of the simulation on an individual organ scale. The evaluation of the static model was discussed with respect to the quality of the surface based light model for the application within a dynamical plant model.

Material and methods

Plant material

Three sets of cucumber crops (*Cucumis sativus* L. cv. Aramon, Rijk Zwaan, De Lier, Netherlands) were cultivated in greenhouses at the Institute of Biological Production Systems in Hannover, Germany (52.5°N, 9.7° E). Plants were transplanted to the greenhouse in the five-leaves stage. They were arranged in either row or isometric patterns with either one or two plants per m² (Table 2.1).

Table 2.1 Canopy architectures with information about distribution, plant density (plant m^{-2}), plant distance (cm) and row distance (cm).

Canopy architecture	Distribution	Plant density (plant m^{-2})	Plant distance (cm)	Row distance (cm)
I1	Isometric	1	107	93
R1	Row	1	53	186
I2	Isometric	2	53	93
R2	Row	2	27	186

Rows were oriented from north to south and the ground was covered by a white plastic film. Measurements for each treatment were conducted on a single plant in the center of the middle row, in the following referred to as "measurement plant". The measurements were taken three weeks after transplanting on 14-16 August 2006, 29-31 May 2007 and 20-22 August 2007, when the plants had on average 20 leaves and reached the supporting horizontal wire at 220 cm above the ground. The plants were attached with plastic clips to a cord to ensure their vertical exposition.

Measurement of light distribution

The light measurements were taken with 14 cosine corrected PAR sensors (LI-190, LI-COR, Lincoln, USA) positioned individually on 14 leaves of the measurement plant (Fig. 2.1a). Each sensor was supported by a deformable steel wire allowing to place the sensor parallel to the midrib orientation of the adaxial leaf lamina without disturbing the leaf's original orientation. The sensor position on the leaf lamina was near to the intersection between petiole and leaf lamina (Fig. 2.1a). All PAR sensors were connected to a data logger (CR1000, Campbell Scientific, Logan, USA) which stored the averaged PAR value of every minute. For each measurement, PAR sensor readings of five succeeding minutes were averaged. All light measurements were taken between 10:00 a.m. and 5:45 p.m. to avoid low sun elevation angles.
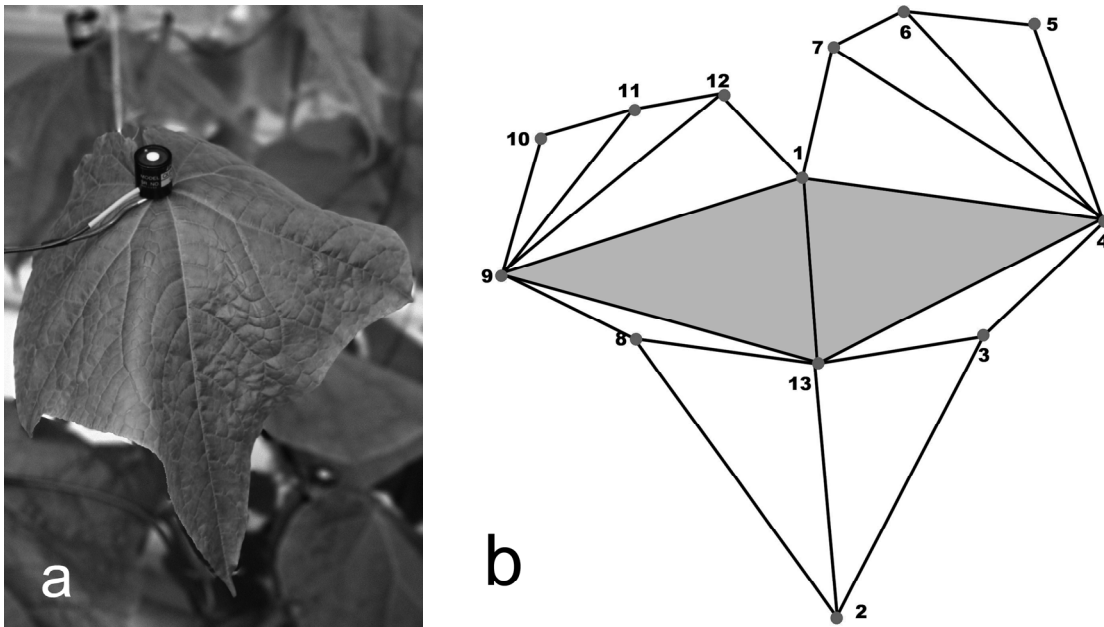
Fig. 2.1 (a) PAR sensors on leaves supported by a flexible wire allowing to place the sensor parallel to the midrib orientation of the adaxial leaf lamina; (b) Digitized points on the leaf lamina with the applied leaf triangulation. Grey shaded areas show the evaluated triangles.

To assess the vertical and horizontal components of radiation transfer a set of four short time side-shading treatments was applied to each canopy architecture (Fig. 2.2). The "closed" treatment (Fig. 2.2a) was designed to measure the vertical gradient down the canopy. It consisted of black fabric placed vertically on both sides of the plant row and between plants within the row. Each fabric also covered a part of the ground, reducing the

reflection of the white ground cover. To reduce shadow casts of structural greenhouse parts a white translucent nonwoven fabric was placed as a diffuser above the plants. Light from the within-row or inter-row spaces was allowed to reach the measurement plant in the "in row open" (Fig. 2.2b) and "between rows open" (Fig. 2.2c) treatments. These were realized by either removing the black fabric between the plants (in row open) or on both sides of the plant row (between rows open). The area opened in the "in row open" treatment was approximately 60% of the area in the "between rows open" treatment. For the "open" treatment (Fig. 2.2d) the black fabric was completely removed and light from all directions was allowed to contribute to the light environment.
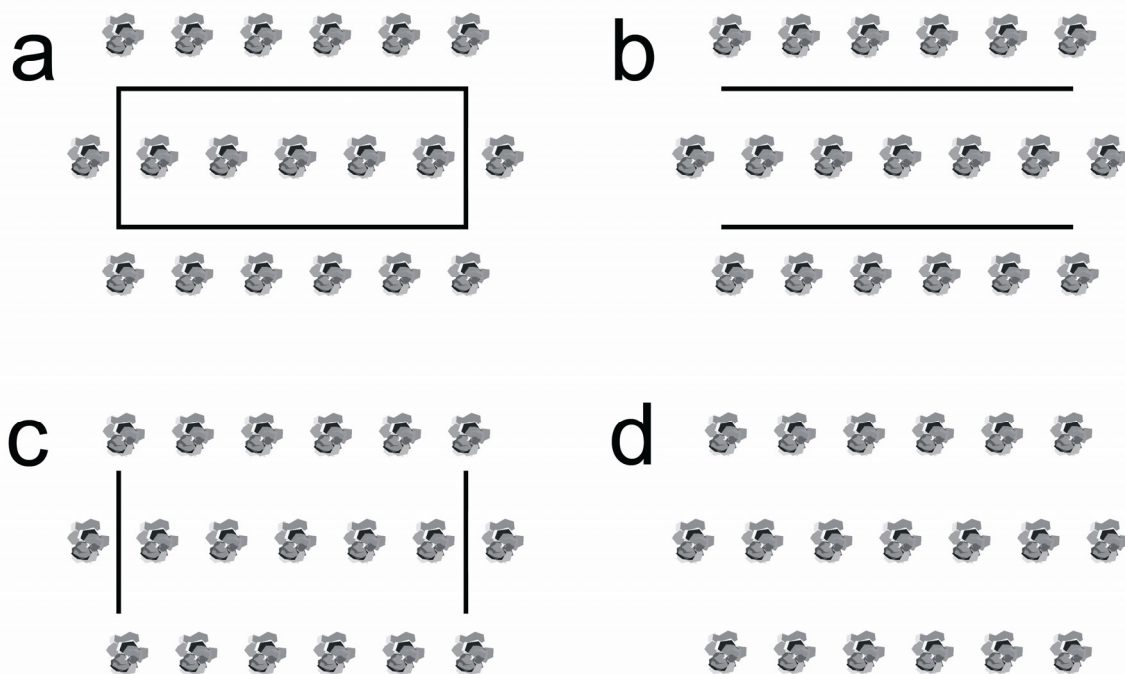
Fig. 2.2 Schematic representation of the four different canopy shadings for a row canopy. (a) "closed", (b) "in row open", (c) "between rows open", (d) "open" shading treatment.

Measurements of plant architecture

Plant architecture was recorded using a 3D digitizer (Fastrak, Polhemus, USA) as Cartesian coordinates in a given sequence of points on the individual plant organs. Predefined sets of triangles representing the individual organs (for details see Kahlen and Stützel, 2007; Wiechers et al., 2006) were used to represent the surface (for a lamina see Fig. 2.1b). Since digitizing of a single plant *in situ* took 30 to 45 minutes, only the measurement plant of each

canopy was recorded. Digitizing was carried out between 7 a.m. and 10 a.m. immediately before light measurements.

Simulation of light distribution

Construction of the virtual scene

To assess the influence of neighboring plants on the light distribution of the measurement plant in the simulation, a mock-up of the canopy surrounding the measurement plant was included. Eight different scenarios with changing combinations of neighboring plants were simulated to provide and assess the variability of the light environment of the real scene. The variation was enhanced by rotating the neighboring plants by +/- 20° around their vertical axis. The canopy surrounding the measurement plant was assembled from virtual clones of measurement plants placed at the position of the neighbor plants. The origins of the neighbor plants were translated on the X- and Y- coordinates corresponding to the distances in the real canopies (Table 2.1). The neighboring plants were taken from the two replications of the same experiment and canopy architecture. The shading and the diffuser fabrics were included in the simulations according to their presence in the measurements.

The virtual plants consisted of internodes, petioles and laminas intercepting light, whereas the effects of flowers and fruits have been neglected. For every given triangle of leaf surface within the virtual scene (Fig. 2.1b), the incident light flux density was calculated using the *Canestra* software (Chelle et al., 1998) implemented in *Caribu* package of the *OpenAlea* Functional-Structural Plant Modeling (FSPM) framework (Pradal et al., 2008). *Caribu* nested a radiosity algorithm into a turbid medium approach. The radiosity algorithm accounts for multiple scattering by calculating the reflectance and transmittance of the objects within a sphere. The influence of the sphere diameter was tested in comparison to a 50 million ray Monte Carlo ray tracing method (Chelle and Andrieu, 1998). Their results revealed for different LAI and leaf dispersions in maize that a sphere diameter of more than one meter resulted in stable RMSE values between 1-2%. To minimize artifacts resulting from edge effects the radiosity calculation was applied over the whole scene. The virtual PAR sensor in the scene was represented by two triangles of each leaf lamina (gray shaded in Fig. 2.1b). The areas mapped the approximate position of the real PAR sensor on the plant. The optical properties of the plants in the virtual plant model were derived from spectroradiometric measurements (LI-1800, LI-COR, Lincoln, USA) following a protocol described by Daughtry et

al. (1989). Measured values in the PAR band for the upper surface reflectance and transmittance were 6%, whereas the lower surface reflectance was 11% and transmittance was 8%. Due to the fact that *Caribu* simulates only Lambertian surfaces, the greenhouse construction was not considered within the scene. The optical properties of the black fabric were specified with 10% reflection, accounting for the possibility of light to enter on the joints of the real fabrics, and 0% transmission. The optical properties of the translucent diffuser were quantified with 10% reflection and 90% transmission, whereas ground reflectance of the plastic film was 80% with 0% transmission.

Light environment

The implemented sky model was made up from 37 light sources. The direct solar radiation with the sun position as a function of the actual latitude, longitude, day of year and the hour at time of light measurement was represented by one of these light sources. The required sun azimuth and zenith angles were calculated with *Solar Tool* software (Autodesk, San Rafael, USA). The diffuse sky radiation was based on the remaining 36 light sources arranged as a standard overcast sky (SOC) generated by the *Gensky* package in *OpenAlea* (Pradal et al., 2008). The proportion of outside global diffuse to total radiation (*Rdiff*) was calculated following Monteith and Unsworth (1990). The calculated mean value for *Rdiff* at the measurement days was 22%. *Rdiff* values were converted from outside global radiation to inside greenhouse PAR values: Accounting for the ratio of diffuse to total radiation in the PAR band according to the SPCTAL2 Model (Bird, 1984) and the different transmissions of direct and diffuse light by the greenhouse glass (Papadakis et al., 2000) resulted in an in-house PAR *Rdiff* of 25%. Under natural sky conditions, scattered radiation from the circumsolar region causes the sky around the sun to appear brighter than the rest of the hemisphere. Including this effect, due to the predominantly open sky during the measurements phases, the ratio was decreased to 23% diffuse light and 77% direct light represented by the single light source. Solar movement within the five minutes of measurement was neglected, so that solar position for the simulation was set to the first minute.

Simulation output and analysis

A simulation of a non-dynamic virtual scene can only result in a static approximation of the real environment, whereas changes of sun position, cloud movement as well as changes in canopy geometry are the key sources of variation for measurements of light *in situ* (Drouet and Kiniry, 2008; Roden, 2003). Thus, the simulation output of the single organ was sensitive to discrepancies between conditions of measurement and simulation. Calculating different scenarios with variations in the surrounding scene e.g. by rotating plants allowed to implement a variation in the simulation of the single organ. Means of measurements and simulations obtained under different sky conditions and time of day are assumed to minimize the impact of extreme differences. Consequently, measurements and simulations averaged over three experiments, each consisting out of three replications, were used for the evaluation. To be able to process measurements and simulations of different days and times during the day, the normalized incident PAR (*niPAR*) values were calculated by dividing the individual leaf PAR value by the maximal PAR level measured.

Statistical analysis

The non-linear fitting of the modified Lambert-Beer law (Monsi and Saeki, 2005) was performed with Sigmaplot 11 (Systat Software, Richmond, USA) for all combinations of treatments and canopy architectures:

$$niPAR = PAR_0 e^{-k\,LAI} \hspace{5cm} (1)$$

Where *niPAR* is the normalized incident photosynthetically active radiation, *LAI* is the leaf area index, parameter PAR_0 represents the amount of light at the top of the plant and parameter *k* maps the intensity of the extinction. The LAI was calculated by averaging the individual leaf areas of the nine replications and cumulating them from top to bottom of the plant and divided by the available ground area per plant. A t-test with an α =0.05, testing for significant differences between measured and simulated data, was performed with Sigmaplot 11 (Systat Software, Richmond, USA).

The evaluation of goodness-of-fit of the parameters and differences between the observed (measured) and simulated data were done on basis of root mean square deviation (*RMSD*) and mean deviation (*Bias*) (Kobayashi and Salam, 2000):

$$RMSD = \sqrt{\frac{1}{n}\sum_{i=1}^{n}(x_i - y_i)^2} \qquad\qquad (2)$$

$$Bias = \frac{1}{n}\sum_{i=1}^{n}(x_i - y_i) \qquad\qquad (3)$$

Where n is the total number of data pairs, i is the sample number, x_i are the observed values and y_i are the predicted values. The mean distance between the measurement and simulation is mapped by the *RMSD*, whereas the difference between the means of simulation and measurement is indicated by the *Bias*.

Results

The *niPAR* values for the "closed" treatment of the R2 canopy architecture (Fig. 2.3a,b), a row canopy with two plants per m², as commonly used in greenhouse horticulture, showed a consistent decline of measured and simulated data towards the base of the plant. This resulted for both data sets in a clear exponential decay function, with the highest standard deviations in the upper and the central plant part. Opening the shading on the within-row sides for the "in row open" treatment (Fig. 2.3c,d) showed only marginal effects on the *niPAR* values and standard deviations. In both treatments the simulated *niPAR* values (Fig. 2.3b,d) at the top of the plant slightly overestimated the measured values (Fig. 2.3a,c). In the case of the "between rows open" treatment (Fig. 2.3e,f), the light components assembling the light environment originated from gap between the rows. The measured and simulated *niPAR* values were similar to the ones of the "open" treatment (Fig. 2.3g,h), resulting in both treatments for the top of the plant in a general reduction of the *niPAR* values compared to the "closed" and "in row open" treatments, whereas the simulations (Fig. 2.3f,h) showed a more distinct decrease within these LAI range. With increasing canopy penetration the *niPAR* decreased to values between 0.2 and 0.4 for the measured (Fig. 2.3e,g) and between 0 and 0.2 for simulated data (Fig. 2.3f,h). This resulted in a less pronounced curvature of the regression function in the measurements (Fig. 2.3e,g) compared to the simulations (Fig. 2.3f,h). The standard deviations for the measured data of both treatments tended to be higher than for the simulations.
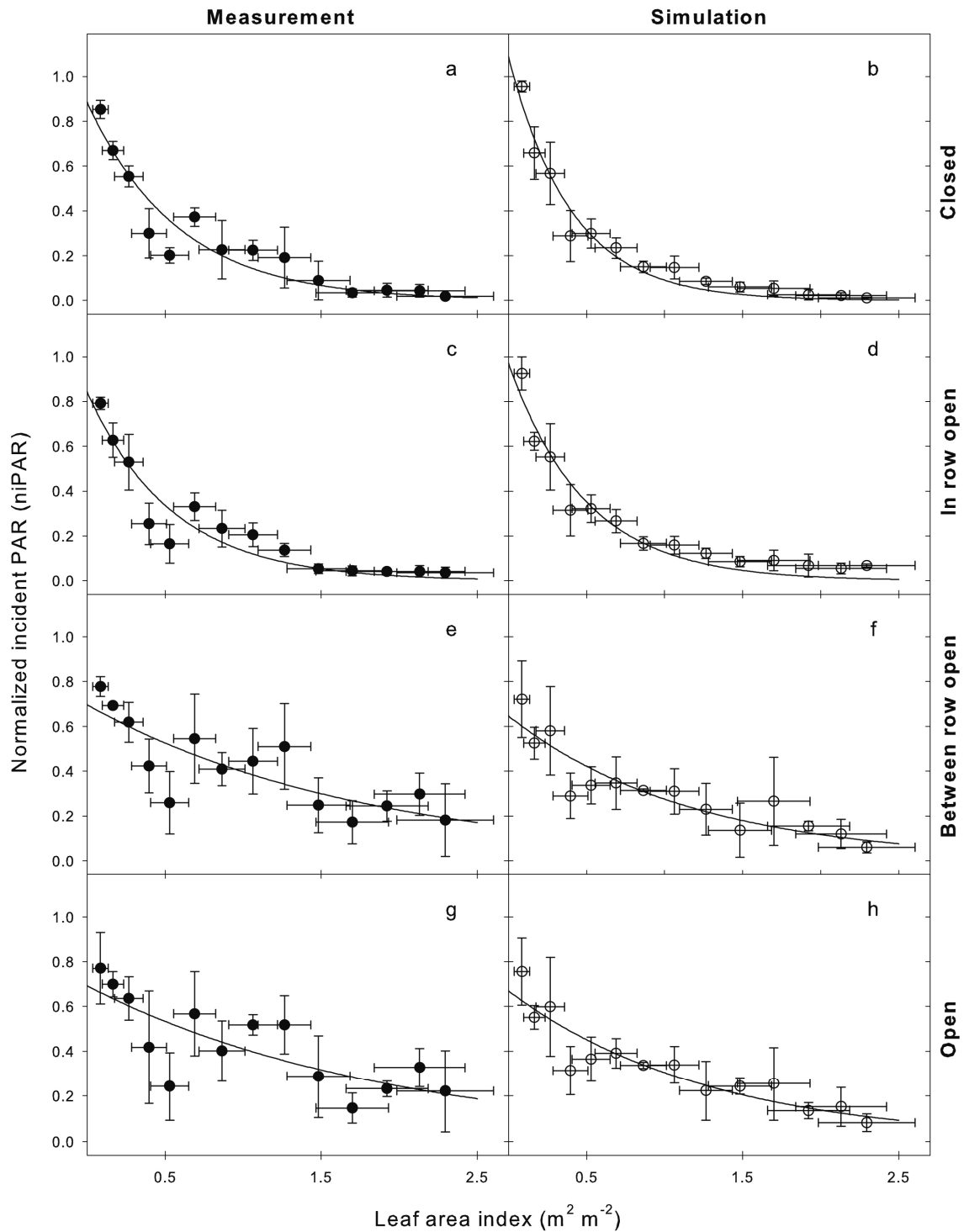
Fig. 2.3 Relationship between measured (left, closed circles) and simulated (right, open circles) normalized incident PAR and the LAI calculated from plant top for a row canopy with two plants per m². The applied shading treatments were either closed in all planes (Closed), open in the in row planes (In row open), open in the between rows planes (Between row open) or open in all planes (Open). With: "Closed" (a) measured, (b) simulated; "In row open" (c) measured, (d) simulated; "Between rows open" (e) measured, (f) simulated; "Open" (g) measured, (h) simulated canopy architecture. Solid line fits a Lambert-Beer law function ($niPAR=I_0*exp(-k*LAI)$) to the data set. Error bars represent standard deviation with N=9.

17

The reduction of the light environment in the "closed" treatment of the isometric canopy with 1 plant per m² (I1) resulted in an exponential regression function showing a strongly curved decay trend with *niPAR* values around 0.1 at the base of the plant (Fig. 2.4a,b). The simulation of the "closed" I1 canopy architecture slightly overestimated the measured *niPAR* values at the top of the plant, whereas the simulated values match the measured values at the base of the plant (Fig. 2.4a,b). The removal of the shading fabrics on the within-row sides of the encasement in the "in row open" treatment affected the light profile in the I1 canopy (Fig. 2.4c,d). For both datasets the additional light components considerably increased the *niPAR* values in the lower part of the plant. The simulated *niPAR* values at the top of the plant were slightly lower, whereas the values at the plant base and the standard deviations over the full LAI range were higher in the simulations than in the measurements. As a consequence, the curvature of the regression function was less pronounced in the simulated data set compared to measured data. The "between rows open" treatment resulted in only minor changes of the simulated *niPAR* pattern compared to the "in row open" treatment (Fig. 2.4d,f). However, the measured *niPAR* values at the top of the plant dropped in comparison with the "in row open" treatment (Fig. 2.4e,c). Accordingly, a change of the curvature of the exponential decay function takes shape only for the measured datasets. For the measured data of the I1 canopy a removal of all lateral shading fabrics in the "open" treatment resulted in marginal changes compared to the "between rows open" treatment (Fig. 2.4e,g). The simulation of the "open" I1 canopy showed a further decrease of the topmost *niPAR* values and a slightly stronger increase at the base of the plant (Fig. 2.4f,h). In consequence, the curvature of the regression fitted to the simulated data was near to linear (Fig. 2.4h). In the measurements the effects on the incident light due to the removal of the shading cloth can be summarized by an approximately 10% decrease in the *niPAR* values at low LAI for all canopy architectures whereas at high LAI values the *niPAR* values increased by 20% in the R2 and by 30% in the I1 canopy (Fig. 2.3&1.4). The simulations mainly overestimated the measurements at the top of the plant for the "closed" shading treatments by up to 20%. With the opening of the encasement this effect disappeared whereas in the R2 canopy the *niPAR* values at LAI higher than 1.5 were underestimated up to 10% (Fig. 2.4e-h).
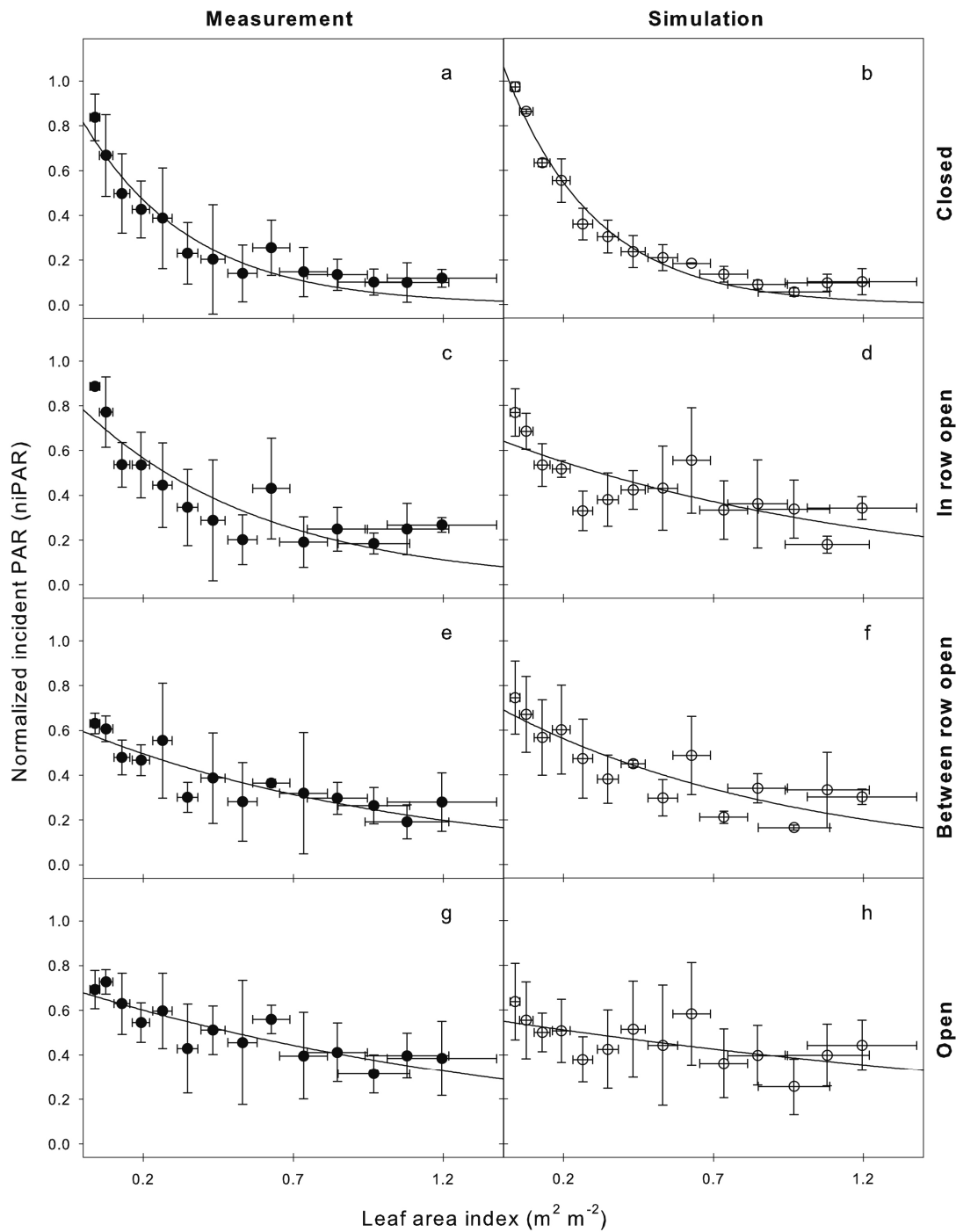
Fig. 2.4 Relationship between measured (left, closed circles) and simulated (right, open circles) normalized incident PAR and the LAI calculated from plant top for an isometric canopy with one plant per m². The applied shading treatments were either closed in all planes (Closed), open in the in row planes (In row open), open in the between rows planes (Between row open) or open in all planes (Open). With: "Closed" (a) measured, (b) simulated; "In row open" (c) measured, (d) simulated; "Between rows open" (e) measured, (f) simulated; "Open" (g) measured, (h) simulated canopy architecture. Solid line fits a Lambert-Beer law function ($niPAR=I_0*\exp(-k*\mathrm{LAI})$) to the data set. Error bars represent standard deviation with N=9.

The relationships described for the R2 and I1 canopy architectures exemplified the different changes in the *niPAR* patterns due to the variation of the shading treatments; hence leaf level data for row canopy with 1 plant per m² (R1) and the isometric canopy with 2 plants per m² (I2) are not shown.

The diversification of the light environments in the canopy architectures could also be retraced in the progression of the shape parameters of the Lambert-Beer law function (Eq. 1) fitted to each combination of canopy architecture × shading treatment (Fig. 2.5). For all canopy architectures, the exposition of the measurement plant to an increasing complexity of the environmental scenes resulted in a general decrease of both shape parameters for the measurement and the simulation. For the individual canopy architecture, the decrease of the regression parameters followed different patterns. The change of the shading resulted in the R2 canopy (Fig. 2.5a,b) in a staggered decrease of measured and simulated parameters with plateaus for the "closed" and "in row open" treatments and for the "between rows open" and the "open" treatment. Compared to the R2 canopy, the decrease of the shape parameters of the "in row open" treatment of the R1 canopy (Fig. 2.5c,d) resulted for the measured parameters in a less staggered decrease, whereas the simulations indicated a continuous decrease. In the I2 canopy (Fig. 2.5e,f) an increase of the shaping parameter PAR_0 in the "between rows open" treatment resulted in a general reduction of the differences between the shading treatments. Both parameters of the measured and simulated values decreased evenly, except for the simulated "open" treatment which stopped on the level of the "between rows open" treatment. The parameters of the simulated I1 canopy (Fig. 2.5g,h) showed a major decrease between the "closed" and the "in row open" treatments resulting in a plateau for the remaining shading treatments, whereas the measured I1 canopy parameters decreased steadily. Within the 32 parameter sets eight significant overestimations and two significant underestimations were detected. Three "clusters" of significances could be stated: (1) four out of eight overestimations were on parameters in the "closed" shading treatment; (2) only the "between row open" treatment in the R1 canopy indicated a significant overestimation of both parameters; (3) both significant underestimations were present in the I1 canopy.
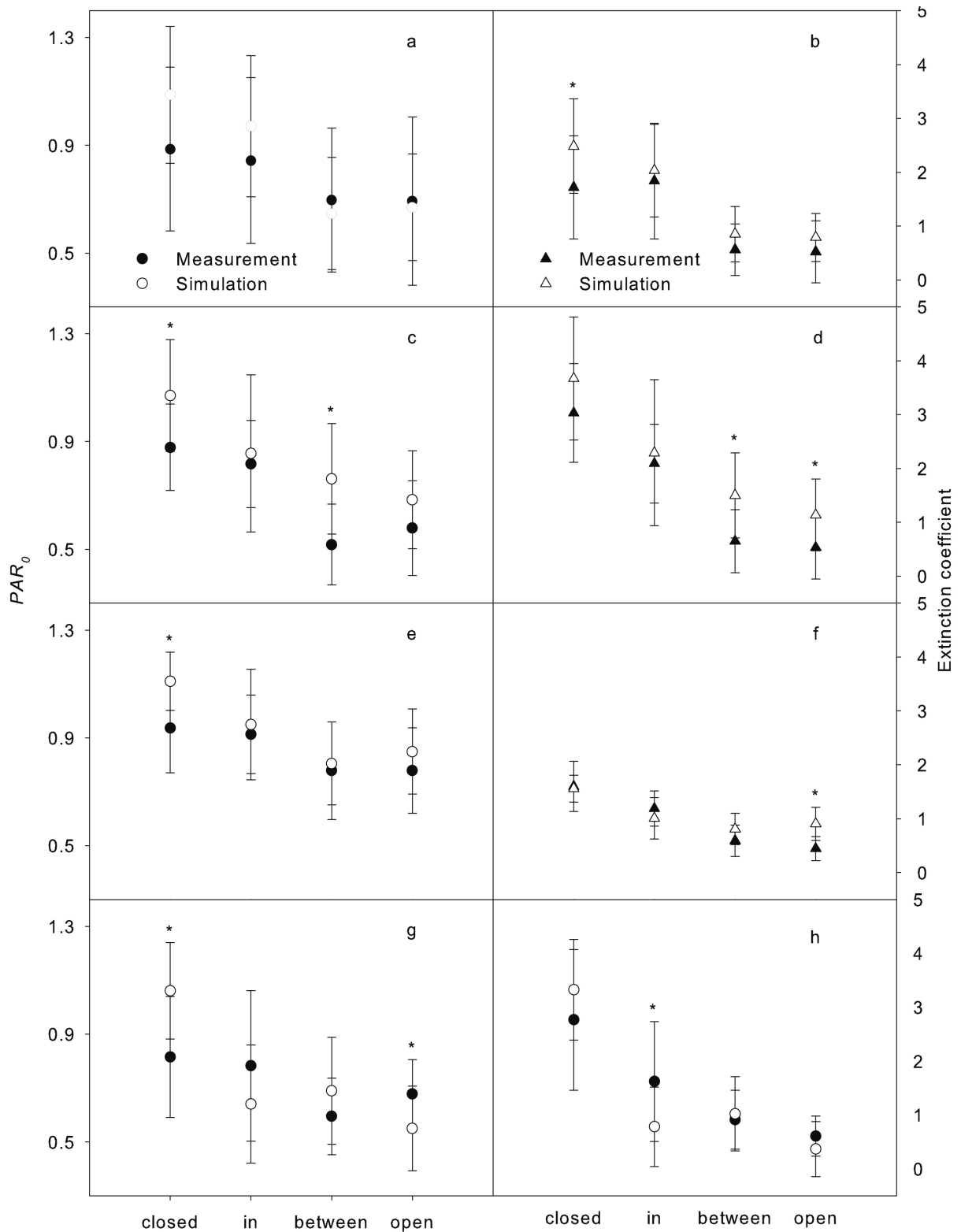
Fig. 2.5 Comparison of regression parameters of the Lambert-Beer law function (niPAR=I0*exp(-k*LAI)) for measured and simulated data for the row canopy with 2 plants per m² (a,b), the row canopy with 1 plant per m² (c,d), the isometric canopy with 2 plants per m² (e,f) and the isometric canopy with 1 plant per m² (g,h). For each canopy architecture shading treatments which were either closed in all planes (closed), open in the in row planes (in), open in the between rows planes (between) or open in all planes (open) were applied. Error bars represent standard deviations with N=14. Stars indicate significant differences by t-test with α=0.05.

The accuracy of the simulations was assessed for every combination of canopy architecture ×

shading treatment by calculation of the *Bias* and *RMSD* (Table 2.2). The examination of the

Bias, representing the deviation between the simulation and the measurement mean,

displayed that the under- or overestimation of the simulation was not greater than +/- 0.08.

The change of the *Bias* with the removal of the shading indicated a slight overestimation the

incident PAR for the "closed" and "in row open" treatments, whereas the "between rows

open" and "open" treatments were somewhat underestimated by the model. The *RMSD*,

indicating the mean deviation between simulation and measurement, ranged from a

minimum of 0.05 for the R2 "in row open treatment" to a maximum of 0.15 for the I2

"open" treatment (Table 2.2). With the stepwise exposition of the measurement plant to an

increasing complexity of the radiation environment, the RMSDs increased for the R2, R1 and

I2 canopy architectures and decreased for the I1 canopy.

Table 2.2 Mean deviation bias (Bias) and root mean squared deviation (RMSD) for comparison of measured and simulated normalized intercepted PAR (niPAR) for the row canopy with two plants per m² (R2), the row canopy with one plant per m² (R1), the isometric canopy with two plants per m² (I2) and the isometric canopy with one plant per m² (I1) canopy architecture. For each canopy architecture shading treatments which were either closed in all planes (closed), open in the in row planes (in), open in the between rows planes (between) or open in all planes (open) were applied. N=14.

Canopy architecture		Shading treatment			
		Closed	In	Between	Open
R2	*Bias*	0.02	-0.02	0.08	0.06
	RMSD	0.06	0.05	0.13	0.12
R1	*Bias*	-0.04	-0.02	0	0.04
	RMSD	0.08	0.08	0.13	0.14
I2	*Bias*	-0.08	-0.07	0.02	0.04
	RMSD	0.11	0.1	0.1	0.15
I1	*Bias*	-0.07	-0.07	-0.04	0.05
	RMSD	0.12	0.12	0.1	0.08

Discussion

The aim of this study was to investigate the light distribution in canopies with different

architectures using a 3D light distribution model with a static 3D reconstruction of the

canopy and to evaluate the simulations with leaf level PAR measurements. Therefore,

measurements and simulations of light distributions on the individual leaf level were

conducted for four cucumber canopy architectures. It has been shown in several studies that

digitizing plants *in situ* for the reconstruction of the architecture *in silico* using an

electromagnetic device is the method of choice (e.g. Drouet and Kiniry, 2008; Kahlen and Stützel, 2007; Louarn et al., 2008), whereas point sensors are widely used to characterize the PAR distribution in plant canopies (Higashide, 2009; Hovi-Pekkanen and Tahvonen, 2008; Kubo et al., 2008; Rosati et al., 2001). The short period of PAR measurements allowed to relate the measurements to a fixed sun position. Measurements may be highly variable due to instantaneous sky cloudiness, canopy heterogeneity, leaf area index and angular leaf distribution (Drouet and Kiniry, 2008).

The ratio of diffuse to total radiation used for the simulations was within the range of reported values of 23% (Spitters et al., 1986) for outside global irradiance and 30% reported by Uchijima et al. (1976) for global irradiance inside a vinyl greenhouse. The approximation of Lambertian optical properties for the leaf surfaces has been shown to be appropriate for the simulation of PAR in dense canopies (Chelle, 2006). PAR penetrating into the canopy is mainly direct light, which is primarily influenced by the canopy structure (Chelle, 2006). An evaluation of the *Caribu* model (Chelle and Andrieu, 1998) by Cieslak et al. (2008) with their own *QuasiMC* software, a Monte Carlo path tracing based model, showed the comparability of both approaches for modeling the light environment of plants.

Complexity of light environment

The "closed" treatments had the smallest standard deviations (Fig. 2.3 & Fig. 2.4a,b). The narrowest spacings were within the row of the R2 canopy showing negligible differences for the standard deviations in the "in row open" treatment (Fig. 2.3c,d) due the high light attenuation. The increased standard deviation in the "in row open" treatment of the I1 canopy (Fig. 2.4c,d) could be related to the sparse arrangement of the plants in the row as well as the unaffected azimuthal orientations of the leaves with respect to the 2/5 phyllotaxis (Kahlen et al., 2008), allowing a more variable amount of light to reach the measurement plant. Similarly, the wide gaps between the rows in the "between row open" treatment of the R2 canopy (Fig. 2.3e,f) increased the ability of incident light to directly access the measurement leaf resulting in highly increased standard deviations compared to "in row open" treatment (Fig. 2.3c,d). The isometry characteristic of the I1 canopy could be related to the unchanged scale of standard deviations of the "in row open" treatment (Fig. 2.4c,d) and the "between rows open" treatment (Fig. 2.4e,f). The "open" treatments (Fig.

2.4g,h) revealed only a small increase in standard deviation compared to "in row open" and "between rows open" treatments (Fig. 2.4c-f) indicating that they were primarily shaped by one of the horizontal light components. In summary, the largest share of the standard deviation for a single leaf in a complex light environment could be explained by differences in 3D plant structure influenced by plant spacing and morphology as well as the light environment.

Light distribution on leaf level

The consequent reduction to a vertical light gradient by the encasement and the Lambertian transmission of the light through the nonwoven diffuser fabric on the top of the canopy resulted for the "closed" treatments, irrespective of the canopy architecture, in a strict representation of the Lambert-Beer law with high extinction coefficients (Fig. 2.3a, b; Fig. 2.4a, b; Fig. 2.5 "closed"). Increased extinction coefficients of 0.87 have been shown to result from enhanced vertical light gradients due to applying supplementary light exclusively from top (Trouwborst et al., 2010). Due to the anisotropy of the light environment, the stepwise removal of the lateral shading fabrics allowed directly lit laminas facing to the sun direction to obtain high PAR levels. As this effect was not strictly correlated to the rank on the plant, the highest PAR levels were not necessarily at the top of the plant. This resulted in unequal attenuation of the exponential coefficients for the different canopy architectures. In the R2 canopy the impact of the horizontal light components was distinct due to the row structure (Fig. 2.3c - h & Fig. 2.5a, b). Through the high plant density in the within-row space the light was highly attenuated, whereas the wide gap between adjacent rows allowed high amounts of direct light to reach the plant from the space between the rows (Table 2.1). Compared to the R2 canopy the doubled plant spacing in the row of the R1 canopy allowed a higher amount of light to reach the measurement plant from the within-row space, resulting in a more gradual decrease of the slope with the removal of the shading fabric (Fig. 2.5c,d). Halving the row to row space while retaining the plant spacing in the row for the I2 canopy (Table 2.1) explained the further balancing of the differences with the stepwise enhancement of the light environment (Fig. 2.5e,f). In the I1 canopy the isometric spacing of plants (Table 2.1) resulted in a virtually not possible differentiation between the horizontal light components (Fig. 2.4). This explained the similar changes between the "closed" (Fig.

2.4a,b) and the "in row open" (Fig. 2.4c,d) as well as the "between rows open" treatments (Fig. 2.4e,f). The decrease of *niPAR* values at the top of the plant and there increase at the plant base, due to the low attenuation of light, affected the high decrease of PAR_0 (Fig. 2.5g), and caused the change from exponentially to a nearly linearly sloping *k*-values (Fig. 2.5h). The extinction coefficients for the "open" treatments (Fig. 2.3g,h, Fig. 2.4g,h, Fig. 2.5) are comparable with literature values for cucumber crops, which ranged from 0.42 (Warren Wilson et al. 1992) up to 0.53 - 0.59 (Peil et al. 2002) and 0.57 for an inter-lighted canopy (Trouwborst et al., 2010).

The slight differences of the *k* and PAR_0 values between the "open" canopy architectures (Fig. 2.5) masked the fact that the *niPAR* with increasing LAI above a certain leaf highly depends on the plant density. Comparing the R2 and I1 canopies the reduction of the *niPAR* on the same leaf rank in the R2 canopy was negligible at the top while it could increase up to 80% at the bottom. The increase of *niPAR* values at the bottom of the plant was also related to the high reflectance properties of the white plastic ground cover, which was uncovered with the removal of the shading fabric (Warren Wilson et al. 1992). In summary, the results highlighted that the 3D model approach precisely simulated incident PAR for the individual leaf under a broad range of canopy architectures and shading treatments.

Precision of simulation

For the parameters of the Lambert-Beer law the aggregation of the significant overestimations in the "closed" shading treatments (Fig. 2.5) supported the overestimations of the *niPAR* values at the top of the plant (Fig. 2.3 & 1.4). The incidence of the two significant underestimations in the non-closed I1 canopy treatments was in line with the shift of the *Bias* (Table 2.2) as well as the reduction of the shading from an overestimation to a moderate underestimation. This alternation also indicated that there was no overall systematic error in the *Caribu* model. The underestimations indicated by the *Bias* and the parameters of the Lambert-Beer law for the less shaded row canopies treatments could be explained by the fact that no morphological interactions of the measurement plants with their neighbor plants were accounted for by the model. As the light intensity on the leaf surface was mainly due to direct light, the negligence of morphological interaction may have led to an increase of light interceptions. In isometric canopies morphological interactions

were less pronounced due to the sparse arrangement of the plants (Kahlen et al., 2008). The overestimation in the encased isometric treatments could possibly be related to an overestimation of the reflectance properties of the shading fabric, which should account for stray light coming through the junction of the shading fabrics. The reduced *Bias* in both encased row treatments could then be a balanced result of both effects described above.

To our knowledge, there have been no studies which analyzed the light distribution in a greenhouse crop at a comparable level of detail. The recent study of Higashide (2009) used a row canopy structure in tomato and fitted exponential regression to the measured and simulated data ("flat" equations Fig. 1 and Fig. 2, Higashide, 2009). The measurements and simulations were done on the individual leaf level, whereas for the comparison the datasets where averaged over five leaves and cumulated over seven days. The cited exponential functions were used to calculate the *Bias* of -0.29 and a *RMSD* of 0.32 (Higashide, 2009). Comparing these values with the "open" canopy treatments which ranged between 0.04 to 0.06 for the *Bias* and 0.08 to 0.15 for the *RMSD* (Table 2.2) showed the higher precision of the approach using detailed plant canopy data obtained by digitizing as supposed by Higashide (2009). Other authors also emphasized the importance of accounting for the spatial heterogeneity of the light distribution within the greenhouse (Chenu et al., 2008) as well as the changes over time and the plasticity of the crop (Drouet and Kiniry, 2008). Further improvements of the precision of the model could be accomplished by increasing the level of detail of the surrounding canopy with representations of the real neighbor plants, incorporating the greenhouse structure and by mapping the diversity of the anisotropic light distribution due to clouds.

Conclusion

Spatial positioning of plants within the canopy has a clear effect on the *niPAR* values on the individual leaf. The method allowed capturing the key characteristics of the light distribution within a canopy under a broad range of environmental factors like plant and canopy architecture, light conditions and time of day. Disregarding morphological interactions of neighboring plants appeared to be less suitable for the precise determination of the light distribution in dense canopies. The combination of a detailed 3D surface based plant model with a 3D light model allowed to precisely simulate incident PAR for individual leaves

offering the opportunity to calculate rates of photosynthesis as a basis for further plant development. Therefore, this study supports the use of surface based radiation models for a precise description of the phylloclimate in plant canopies.

Chapter 3

Influence of canopy architecture and environmental conditions on the dry matter production of a functional-structural plant model including leaf-level photosynthesis

Dirk Wiechers, Katrin Kahlen, Hartmut Stützel

Abstract

Background and Aims: In spatially discontinuous canopies of indeterminately growing plants, like greenhouse cucumber, canopy structure may have a variable influence on yield formation, depending on environmental conditions. The aim of this study was to gain a better quantitative understanding of the interdependence between canopy architecture, light interception and plant growth. This requires an accurate representation of growth, radiation transfer and canopy structure. Therefore, we combined models of photosynthesis, dry matter distribution, light interception and plant architecture to a functional-structural plant model (FSPM) of greenhouse cucumber and analyzed its performance under various canopy conditions.

Methods: Based on the biochemical model of leaf photosynthesis of Farquhar *et al.*(1980), a combined model (Kim and Lieth, 2003) including stomatal conductance, was parameterized for cucumber and implemented into L-Cucumber (Kahlen *et al.*, 2008), a dynamical FSPM. Dry matter production was simulated for four different canopy architectures as well as for different CO_2 concentrations and light intensities, and evaluated with measured data and values from literature.

Key Results: The model predictions of dry matter production were in good agreement for different plant architectures. Deviations in the dense isometric canopy could be related to underestimations of leaf area and light interception. Scenarios with varying CO_2 and light

agreed with cited changes and varying responses of the canopy architectures could be related to different sensitivities of the photosynthesis model.

Conclusion: This FSPM provides the possibility to account for spatial gradients of environmental factors induced by the spatial structure of the plant and the canopy, which are necessary for an accurate estimation of plant productivity. Thus, the FSPM could serve as a tool to analyze the impact of environmental control strategies on productivity for greenhouse production, which aims at optimized resource usage.

Introduction

In indeterminate plants, which are continuously producing new fruits, yield is highly alternated by the non-uniform growth of the individual fruits (Wubs *et al.*, 2009b; Schapendonk and Brouwer, 1984; Heuvelink, 1996). In these crops, also variations of yield depending on plant arrangement and plant density have been observed (Kahlen, 2007). Moreover, influences of the canopy architecture on the growth and quality of the harvested fruits have been shown (Klieber *et al.*, 1993; Wiechers *et al.*, 2011a). Thus, in order to understand yield formation, a detailed representation of plant structure and growth is needed. Existing models for reproductive and indeterminate plants cultivated in discontinuous canopies are process based (Marcelis, 1994; Heuvelink, 1996), or do not explicitly consider canopy conditions (Ma *et al.*, 2011). Thus, they do not allow for feedback from the organ level to the functioning on plant or crop level. This makes these models not well suited for studies of parameters with an underlying spatial distribution, e.g. light, temperature or nitrogen distribution (Vos *et al.*, 2007). To simulate the environmental influences on the development of individual organs, models which are capable of accounting for interactions between organ based physiological processes and plant morphology influenced by the canopy, structure are essential (Fourcaud *et al.*, 2008).

Photosynthesis is one of the key physiological processes in plants determining dry matter production, driven by the available quantity of light as one of the major environmental factors (Chenu *et al.*, 2005). Different approaches to simulate photosynthesis, like light use efficiency and light response curve models have been developed (Vos and Heuvelink, 2007). The light use efficiency concept (Monteith and Moss, 1977) was designed to work on the canopy level, whereas the light response model can be used for individual leaves. Both approaches are restricted to the influence of light, and interactions between light and other environmental factors are not generally included. The model of leaf photosynthesis developed by Farquhar and coworkers (Farquhar et al., 1980) relating the actual rate of photosynthesis (A) to the underlying biochemical processes has been widely implemented. This model is also capable of predicting the rate of photosynthesis for a variety of environmental factors like: CO_2 concentration, light, temperature and relative humidity (von Caemmerer, 2000). Photosynthesis is also affected by physiological processes like ontogenesis (Marcelis, 1991) or the distribution of nitrogen (Müller *et al.*, 2005). For the Farquhar model, the dependency of A on CO_2 concentration is most precisely described on

the level of CO$_2$ concentration in the chloroplast (C_c), involving the internal conductance (g_i) for the pathway of CO$_2$ from the substomatal cavities to the chloroplast into the model (Sharkey *et al.*, 2007; Dubois *et al.*, 2007). The concentration of CO$_2$ in the substomatal cavities (C_i) has a major influence on the apparent rate of photosynthesis. One of the most commonly used models relates stomatal conductance (g_s) to the net rate of photosynthesis (A_n), relative humidity (rh) and the CO$_2$ concentration at the leaf surface (Ball et al., 1987) to predict C_i. Besides its proven accuracy under a wide range of environmental conditions, the advantage of the model is the simplicity of parameterization (Damour *et al.*, 2010). A combination of both models was developed to simulate the photosynthesis of single leaves (e.g. Kim and Lieth, 2003), but this model is not designed to estimate the photosynthesis of whole plants. To be applied at the plant level, a leaf level model needs information on the plant and canopy structure. Thus, due to the non-linear response of photosynthesis to light, a detailed simulation of the plant structure and the surrounding canopy architecture is essential (De Pury and Farquhar, 1997; Chelle, 2005). This is of special importance in vertically trained row canopies like greenhouse cucumber with their discontinuous canopy structures, which causes the distribution of light fluctuating with time and space (Wiechers *et al.*, 2011b).

One of the most elaborated methods to model the development of plants are defined as functional-structural plant models (FSPM, Fourcaud *et al.*, 2008; Vos *et al.*, 2010). These models allow combining the approaches of physiological models with information of the three-dimensional (3D) plant and canopy structure for the dynamic representation of plant development. This allows mimicking interactions between plant physiology, morphology and environment (Chelle, 2005; Kahlen and Stützel, 2011). A major advantage is the possibility of a precise simulation of the incident light on the leaf surface (Cieslak *et al.*, 2008; Wiechers *et al.*, 2011b). So far, only a small number of dynamic models, which combine a detailed model of photosynthesis with a precise description of the plant and canopy structure, have been developed: L-Peach a FSPM for the growth of peach does not explicitly accounts for the interactions of a canopy (Allen *et al.*, 2005). For the reproduction of major features of the growth of kiwifruit vines a FSPM was conceptualized, but a parameterization with appropriate data has not yet been done (Cieslak *et al.*, 2010). For cereal crops, combinations of a 3D model and an organ-based model of photosynthesis simulating the effect of plant density on biomass production and tillering (Evers *et al.*, 2010) or the influence of

quantitative trait loci (QTL) on the phenotype (Xu *et al.*, 2011) have been developed. However, cereal crops are characterized by a relatively homogenous distribution of leaves in space, which reduces the variability of the light distribution within the canopy (Disney *et al.*, 2006).

The objective of this study was to predict and evaluate the growth and development of greenhouse cucumber as a model for a reproductive and indeterminate plant with spatially discontinuous canopy structure, for a variety of environmental conditions. Therefore we extended L-Cucumber (Kahlen et al., 2008) a FSPM for dynamic greenhouse cucumber growth, with a leaf level model of photosynthesis and stomatal conductance(Kim and Lieth, 2003), which was extended to take the g_i into account. The parameterization of the underlying Farquhar model (Farquhar *et al.*, 1980) followed a simultaneous parameter estimation approach (Dubois *et al.*, 2007). The stomatal conductance and photosynthesis sub models were evaluated against independent photosynthesis data. The extended L-Cucumber was evaluated for different canopy architectures by comparing the simulated dry matter production, based on simulations of the radiations transfer using Caribu (Chelle *et al.*, 1998), with non-destructive measurements. The sensitivity of the dry matter production of the different canopies to changes in environmental conditions was simulated using L-Cucumber and was evaluated with measurements cited in literature.

Materials and Methods

Coupled model of stomatal conductance and photosynthesis

The model of stomatal conductance (Ball *et al.*, 1987) relates g_s (mol H_2O m^{-2} s^{-1}) to A_n (µmol CO_2 m^{-2} s^{-1}), relative humidity at leaf surface (h_s), the CO_2 partial pressure at the leaf surface (C_s, µbar) and atmospheric pressure (P_a, kPa):

$$g_s = b + m A_n h_s / (C_s / P_a) \qquad (1)$$

where b (mol H_2O m^{-2} s^{-1}) is the minimum stomatal conductance and m is an empirical parameter representing the sensitivity of the stomatal conductance to the related environmental influences.

The parameters of the two-phase photosynthesis model were estimated simultaneously, whereupon the estimation of the model parameters was accomplished without a predetermination of the transition between Ribulose-1,5-bisphosphate carboxylase oxygenase (Rubisco) and ribulose 1,5-bisphosphate (RuBP) regeneration limited photosynthesis (C_{itr25}, µmol mol^{-1}). A_n is modeled as the minimum of the Rubisco limited assimilation rate (A_c, µmol CO_2 m^{-2} s^{-1}) and the RuBP regeneration-limited assimilation rate (A_j, µmol CO_2 m^{-2} s^{-1}):

$$A_n=\min(A_c,A_j)-R_d \qquad\qquad (2)$$

with

$$A_c=V_{cmax}(C_c- \Gamma^*)/C_c+K_c(1+O/K_o) \qquad\qquad (3)$$

$$A_j= J_{max}(C_c- \Gamma^*)/(4C_c+8 \Gamma^*) \qquad\qquad (4)$$

where R_d (µmol CO_2 m^{-2} s^{-1}) is the rate of non-photorespiratory CO_2 evolution, V_{cmax} (µmol CO_2 m^{-2} s^{-1}) is the maximum rate of carboxylation and J_{max} (µmol CO_2 m^{-2} s^{-1}) is the rate of electron transport at a given temperature. V_{cmax} and J_{max} can either be estimated by using C_i based kinetic constants, which are not stable within and among plant species or based on apparent constants determined at the CO_2 partial pressure at the chloroplast (C_c, µmol mol^{-1}) (Warren, 2008). The C_c based Michaels-Menten constants and their kinetic constants of Rubisco to CO_2 (K_c, µmol mol^{-1}) and to O_2 (K_o, mmol mol^{-1}) concentration as well as the CO_2 compensation point in the absence of dark respiration (Γ^*, µmol mol^{-1}) were chosen *a priori* from *in vivo* measurements (Bernacchi et al., 2002). To be able to employ these apparent C_c based parameters, the internal conductance (g_i, µmol mol^{-1}) based on measurements for cucumber is used (Loreto et al., 1992).

$$C_c= C_i-A_n/g_i \qquad\qquad (5)$$

The dependency of J_{max} on PAR was adjusted following De Pury and Farquhar (1997). To minimize temperature effects in the parameterization the estimates were standardized to 25°C for further analysis. Temperature dependencies were calculated according to Bernacchi *et al*. (2002) and Sharkey *et al*. (2007). This includes the estimation of the maximum rate of carboxylation (V_{cmax25}), the maximum rate of electron transport (J_{max25}), and the rate of non photorespiratory CO_2 evolution (R_{d25}) at 25°C. The models of stomatal conductance and

photosynthesis are coupled with the Newton-Raphson method, which successively approximates the C_i value until a predefined accuracy (< 0.001 ppm) is reached (Kim and Lieth, 2003).

Functional structural plant model

We combined L-Cucumber (Kahlen et al., 2008), the existing FSPM for dynamic structural plant growth, with the coupled model of photosynthesis and stomatal conductance (Kim and Lieth, 2003). The FSPM was implemented as cpfg code into L-Studio software (Mech, 2004). The model calculated the rate of photosynthesis at individual leaf level on an hourly basis, depending on the incident radiation, temperature, CO_2 concentration and relative humidity. Parameters for stomatal conductance and photosynthesis were derived from the measurements. As the original model (Farquhar *et al.*, 1980) was not parameterized for wider temperature ranges (Bernacchi *et al.*, 2003), exponential functions to account for the temperature responses of the model parameters, summarized in Sharkey *et al.*(2007) were implemented. The radiation incident on each leaf was calculated by the L-System with the Caribu software (Chelle et al., 1998) based on the plant and canopy architecture. For the light environment 36 light sources were used to simulate a standard overcast sky. The daily course of light intensity and temperature was mapped by a normalized sine function and scaled with the daily incident light intensity and temperature of the experiments. For the concentration of CO_2 (400 ppm) and relative humidity (70%) no spatial or temporal gradients were assumed. Leaf temperature was assumed to be equal to the ambient air temperature. Simulations were run for 47 days, the same time span as the duration of the experiment. Corresponding to the greenhouse experiment, four canopy architectures were simulated (Table 3.1).

Table 3.1 Canopy architectures with information about distribution, plant density (plant m^{-2}), plant distance (cm), row distance (cm) and specific leaf area (cm² g^{-1})

Canopy architecture	Distribution	Plant density (plant m^{-2})	Plant distance (cm)	Row distance (cm)	Specific leaf area (cm² g^{-1})
R2	Row	2	27	186	395
R1	Row	1	53	186	335
I2	Isometric	2	53	93	395
I1	Isometric	1	107	93	335

Only the arrangements of the canopies and differences in specific leaf area (SLA) were changed to simulate the four different canopy architectures. Simulations were run with 15 plants in row, and 19 plants in isometric canopies. As in the experiment, plants grew monopodially without side shoots, were topped at the highwire, and each fruit bearing rank had one fruit. The first fruit was allowed to grow at rank seven.

In the simulations, hourly rates of photosynthesis were calculated for each leaf individually. The hourly rates of photosynthesis were accumulated and converted to a daily rate of dry matter gain which was transferred to a common assimilate pool (Warren Wilson et al., 1992). A time dependent partitioning of assimilates between vegetative shoot parts and fruits was implemented as described by (Wiechers *et al.*, 2011a).

Simulation scenarios

In the experiment the plants were transplanted with the first leaf approximately oriented towards the south. To represent the unavoidable variation in the initial orientation in the simulation, the south orientation of the first leaf of each plant was varied between ±15° by rotating it around the vertical axis for three rotation scenarios. Overall, this resulted in nine simulated plants per canopy architecture, which were evaluated.

Environmental scenarios

The sensitivity of the model to environmental conditions was evaluated by either raising or lowering the light intensity for all four canopy architectures by 30%. All other factors were kept as in the simulation of experimental conditions of the greenhouse conditions. Similarly, the influence of the ambient CO_2 concentration on the dry matter production of the different canopy architectures was analyzed by increasing the ambient CO_2 to 600 ppm or dropping the concentration to 200 ppm.

Parameterization of the coupled model of photosynthesis

The experiments for parameterization and evaluation of the functional models, i.e. the model of stomatal conductance and the photosynthesis model, were conducted in growth chambers at the Institute of Biological Production Systems in Hannover, Germany. Cucumbers (*Cucumis sativus* L. Aramon, Rijk Zwaan, De Lier, Netherlands) were cultivated on rock wool slabs (Grodan, Roermond, Netherlands). The irradiance above the plants was approximately 500 µmol m^{-2} s^{-1} photosynthetic active radiation (PAR). Lights were switched on at 6 a.m. for 14 hours. Temperature was set to 25/20°C day/night and relative humidity was maintained at 70%. Irrigation and nutrition was applied manually twice a day using a water soluble fertilizer (Universol Orange, Scotts B.V., Geldermalsen, The Netherlands). The BWB model was parameterized with data from 121 measurements. All measurements were conducted on fully expanded leaves which were 14 to 17 after unfolding. For the measurements either relative humidity (46-73% *rh*), temperature (21-35 °C), light (200-1500 µmol m^{-2} s^{-1} PAR) or CO_2 (100-1500 ppm) were varied, while all other conditions were kept constant. Plants were sown on 09 Jan 2007, transplanted on 03 Feb 2007 and measurements started on 19 Feb 2007. Measurements for the parameterization of the photosynthesis model (Farquhar *et al.*, 1980) were taken on eight plants one, two and three weeks after unfolding of the leaf. The exposition of the measured leaves was controlled by a mechanical support to ensure that their irradiation remains constant. For the parameterization of the model of photosynthesis 46 A/C_i response curves with 12 C_i levels between 50 and 1000 µmol mol^{-1} CO_2 at 800 µmol m^{-2} s^{-1} PAR, 25°C leaf temperature and approximately 70% relative humidity were measured in total. For the validation 15 A/C_i response curves with 9 C_i levels between 100 and 1500 µm at 1500µmol m^{-2} s^{-1} PAR, 25° C leaf temperature and approximately 70% relative humidity of leaves between eight and 22 days after unfolding were measured. Plants were sown on 09 Jan 2008, transplanted on the slabs on 30 Jan 2008 and measurements started on 13 Feb 2008. All measurements were conducted with the LI-6400 photosynthesis system (LI-COR Inc., Lincoln, NE, USA).

Greenhouse evaluation

Four cucumber crops with different canopy architectures were cultivated in greenhouses from July to September 2007 at the Institute of Biological Production Systems in Hannover,

Germany (52.5°N, 9.7° E). The experiment was set up as a randomized complete block design with three replications. The canopy architectures were arranged in either row or isometric patterns with either one or two plants per m² (Table 3.1). The ground was covered by a white plastic film and rows were oriented from north to south. Plants were transplanted to the greenhouse in the five-leaves stage on 30 July 2007. To ensure their monopodial growth plants were attached to a cord with plastic clips until the main stem reached the supporting horizontal wire at 220 cm above the ground. At this time the plants were topped. The number of fruits per rank was reduced to one and all side shoots were pruned. To enhance vegetative growth in the initial phase all fruits in the first six fruit bearing ranks were pruned. The row canopies were composed of three rows with six plants, and the isometric canopies of four rows with either three or four plants. Measurements for each treatment were conducted on two plants in the center of the middle row ensuring at least one border plant to each side. With the start of fruit growth non-destructive measurements of fruit length and leaf width were taken every two to three days. Measurements of the organs started at approximately 5 cm length and fruits were harvested when they had reached approximately 30 cm length. Allometric relations were used to calculate the dry weights of the individual organs (Kahlen and Stützel, 2007).

Statistical analysis

The parameters of the photosynthetic model were statistically analyzed with the SAS software using the GLM procedure and a Tukey multiple comparison test (p=0.05) (SAS Institute Inc., Cary, NC, USA). For a continuous description leaf aging over time (t), the estimated parameters of V_{cmax25} and J_{max25} were normalized and fitted to a logistic peak function, $P(t)$, with Sigmaplot 11 (Systat Software, Richmond, USA):

$$P(t)= a*\exp(-0{,}5*(\log(t/b)/c)^2)/t \qquad\qquad (6)$$

where a, b and c were parameters. The parameters of the logistic peak function of V_{cmax25} and J_{max25} were compared with a t-test in Sigmaplot 11. To evaluate the performance of the stomatal conductance model and the combined model of photosynthesis the root mean square deviation (RMSD) and the systematic error (bias) between both data sets were calculated (Kobayashi and Salam, 2000). Produced total dry weight of the experiment and the simulation were compared using a t-test in Sigmaplot 11. Simulated light interception of

the different canopies was compared to Lambert-Beer law light extinction function based on measurements for the different canopies (Wiechers *et al.*, 2011b). These functions used normalized values of the incident PAR (*niPAR*) to allow comparison of measurements and simulation for different light environments. For comparisons between measurements and simulation bias and RMSD were calculated. The final dry weights of the environmental scenarios were analysed with the GLM procedure and a Tukey multiple comparison test (p=0.05).

Results

Parameterization and validation of the leaf photosynthesis sub model

The estimate for the parameter *b* of the BWB model minimum stomatal conductance was not significantly different from zero, while *m* was 7.8 (Figure 3.1). The validation of the BWB model with an independent data set revealed a minor systematic overestimation of the measured data indicated by the bias with 0.0404 mol m^{-2} s^{-1} and a marginal residual error indicated by the RMSD of 0.1055 mol m^{-2} s^{-1} (Table 3.2).
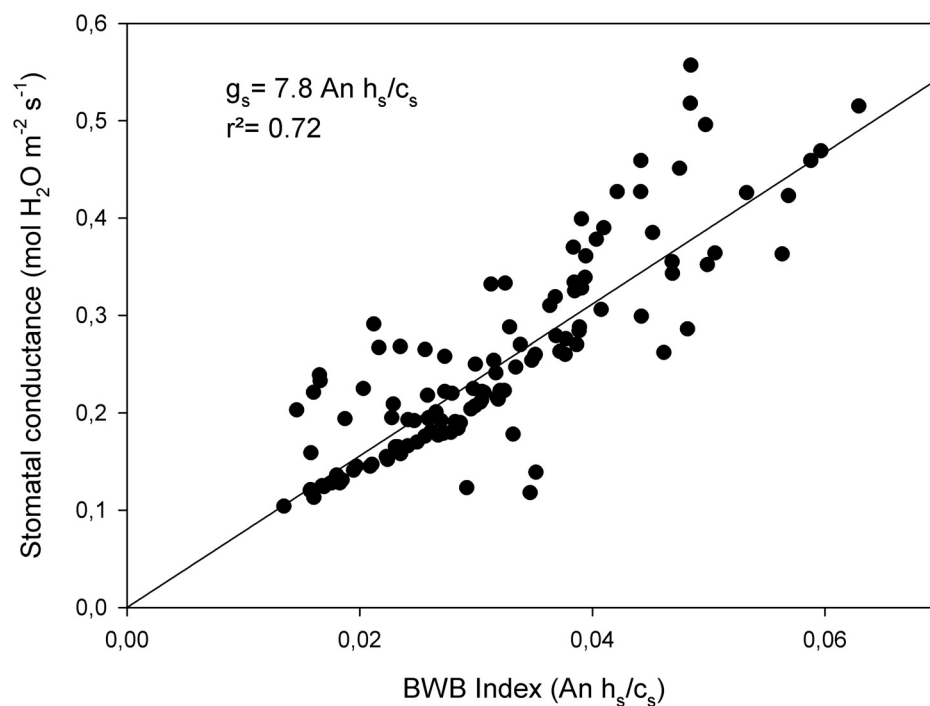
Fig. 3.1 Linear regression of measured stomatal conductance and the prediction of from the BWB model (Eq. 1). N= 121.

Table 3.2 Performance of the stomatal conductance model and the combined model against validation data. Shown are values for the bias and the root mean square deviation (RMSD) of observed values and model prediction for net photosynthetic rate (*An*) and stomatal conductance (*gs*). N= 135.

	Bias	RMSD
gs (mol H_2O m^{-2} s^{-1})	0.0404	0.1055
An (μmol CO_2 m^{-2} s^{-1})	0.2475	5.3135
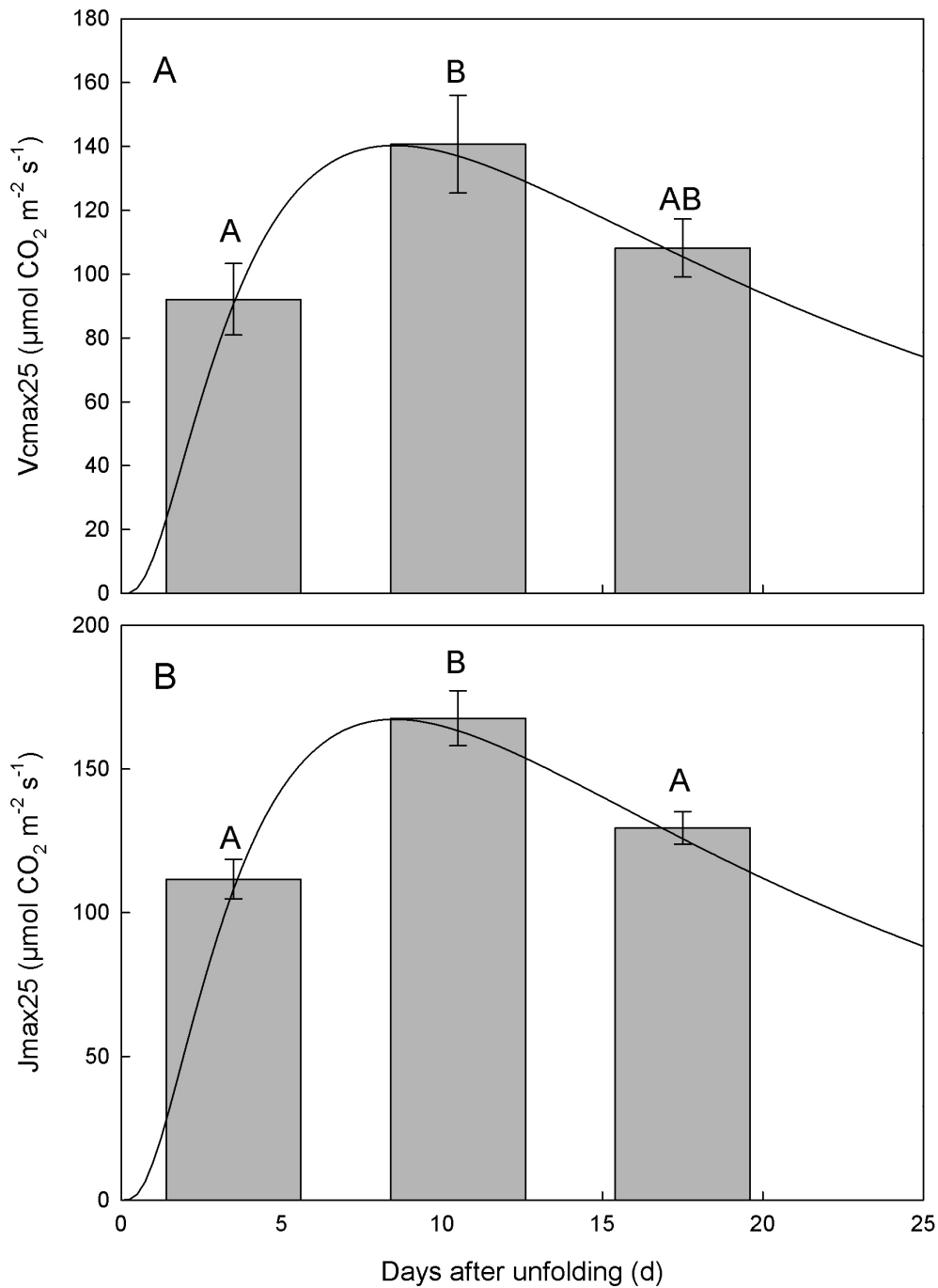
Fig. 3.2 (A) Maximum rate of carboxylation (V_{cmax25}) and (B) maximum rate of electron transport (J_{max25}) at 25°C. Bars indicate estimates ± s.d. for one (n=15), two (n=8) and three (n=23) weeks after unfolding. Curve shows non-linear it of Eq. 6.

The parameters for V_{cmax25} and J_{max25} differed significantly between succeeding weeks with a peak in the second week (Figure 3.2). A continuous description of these parameters was obtained by fitting a logistic peak function (Eq. 6) to the normalized data. The trajectory of the function was characterized by a steep increase and a less pronounced drop. As the parameters of the logistic peak function did not significantly differ between V_{cmax25} and J_{max25} a common parameter set with a=13.8, b=21.1 and c=0.952 was used to scale the maximum values of the second week V_{cmax25}= 140.7 µmol CO_2 m^{-2} s^{-1} and J_{max25}= 163.5 µmol CO_2 m^{-2} s^{-1} over time (Figure 3.2).

The statistical analysis of the values for R_{d25} and C_{itr25} revealed no significant changes over time, thus mean values could be used (Table 3.3).

Table 3.3 Estimates of the the rate of non- photorespiratory CO_2 evolution (Rd25) and the transition point from *Ac* to *Aj* (*Citr*25) for one (n=15), two (n=9) or three (n=23) weeks after unfolding and the mean of all weeks. Values are means ± s.d. for the estimates. Different letters in a column indicate significant differences based an Anova and a Tukey multiple comparison (p=0.05).

	Week 1	Week 2	Week 3	Mean
Rd25 (µmol CO_2 m^{-2} s^{-1})	1.1 ± 0.3a	1.3 ± 0.5a	2.0 ± 0.3a	1.5
Citr25 (µmol mol^{-1})	175.2 ± 29.0a	182.9 ± 39.6a	228.7 ± 23.5a	205.9

Implementing all parameters for the stomatal conductance and photosynthesis model, and validating the coupled model against independent data showed that the bias was also quite small, whereas the RMSD was more prominent (Table 3.2).

Simulation of canopy dry matter production

The measured final dry weights of the four canopies differed by nearly 80 g plant[-1] (Figure 3.3). The simulation of dry matter production for the experiments closely mapped the measured dry matter production. For all four canopy architectures, dry matter production could be separated in an initial phase in which only vegetative organs were produced. With the beginning of fruit set around day 20 a clear increase in total dry matter could be observed in all four canopies. The rise was least pronounced in the R2, and most conspicuous in the I1 canopy. The simulated final total dry weights ranged from 318.0 g plant[-1] for the R2, over 351.5 g plant[-1] in the I2, and 394.9 g plant[-1] for the R1, up to 414.5 g plant[-1] for the I1 canopy (Figure 3.3).
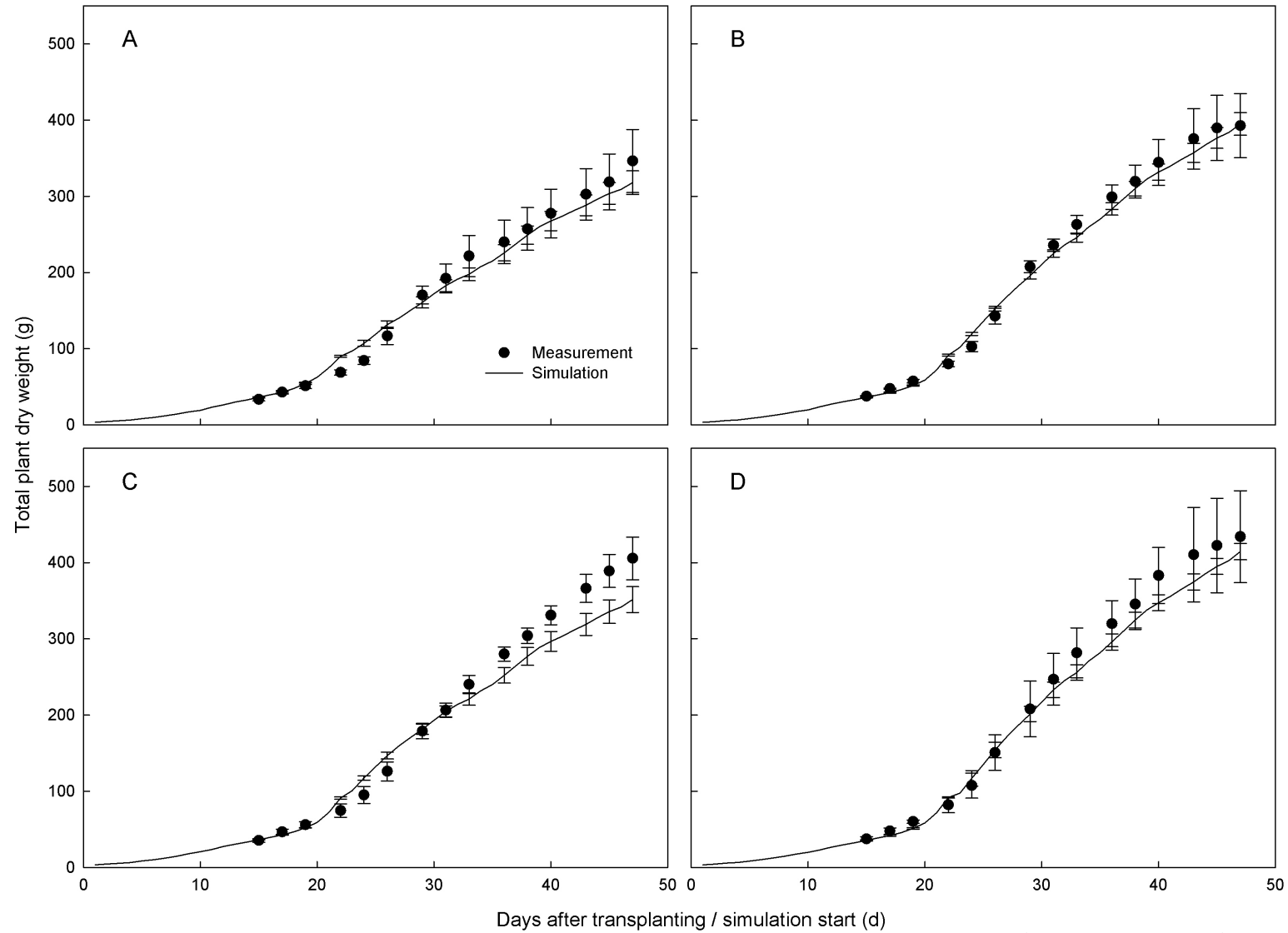
Fig. 3.3 Measured and simulated time curse of accumulated total dry weight for a row canopy with two plants m^{-2} (A) and one plant m^{-2} (B) and an isometric canopy with two plants m^{-2} (C) and one plant m^{-2} (C). Measurements (n=6) and simulations (n=9). Error bars represent standard deviations.

The simulations of the final total dry matter for the R1 canopy resulted in a non significant overestimation of 2.3 g plant^{-1} compared to the measured. The simulations of the R2 and I1 canopy structures underestimated the dry matter of the measurements by approximately 20- 30 g plant^{-1} but did not differ significantly from the measurements. The simulation of the I2 canopy was the only canopy architecture, which significantly underestimated the measured result by 54 g plant^{-1} dry weight (Figure 3.3). At the end of the experiment, the ratio of the measured generative to vegetative plant parts showed only small differences between the canopies (Table 3.4). The resulting final ratio in the simulations differed only within 1 and 2 % from the measurements.

Table 3.4 Ratio of generative and vegetative parts in percentage at the end of the experiment (n=6) and the simulation (n=9) for a row canopy with two plants m^{-2} (R2) and one plant m^{-2} (R1) and an isometric canopy with two plants m^{-2} (I2) and one plant m^{-2} (I1).

Canopy architecture	Measured		Simulated	
	generative part (%)	vegetative part	generative part (%)	vegetative part
R2	76	24	75	25
R1	76	24	75	25
I2	77	23	78	22
I1	77	23	75	25

Except for the I2 canopy, simulations marginally overestimated the vegetative parts in all canopy architectures. The progression of the leaf area per plant over time was closely reproduction in the dense row canopy (Figure 3.4). In this canopy, only marginal overestimations before day 20 and a short period of underestimation around day 30 could be traced. Leaf area of the row and isometric canopies with one plant m^{-2} were closely estimated by the model at beginning of fruit set, but were underestimated thereafter. This led to a delay of approximately five days for the simulations to reach maximal leaf area. The final leaf areas per plant were slightly underestimated. For the I2 canopy, the simulated leaf area per plant matched the measurements up to day 20. Thereafter, a clear underestimation was apparent, leading to a final discrepancy of about 0.2 m² (Figure 3.4).
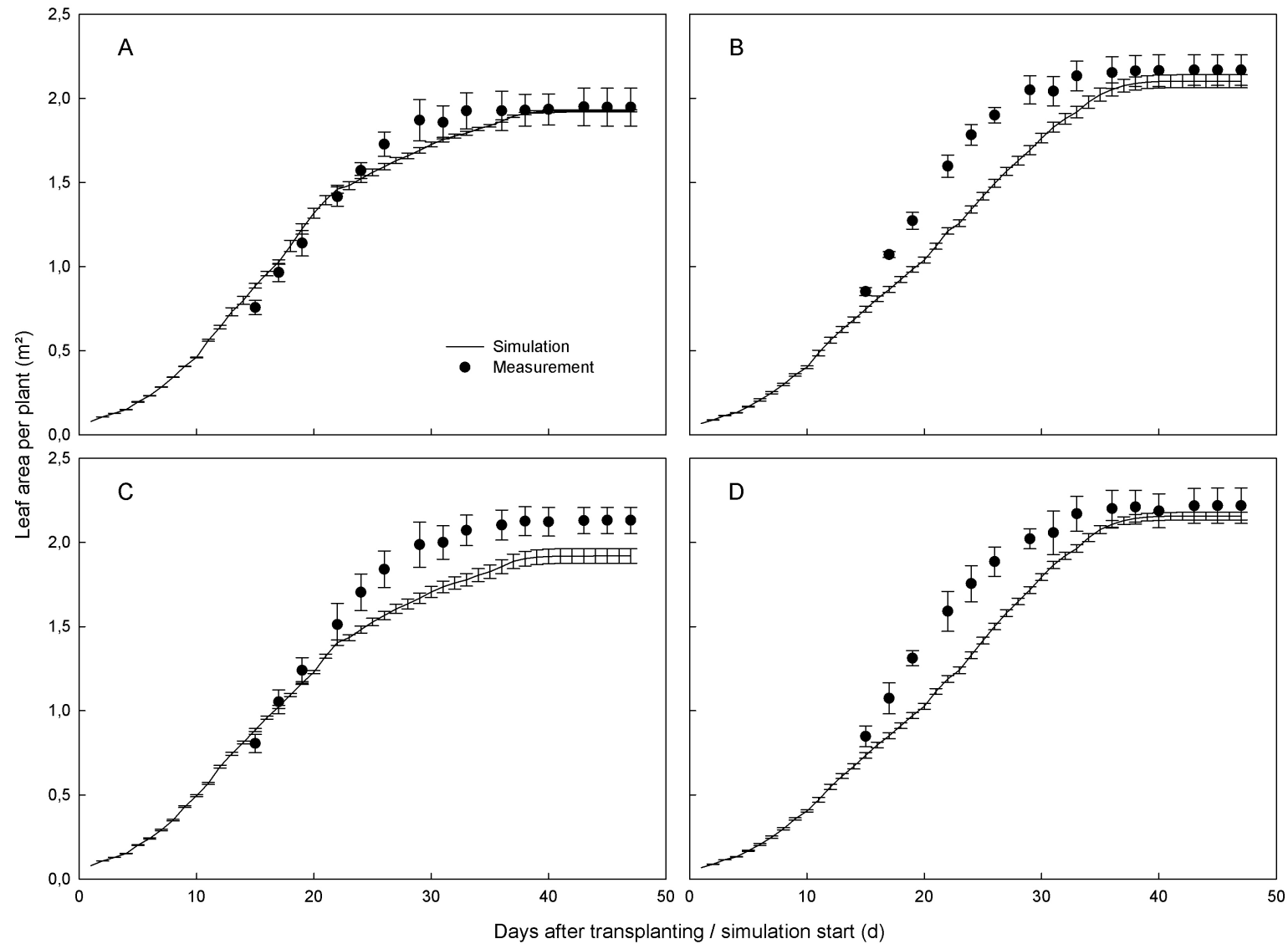
Fig. 3.4 Measured and simulated time curse of accumulated leaf area per plant for a row canopy with two plants m^{-2} (A) and one plant m^{-2} (B) and an isometric canopy with two plants m^{-2} (C) and one plant m^{-2} (C). Measurements (n=6) and simulations (n=9). Error bars represent standard deviations.

Light interception

The bias for the day 47 indicated that light interception was somewhat overestimated by the model for both row canopies, whereas the isometric canopies were slightly underestimated (Table 3.5). The RMSD showed no obvious differences between the four canopies. For earlier stages with lower leaf area indices, comparisons between simulated and measurement-based *niPAR* revealed only small absolute biases and RMSD values. Only in the sparse canopies both values were slightly increased for the days 17- 27 (Table 3.5). For the I1 the systematic underestimation was only present in the last ten days, whereas the bias for the I2 canopy indicated a longer period of underestimation.

Table 3.5 Bias, root mean square deviation (RMSD) and leaf area index (LAI) for a row canopy with two plants m^{-2} (R2) and one plant m^{-2} (R1) and an isometric canopy with two plants m^{-2} (I2) and one plant m^{-2} (I1) for seven dates at the second half of the experiment/simulation.

	R2			R1			I2			I1		
Days	Bias	RMSD	LAI	Bias	RMSD	LAI	Bias	RMSD	LAI	Bias	RMSD	LAI
17	0.08	0.17	2.05	0.16	0.24	0.86	0.03	0.17	2.05	0.14	0.22	0.85
22	0.06	0.15	2.92	0.15	0.26	1.21	0.03	0.17	2.81	0.12	0.23	1.19
27	0.02	0.20	3.26	0.09	0.26	1.57	-0.02	0.23	3.21	0.07	0.25	1.58
32	0.03	0.13	3.55	0.06	0.20	1.88	-0.04	0.13	3.52	0.04	0.19	1.92
37	0.02	0.12	3.79	0.01	0.17	2.07	-0.02	0.12	3.78	-0.02	0.17	2.13
42	0.04	0.13	3.85	0.01	0.16	2.10	-0.02	0.11	3.84	-0.03	0.16	2.14
47	0.05	0.13	3.85	0.02	0.15	2.10	-0.03	0.11	3.84	-0.02	0.14	2.16

Environmental scenarios

A reduction of the ambient CO_2 concentration to 200 ppm had greatest effects in the low density canopies with a reduction of the final dry matter production by more than 60%, compared to about 50% in the high densities (Table 3.6). An increase of the ambient CO_2 concentration to 600 ppm simulated a significantly higher increase of dry matter production with 19.7% for the R2 canopy compared to all other canopy architectures. The reduction of the incident PAR by 30% simulated a reduction of the final dry matter production by approximately 25% for the dense canopies and about a third in the sparse canopies. The increase of the PAR by 30% increased simulated dry matter production in the R2 canopy significantly more than in both isometric canopies.

Table 3.6 Relative changes in total dry matter production at the end of the experiment/simulation in relation to standard condition (Table 3.3). Environmental scenarios were conducted with either CO_2 at 200 ppm or 600 ppm or PAR at 30% lower or 30% higher values than standard conditions, while all other conditions were kept constant. For a row canopy with two plants m^{-2} (R2) and one plant m^{-2} (R1) and an isometric canopy with two plants m^{-2} (I2) and one plant m^{-2} (I1). Different letters in a column indicate significant differences based an Anova and a Tukey multiple comparison (p=0.05). Values are means ± s.d. for the estimates. N= 9.

| Canopy | CO_2 | | PAR | |
	200ppm	600ppm	-30% PAR	+30 PAR
R2	-50.2 ± 1.2 [a]	19.7 ± 6.0 [a]	-24.9 ± 4.9 [a]	25.1 ± 8.0 [a]
R1	-62.2 ± 1.1 [c]	14.1 ± 1.9 [b]	-33.6 ± 3.0 [b]	19.9 ± 2.9 [ab]
I2	-47.2 ± 1.7 [b]	13.3 ± 3.4 [b]	-26.1 ± 2.3 [a]	16.6 ± 2.3 [b]
I1	-64.2 ± 1.8 [d]	13.6 ± 2.9 [b]	-37.3 ± 3.2 [b]	16.5 ± 3.3 [b]

Discussion

The aim of the study was to analyze the impact of canopy architecture and environmental conditions on dry matter production using a FSPM which explicitly accounts for plant morphology and photosynthesis. Analyzing the simulation results of a FSPM is quite complex as such a model combines detailed sub models of organ functioning to model the plant growth and development at higher scales (Vos *et al.*, 2007). Before testing the behavior of such a complex model it is first of all necessary to analyze the individual model parts as has been done for the sub model for light environment in discontinuous canopies (Wiechers *et al.*, 2011b) and the sub model for dry matter partitioning on the fruits growth (Wiechers *et al.*, 2011a). Here, we evaluated the performance of the photosynthesis sub model and the overall dry matter production of the FSPM und different combinations of spatial discontinuous canopy architectures and for scenarios with different ambient CO_2 and light conditions. The description of the functional and structural elements of the FSPM used in this study were similar to models developed spatially continuous cereal crops (Evers *et al.*, 2010; Xu *et al.*, 2011).

Evaluation of the photosynthesis sub model

The parameters of the stomatal conductance model estimated from experimental data (Figure 3.1) were comparable to those obtained in other studies under greenhouse conditions (Liu et al., 2008). Evaluating these with an independent data set (Table 3.2) resulted in a prediction quality of g_s similar to those reported for rose (Kim and Lieth, 2003). The results of our parameterization for V_{cmax25}, J_{max25} (Figure 3.2) and R_{d25} (Table 3.3) were in

the same range as was reported for leaves of different ages under greenhouse conditions (Pettersen et al., 2010). Furthermore, the time courses for V_{cmax25} and J_{max25} (Figure 3.2) were comparable to the function used by Kim and Lieth (2003) to describe the maximum rates of photosynthesis over time. The estimate for the transition phase between the Rubisco-limited and the RuBP-regeneration limited phases, C_{itr}, was in the lower range of the commonly used C_{itr} values (Table 3.3). This commonly *a priori* fixed transitions of the model was derived from measurements of *Phaesolus vulgaris* (von Caemmerer and Farquhar, 1981). Recently, it was stressed that an *a priori* fixation of the cut-off value has an influence on the prediction of the model and that a common threshold is not generally applicable across all plants (Dubois *et al.*, 2007). The introducion of refinements to the original model, like g_i and the simultaneous estimation of parameters without an *a priori* cut-off (Dubois *et al.*, 2007), resulted in biologically meaningful parameters. Validating the derived parameters in the combined model of stomatal conductance and photosynthesis with an independent data set gave a bias that was almost equal to the parameterization of the model of (Kim and Lieth, 2003), whereas the RMSD was higher but still the range of natural variations (Table 3.2). In conclusion, the sub model of photosynthesis was appropriate to simulate the leaf level photosynthesis of cucumber under greenhouse conditions.

Influence of different canopy architectures on dry matter production

Light availability is a major determinant of yield (Hovi-Pekkanen and Tahvonen, 2008). Lower plant density and a more continuous canopy architecture increases light transmittance through the canopy (Drouet and Kiniry, 2008; Wiechers *et al.*, 2011b). The simulations allowed us to accurately estimate the production of dry matter over time (Figure 3.3). The order of final dry matter production of the four canopies corresponded to the light transmittances determined for the canopies in our previous work. This also showed that not only decreasing plant density but also the change of arrangement plants from a row to an isometric arrangement can increase the transmittance (Wiechers *et al.*, 2011b). For three out of four canopy structures the simulation was able to estimate the final dry matter with non-significant differences to the measurements (Figure 3.3). The canopy architectures with the maximal und minimal final plant dry weights were exactly estimated, but the range between the extremes was 20 g per plant higher in the simulations than in the measurements. With an average final plant dry weight of close to 400 g this meant a rather

small deviation of 5%, or, expressed in number of fruits, an estimation error of less than a single harvestable fruit.

The significant underestimation of final total dry matter in the I2 canopy might have been caused by an underestimation of: (a) the ratio between vegetative and generative parts, (b) the leaf area and (c) the *niPAR*. I2 was the only canopy architecture which showed a smaller amount of dry matter in the vegetative part compared the measurement (Table 3.4). The underestimation was even distinct for the estimation of leaf area per plant (Figure 3.4). The course of the leaf area over time in the sparse canopies revealed that an underestimation at an early stage could be compensated at a later stage. Although a smaller leaf area should have increased the penetration of light into the canopy, the comparison to the experimentally derived light extinction revealed the opposite for the I2 canopy (Table 3.5). Due to the close relation between the incident light and the production of assimilates, the underestimation of *niPAR* over the second half of the simulation period enhanced the divergence between simulation and measurements. This combination might explain the significant underestimation in the I2 canopy.

Evaluating the results, we must keep in mind that the adaptations for the different canopy architectures just accounted for the plant to plant distances and the SLA. L-Cucumber was capable of leaf phototropism to dynamically avoid shading (Kahlen *et al.*, 2007), but additional morphological adaptations were not incorporated. These adaptations can evoke from changes in the red to far-red ratio and the blue radiation, which can be related as a sensing of neighbors in a canopy (Ballare and Scopel, 1997). The corresponding phenotypic responses can alter e.g. the internode growth (Kahlen and Stützel, 2011), leaf curling (Trouwborst et al., 2010) or leaf elevation angle (Ballare and Scopel, 1997). Furthermore, the phylloclimate, defined as the physical environment sensed by an organ, also includes other features like temperature, humidity and wind speed (Chelle, 2005). Effects resulting from these interactions between canopy and the environment were not accounted for by the model. Nevertheless, the model approach was capable by only adapting a few parameters to simulation different spatial arrangements, in contrast to solely process based model which are not designed to account spatial changes of the environment (Vos *et al.*, 2007).

Influences of CO$_2$ and light on dry matter production

The general effect of CO$_2$ enrichment is characterized by a gradual decrease of the relative production gains, whereas a lowering of CO$_2$ results in more and more pronounced decreases in the relative production gains (Nederhoff, 1994). These changes are similar to the saturating response of the photosynthesis to CO$_2$ (von Caemmerer, 2000). The model was able to depict these effects of CO$_2$ concentrations, as the final dry weight loss in case of a reduction to 200 ppm ambient CO$_2$ was higher than the gain when increasing CO2 concentrations to 600 ppm (Table 3.6). The reduction of the final total dry weight due to the lowering of the ambient CO$_2$ concentration to 200 ppm was higher than reported for other experiments with cucumber (Kläring et al., 2007). The reduction of the ambient CO$_2$ concentration in their experimental set up was lower, explaining the lower reduction of total dry weight compared to our simulations. Other studies reported increases in the final total dry weight by up to 25% (Nederhoff, 1994) or fruit fresh yields by20% (Sánchez-Guerrero et al., 2005), due to an CO$_2$ CO$_2$ enrichment of up to 700 ppm. This was approximately 10% higher as the results of our simulations of 600 ppm.

It is known that the increase of produced biomass induced by higher CO$_2$ levels decreases at high plant densities (Wayne *et al.*, 1999; Retuerto *et al.*, 1996). To our knowledge, there were no studies for the differences of the effects of the spatial arrangement on dry matter production. Reduction of CO$_2$ results in a flattened light response characteristic in the initial phase, and a reduction of the maximum rate of photosynthesis (von Caemmerer, 2000). This change of the photosynthesis responses curve might explain the higher sensitivity of the sparse canopies (Table 3.6). The stronger increase predicted for the R2 canopy by the increase of CO$_2$ or PAR could be related to the non-linear response of photosynthesis model of both factors. Under experimental conditions, the productivity of the R2 canopy was the lowest of all four architectures (Figure 3.3). Hence, the actual rates of photosynthesis under these conditions were likely to be more in the non saturating phase as in all other canopies. This allowed the increases of CO$_2$ and PAR to be more distinctive in the R2 than in the other canopies (Table 3.6). In consequence, by trend the changes of dry matter production caused by CO2 were estimated in a realistic way, and differences between the canopies could be related to the properties of the photosynthesis response curves.

The response of photosynthesis to changes of the incident light can be characterized by the maximum light use efficiency at low values and an approaching of a saturation at high light levels (von Caemmerer, 2000). Hao and Papadopoulos (1999) reported for the response to an increase of light that increases of 20 - 26% in final dry weight were obtained with 10 - 30% supplementary light. This matches to our estimates (Table 3.6). In our simulation under experimental conditions the final total dry matter production of the sparse canopies was 20% higher than in the dense canopies (Figure 3.3). This implied that the photosynthesis model in these canopies was producing assimilates at a higher level. Under the same environmental conditions this could be mainly achieved by a larger assimilating leaf area or higher availability of radiation. The leaf area between the sparse and dense canopies varied by 10% but this can not fully explain the differences (Figure 3.4). Thus, they might be also related to the reaction of the model of photosynthesis. The A_c phase of the photosynthesis model is insensitive to irradiance, whereas the asymptotes defined by A_j is sensitive to changes in the incident radiation (von Caemmerer, 2000). In the sparse canopies which allow the light to penetrate deeper into the canopy (Wiechers et $al.$, 2011b) it was more likely that the photosynthesis of a large proportion of individual leaves was in the A_j phase. This would explain why these canopies were more sensitive to a reduction of the ambient light compared to the dense canopies (Table 3.6). The highest increments of the final dry matter in the R2 canopy due to an increase of PAR might be related to the low transmission of light in this canopy. Thus, under experimental conditions, leaves in the A_j were not so likely to be close to the saturation phase, which would explain the higher sensitivity to additional PAR.

The simulation of environmental scenarios with the FSPM gives the opportunity to relate variations of productivity to properties of the underlying photosynthetic processes. Establishing this link made it worth to use the combination of a 3D surface based model and a Farquhar model of photosynthesis. As the model is not limited to the influences and spatial resolutions applied in the present study it is an appropriate approach offering multiple possible applications: Introducing higher spatial resolution of environmental factors like light, CO_2, temperature and relative humidity enabled to simulate the impact of the precise spatial and temporal control of these factor on productivity. To be able to analyze different control strategies is essential for the optimization of the production process under the aim of reduced resource usage. Furthermore, changes of the environmental factor due to alternations greenhouse design could be studied.

Conclusion

The evaluation of the combined model of photosynthesis and stomatal conductance revealed that the sub model results were capable to be used for a simulation of greenhouse cucumber grow. Implementing the combined model into L-Cucumber allowed us to simulate the dry matter production in different canopy architectures. Simulating different environmental scenarios for the canopies resulted in different productivities which could be related to the properties of the photosynthesis model. To improve the modeling of plants, introducing more detailed representations of phylloclimate models allows accounting for the interaction of the plant with its surrounding and the corresponding physiological processes of the plant which offers a wide field of application option to the FSPM approach.

Chapter 4

Dry matter partitioning models for the simulation of individual fruit growth in greenhouse cucumber canopies

Dirk Wiechers, Katrin Kahlen, Hartmut Stützel

Abstract

Background and Aims: Growth imbalances between individual fruits are common in indeterminate plants like cucumber (*Cucumis sativus*). In this species, these imbalances can be related to differences in two growth characteristics, fruit growth duration until reaching a given size and fruit abortion. Both are distribution related and environmental factors as well as canopy architecture play a key role for their differentiation. Furthermore, events that a fruit reaches its harvestable size before or simultaneously with a fruit set prior could be observed. Functional-structural plant models (FSPM) allow for interactions between environmental factors, canopy architecture and physiological processes. Here, we tested hypotheses which account for these interactions by introducing dominance and abortion thresholds for the partitioning of assimilates between growing fruits.

Methods: Using the L-System formalism, a FSPM was developed which combined a model for architectural development, a biochemical model of photosynthesis and a model for assimilate partitioning, which includes a fruit growth model based on a size related potential growth rate (R_P). Starting from a distribution proportional to R_P, the model was extended by including abortion and dominance. Abortion was source strength and dominance was sink strength related. Both thresholds were varied to test their influence on fruit growth characteristics. Simulations were conducted for a dense row and a sparse isometric canopy.

Key Results: The simple partitioning models failed to simulate individual fruit growth realistically. The introduction of abortion and dominance thresholds gave the best results. Simulations of fruit growth durations and abortion rates were in line with measurements, and events that a fruit was harvestable earlier than an older fruit were reproduced.

Conclusion: Dominance and abortion events need to be considered when simulating typical fruit growth traits. By integrating environmental factors, the FSPM can be a valuable tool to analyse and improve existing knowledge about the dynamics of assimilates partitioning.

Introduction

Fruits of greenhouse cucumber (*Cucumis sativus*) show unbalanced individual growth rates and abortion of individual fruits (Schapendonk and Brouwer, 1984). These characteristics result in a non-uniform growth of fruits and can also be observed in other reproductive and indeterminately growing crops like bell pepper and tomato (Heuvelink, 1996; Wubs *et al.*, 2009b). Reasons for differences in growth have been related to environmental factors (Marcelis, 1993b; Pettersen *et al.*, 2010; Wubs *et al.*, 2009a) and canopy architecture (Kahlen, 2007). Variations in dry matter partitioning have been explained by competitive growth under limitation of assimilates (Marcelis *et al.*, 1998) and by hormone regulation (Bangerth *et al.*, 2000), or discussed as a combination of both (Marcelis *et al.*, 2004).

To analyse how growth processes on individual positions of a plant interact with the environment, models are required which integrate key physiological processes on the organ level under consideration of plant morphology on the canopy scale (Fourcaud *et al.*, 2008). These interactions are explicitly provided for by functional-structural plant models (FSPM) which simulate plant systems dynamically allowing for feedback between plant physiology and morphology (Vos *et al.*, 2010). Furthermore, representing the morphological plasticity of the developing plant using surface based three-dimensional (3D) models allows incorporating detailed environmental models and the responses of biological processes with the plant (Chelle, 2005; Kahlen & Stützel, 2011). In FSPMs, the partitioning of assimilates between individual organs is commonly modelled with a source:sink approach (Vos *et al.*, 2010). When assimilates are limited a proportional partitioning concept is frequently assumed. Based on an experimentally determined potential growth rate of an organ, R_P, the proportional sink limitation is calculated by dividing R_P through the sum of all R_P indicating the total demand of the plant (Heuvelink, 1996; Marcelis, 1994; Schapendonk and Brouwer, 1984; Wubs *et al.*, 2009b). This concept does not model the individual fruit growth independently as the limitation affects all fruits proportionally. It also fails to account for fruit abortion and does not provide for young fruits to accumulate dry matter faster than fruits on lower nodes, which would allow a fruit to reach harvest before a prior initiated fruit. In literature related observations, describing that a fruit starting to grow at high growth rates sooner than a prior fruit can be found (Marcelis, 1994). R_P is commonly described as a peak function of organ age with the maximum growth rate shortly after anthesis (Heuvelink, 1996; Marcelis, 1994; Wubs *et al.*, 2009b). For cucumber and tomato it has been shown that

fruits do not irreversibly lose their sink strength in periods of limited or discontinued growth (de Koning, 1989; Marcelis, 1993a). The commonly used peak function decreases rapidly after the peak. If the growth of a fruit is limited over a longer period around the peak the low potential growth rates are limiting growth at a later stage. This can lead to the loss of the capability to regain higher growth rates and may even inhibit the fruit to reach a harvestable size. The potential fruit growth rate between anthesis and harvest can be defined by a power function of organ size (Kuwar, 2007) which allows the fruit to grow at appropriate rates under ample assimilate supply at any stage of fruit development.

Fruit abortion is the most evident change in fruit growth characteristics and has frequently been implemented into plant growth models. Commonly, a sensitive phase of up to ten days after anthesis in which fruits can be aborted has been observed (Marcelis, 1992; Schapendonk and Brouwer, 1984). Fruit abortion was modelled using a defined source:sink ratio as a threshold in pepper (Wubs *et al.*, 2009b) or as a linear decrease with increasing source:sink ratio in cucumber (Marcelis, 1994). The latter approach was combined with a priority function implemented as the K_m constant in a Michaelis-Menten kinetic to describe dominance among cucumber fruits. The priority function increased with total potential growth rate and decreased with the age of the individual fruit (Marcelis, 1994). This model did not account for events in which a fruit reached harvest earlier than an older fruit and longer periods of reduced growth could result in a growth cessation of individual fruits even at later stages. Abortion rate was related to the source:sink ratio but not explicitly with the priority function. A different approach to account for fruit competition was based on the concept that if a proportional growth rate of a certain fruit is lower than R_P, this fruit can reduce the growth rate of the subsequent fruit by 90% to its own favour (Schapendonk and Brouwer, 1984). This assumption was supported by observations which showed that a fruit did not dominate all subsequent fruits. In combination with an age dependent R_P this resulted in a discontinued fruit growth which was interpreted as fruit abortion. Due to the fact that after a prolonged period of limited growth fruits could not regain high growth rates the model was not able to reproduce the case that a younger fruit reached harvest size prior to an earlier initiated fruit.

In the present study we implemented fruit partitioning models into the existing FSPM L-Cucumber (Kahlen *et al*., 2008) aiming to reproduce fruits growth characteristics which are

not accounted for in existing models, like a fruit being harvestable before or simultaneously with an earlier formed fruit, and a fruit to regain high growth rates. The partitioning models were designed to test the hypotheses whether fruit growth of cucumber follows (1) a proportional distribution of assimilates, (2) a proportional distribution of assimilates with an abortion threshold or (3) a dominant distribution of assimilates among fruits with abortion. The hypotheses were tested by comparing model results with measured fruit growth of plants cultivated under canopy conditions. As the FSPM approach allowed integrating feedbacks between plant morphogenesis and developmental physiology, the individual fruit growth was evaluated under different canopy architectures.

Materials and Methods

Experimental set-up

Cucumber (*Cucumis sativus,* cv. Aramon, Rijk Zwaan, De Lier, The Netherlands) plants were cultivated in greenhouses at the Institute of Biological Production Systems in Hannover, Germany (52.5°N, 9.7°E). In the five-leaves stage on 30 July 2007 they were transplanted on rockwool slaps and trained to a high wire system. Fruits were reduced to one fruit per rank and all tendrils and side shoots were pruned to allow an undisturbed monopodial growth. Plants were decapitated when they reached the high wire at 220 cm. Canopies were either arranged as a row canopy with two plants m^{-2} (R2) or as an isometric canopy one plant m^{-2} (I1). In the R2 canopy the distance in the rows was 0.27 m and the distance between the rows was 1.86 m, whereas the I1 canopy had a distance of 1.08 m in the row canopy and 0.93 m between the rows. The experiment was set up as a randomized complete block design, with three replications. The R2 canopy was composed of three rows with six plants each, and the I1 canopy of four rows with either three or four plants per row. Measurements were taken on two plants in the middle rows with at least one border plant to each side. In the experiment, the average day temperature was 25.1 ± 2.1 °C inside the greenhouse.

Measurements

Non destructive measurements were taken every two to three days from 13 August 2007 till 14 September 2007. Each time, the length of each fruit and the width of each leaf on the

plant were measured. Measurements of fruit length and leaf width started at approximately 5cm organ length. Under canopy conditions the measurement of small fruits and leaves is very error-prone and there was a high risk to injure or even break an organ. Individual organ dry weights and growth rates were calculated based on allometric relations (Kahlen and Stützel, 2007). Fruits were harvested twice a week when they had reached approximately 30 cm length. For model evaluation the proportion of aborted fruits, the duration of fruit growth and the frequency of fruits reaching harvest size before or simultaneously with an earlier initiated fruit were recorded and analyzed.

Model

The FSPM was based on the dynamic structural plant growth model L-Cucumber (Kahlen *et al.*, 2008) implemented as cpfg code into L-Studio (Mech*, 2004). The simulations were run for 65 d. The model parameterisation accounted for the conditions of the experiments by reproducing the daily light conditions, the arrangement of the plants in the canopy and the differences in specific leaf area (SLA) in the canopies. As in experiments, each fruit bearing rank had one fruit which had a length of 5 cm at initiation. Plants grew monopodially without side shoots. The decapitation at the high wire was accounted for in the simulations by limiting the number of leaves to 23. This corresponded to the average number of 22.9 ± 0.5 leaves in the experiment. Furthermore, L-Cucumber was expanded by a more detailed description of leaf level photosynthesis and a fruit growth model part, which allowed a specific description of the growth of individual fruits.

The model calculated light interception of individual leaf surfaces with the Caribu software (Chelle *et al.*, 1998) which interfaced with the L-Studio software. The virtual crop was reconstructed of 16 to 19 plants dependent on the canopy structure, to avoid border effects on the three evaluated plants in the middle of canopy. A standard overcast sky with 36 light sources was used to simulate the light environment. The reflectance of the plastic film covering the greenhouse floor was 80%. Optical properties of the leaf laminae were parameterized using a given protocol (Daughtry *et al.*, 1989). The protocol specifies a series of reflectance and transmittance measurements using an integrating sphere and a spectrometer which allowed calculating leaf optical properties. The upper surface reflectance and transmittances of the leaf laminae were 6%, whereas the lower reflectance

and transmittance was 11% and 8%, respectively. The calculation of light interception was performed on a daily basis to account for the dynamic growth of the plants. An evaluation of the combination of the 3D surface based plant model and the light distribution model showed the appropriateness of the approach for heterogeneous canopy structures (Wiechers *et al.*, 2011).

Assimilate production and partitioning

The rate of photosynthesis of the individual organs was calculated using a Farquhar *et al.* (1980) photosynthesis model coupled with a model of stomatal conductance (Kim and Lieth, 2003). A two-phase description of the model was implemented and parameterized with the maximum rate of carboxylation (105.6 μmol CO_2 m^{-2} s^{-1}) and the potential rate of electron transport (201.1 μmol CO_2 m^{-2} s^{-1}). The conversion to plant dry matter was performed using a factor of 0.68 (Warren Wilson, 1992). Maintenance respiration was not separately accounted for as a minor fraction with approximately reduction 2% of the daily dry matter (Marcelis, 1994). This model part provided a good estimate of the total measured dry matter. Temperature (25 °C), humidity (70% RH), CO_2 concentration (400 ppm) and wind speed (0.5 m s^{-1}) were assumed to be homogenous for the simulation, and leaf temperature was assumed to be equal to air temperature. Based on the simulated daily incident light intensities the rate of photosynthesis was calculated on an hourly basis to account for the non linear response of photosynthesis to light. The daily course of light intensity was mapped by a normalized sine function and scaled with the daily incident light intensity. The resulting hourly rates of photosynthesis were accumulated to a daily rate of dry matter gain which was transferred to a common assimilate pool. Excess dry matter was added to the pool when the daily demands of all organs were fulfilled.

Assimilates were partitioned to the organs on a daily basis. In the vegetative phase 15% of the produced assimilates were partitioned to the root (Kharkina *et al.*, 1999), from the beginning of fruit growth this fraction was reduced to 3% which corresponded to final root dry weights fractions cited in literature between 5% (Kharkina *et al.*, 1999) and 2.6% (Marcelis, 1992). A time dependent partitioning of assimilates between vegetative shoot parts and fruits was implemented. In accordance with production practice the fruits of the first six ranks were pruned to enhance the vegetative growth. In this initial vegetative phase

90% of the assimilates available for the shoot were allocated to the vegetative part, $A_V(t)$ (g dw d^{-1}). The residual 10% were allocated to the assimilate pool and became available in the following simulation steps. The allocation of only 90 % of the shoot assimilates to the vegetative part was implemented because the vegetative dry matter production in the initial phase would have been overestimated if all shoot assimilated would have been allocated directly to the vegetative parts. The physiological background might be that cucumber plants tend to retain assimilates in the late vegetative phase in order to enable rapid fruit growth. With the beginning of fruit set the share partitioned to the fruits, $A_F(t)$ (g dw d^{-1}), increased linearly until it reached 80% of the dry matter available for shoot growth, with the remaining 20% going to the vegetative parts. From then on these proportions were kept constant. Keeping this ratio fixed agreed with other studies which also showed that dry matter allocation to the fruits was insensitive to short term changes in irradiance (Marcelis, 1993c). Similar patterns of dry matter distribution among above-ground plant parts for cucumber were described in literature with a plateau between 40% and 90% allocated to the vegetative part in fruiting cucumber plants (Marcelis, 1992). The reduction of vegetative growth due to topping resulted in a relatively high ratio within the reported range.

For the growth of the individual fruits a set of partitioning concepts with increasing complexity of rules was implemented into L-Cucumber. The resulting fruit growth was evaluated with regard to the measured growth. The basic concept implemented into the model was the proportional partitioning of assimilates among all growing fruits. From experiments the potential growth rate of a fruit i, on a given day t after initialisation (5 cm), $R_{P,i}(t)$ (g dw d^{-1}), was derived from the fruit length of the previous day, $L_{F,i}(t\text{-}1)$ (cm), (Kuwar, 2007).

$$R_{P,i}(t) = 0.0025 L_{F,i}(t\text{-}1)^{2.6587} \tag{1}$$

$R_{P,i}(t)$ determined the maximum demand of each fruit. Fruit length was calculated from fruit dry weight using an allometric power function. All $R_{P,i}(t)$ of one simulation step were added up to calculate the total maximum demand of all fruits of day t, $D_{TMF}(t)$ (g dw d^{-1}):

$$D_{TMF}(t) = \Sigma\, R_{P,i}(t) \tag{2}$$

For the first hypothesis the proportional growth rate, $R_{\text{Prop},i}(t)$ (g dw d^{-1}), was calculated using the ratio of $R_{\text{P},i}(t)$ to $D_{\text{TMF}}(t)$ and the assimilates available for the fruit growth, $A_{\text{F}}(t)$. In consequence, this distribution is scaled by the source strength:

$$R_{\text{Prop},i}(t) = (R_{\text{P},i}(t) \, / \, D_{\text{TMF}}(t)) \, A_{\text{F}}(t) \quad\quad\quad\quad (3)$$

For the second hypothesis the concept of proportional assimilate distribution was extended by the instance of fruit abortion. Abortion was determined by the ratio $r_{\text{AD}}(t)$ of the assimilates available for the fruit growth, $A_{\text{F}}(t)$, and the total maximum demand of all fruits, $D_{\text{TMF}}(t)$:

$$r_{\text{AD}}(t) = A_{\text{F}}(t) \, / \, D_{\text{TMF}}(t) \quad\quad\quad\quad (4)$$

If $r_{\text{AD}}(t)$ was below a predefined abortion threshold, A_{T}, at a single day all fruits within six to ten days after anthesis stopped growth and were aborted. The fruit was sensitive to this event. The A_{T} threshold, which was therefore source strength dependent, was set to 10%, 20%, 40%, 60% or 80%.

For the third hypothesis the concept of abortion was retained and a dominant growth characteristic of earlier initiated fruits was implemented in addition. Instead of distributing assimilates proportionally among all growing fruits irrespective of the degree of limitation, the sink strength of a fruit could be increased in favour of a growth decrease of the following fruit. This dominance was only applied if $r_{\text{AD}}(t)$ did not reach a threshold, D_{T} :

$$R_{\text{D},i}(t) = \min \, (R_{\text{Prop},i}(t) + 0.5 \, R_{\text{Prop},i+1}(t); \, R_{\text{P},i}(t)) \quad\quad\quad\quad (5)$$

The dominant growth rate, $R_{\text{D},i}(t)$ (g dw d^{-1}), of the dominant fruit was increased to $R_{\text{P},i}(t)$ at maximum. The increase was established by up to 50% of the proportional growth rate of the dominated fruit. For the dominated fruit a reduction of the proportional growth rate by the corresponding amount was implemented. Similar to the abortion event, dominance was directly applied on the day at which D_{T} was not reached. Furthermore, it was assumed that D_{T} had to be higher than the A_{T} threshold. For a dominated fruit no further alternations of growth rates were allowed in this day. For the simulations, the A_{T} thresholds were either set to 10%, 20% or 30% and were varied with D_{T} threshold of either 40%, 60%, 80% or 100%. Dependent on the implemented fruit growth model the actual growth rate was either proportional, proportional with abortion or dominant with abortion.

Simulation scenarios

In the mock up of the simulation scene an initial orientation was given to each plant. In the experiments, the first leaf of the plants was manually oriented at transplanting to the south with an unavoidable variability. In the simulation this variability was accounted for by three scenarios with alternated starting orientation of the evaluated plants. For each scenario the south orientation of the first leaf for each plant was varied between ±15° by rotating the plant around the vertical axis.

Data Analysis

For the measurements and simulations fruit growth duration of all fruits which had reached their harvest size and the abortion rate was calculated. Fruit growth duration was defined as the number of days from 5 cm to 30 cm fruit length. Averages and standard deviations of the individual ranks were calculated based on the six measured plants or the nine simulated plants. The abortion rate was defined as the number of aborted fruits divided by the number of evaluated plants in the measurements and simulations, respectively. Average growth durations and average abortion rates were calculated as means over ranks 7 to 19. For both traits absolute differences between the averages of measured and simulated plants were calculated. To assess the prediction quality for both traits simultaneously, the absolute differences were divided by the measured values to obtain relative values. The relative values were added up to obtain the total relative deviation. In addition, the occurrence of events when a later initiated fruit had reached 30 cm length on the same day or earlier as a prior initiated fruit was quantified. Comparison of measured and simulated final vegetative and generative dry matter was performed using a t-test with a p-value of 0.05 using Sigmaplot (Systat Software Inc., Chicago, IL, USA).

Results

Proportional assimilate distribution

In the R2 canopy, the measured growth duration of individual fruits increased in an irregular pattern from less than ten days for the fruits on the low ranks up to a maximum of nearly 20 days for the fruits on the high ranks (Fig. 4.1A). The increase was accompanied by a rise in

the variability of growth duration as indicated by higher standard deviations. For the fruits on ranks 7 - 19 the average growth duration was 14.5 days and the average fruit abortion was 20.5% (Table 4.1). The simulation of fruit growth duration using a proportional distribution of assimilates resulted in a good estimate for fruit ranks 7 to 12 followed by an increasing overestimation due to a steady increase of growth durations up to 30 days (Fig. 4.1A). None of the fruits on the ranks higher than 17 reached harvest size until the end of the simulation run and no fruit was aborted. On average, the simulated growth duration of fruits that reached harvest size during simulation was approximately 4 days longer than the measured (Table 4.1).
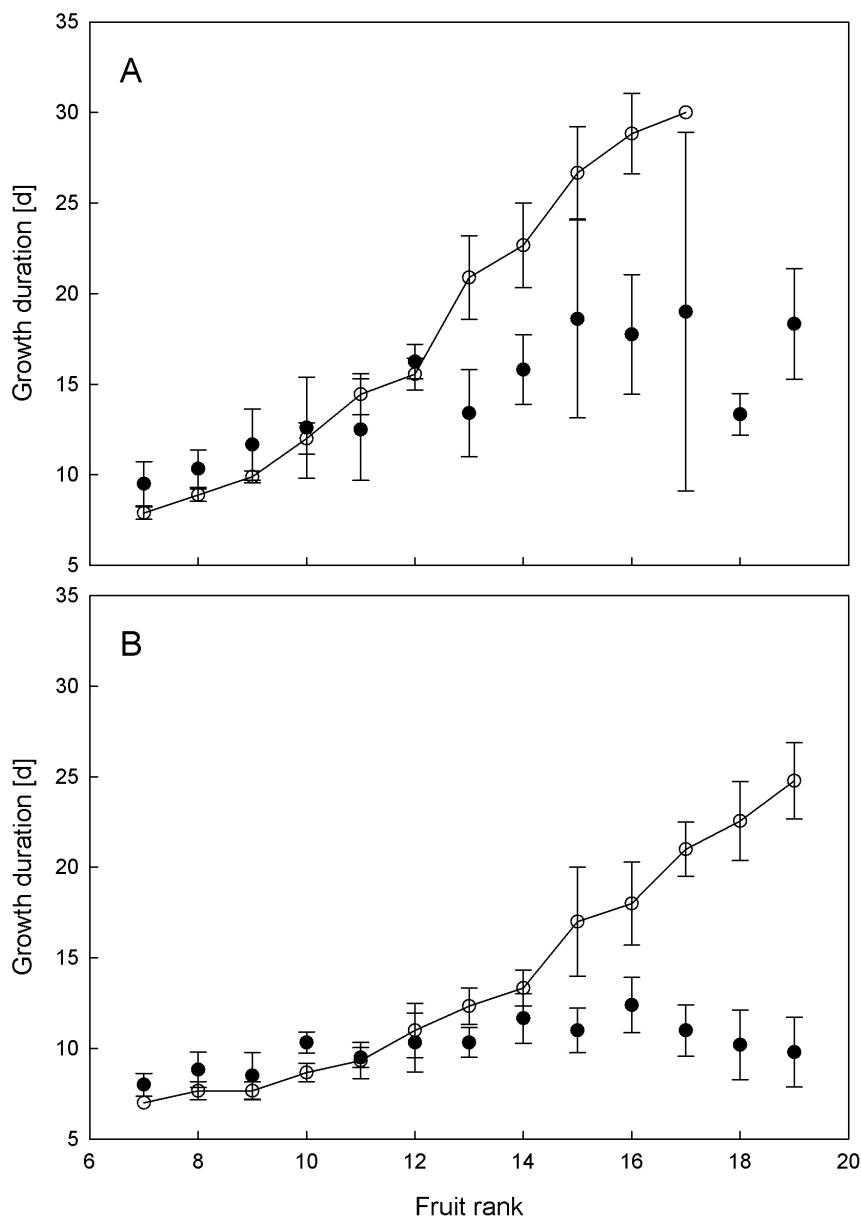
Fig. 4.1 Individual fruit growth durations for a row canopy with two plants m^{-2} (A) and isometric canopy with one plant m^{-2} (B). Closed circles represent measurements (n=6) and open circles indicate simulations assuming proportional distribution of assimilates (Eq. 3) (n=9). Error bars indicate standard deviations.

Table 4.1 Average fruit growth duration, average fruit abortion rate and total relative deviation for measured and simulated fruit ranks 7-19 per plant in a row canopy with two plants m^{-2} (R2) and an isometric canopy with one plant m^{-2}(I1). Simulations distributed assimilate to the fruits proportional, proportional with abortion or dominant with abortion. Measurements *n*=6 and simulations *n*=9.

	R2							I1						
	Measurement	Simulation						Measurement	Simulation					
		Proportional	Proportional with abortion						Proportional	Proportional with abortion				
Dominance [%]		0	0	0	0	0	0		0	0	0	0	0	0
Abortion [%]		0	10	20	40	60	80		0	10	20	40	60	80
Growth duration [days]	14.5 ± 3.2	18.0 ± 8.2	18.4 ± 8.8	13.3 ± 3.8	9.0 ± 1.1	8.0 ± 0	7.7 ± 0.5	10.1 ± 1.2	13.9 ± 6.2	13.6 ± 6.0	12.5 ± 4.7	8.7 ± 1.2	7.8 ± 0.4	7.8 ± 0.4
Fruit abortion [%]	20.5 ± 22.7	0 ± 0	0 ± 0	36.8 ± 48.7	53.0 ± 46.1	59.8 ± 46.6	61.5 ± 50.6	7.7 ± 14.6	0 ± 0	0 ± 0	10.3 ± 19.5	43.6 ± 45.9	51.3 ± 46.4*	51.3 ± 37.6*
Rel. dev. growth duration		0.24	0.27	0.09	0.38	0.45	0.47		0.37	0.35	0.24	0.14	0.23	0.23
Rel. dev. fruit abortion		1.00	1.00	0.79	1.58	1.92	2.00		1.00	1.00	0.33	4.66	5.66	5.66
Total relative deviation		1.24	1.27	0.88	1.96	2.37	2.47		1.37	1.35	0.57	4.80	5.89	5.89

Table 4.2 Average fruit growth duration, average fruit abortion rate and total relative deviation for simulations of ranks 7-19 in a row canopy with two plants m^{-2} (R2) including dominance and abortion which fulfilled all three criteria. For comparison with measured data see Table 4.1. *n*=9.

	R2							I1						
	Measurement	Simulation						Measurement	Simulation					
Dominance [%]		40	40	60	60	80	100		40	60	80	100	100	100
Abortion [%]		20	30	20	30	30	30		30	30	30	10	20	30
Growth duration [days]	14.5 ± 3.2	18.0 ± 7.2	13.4 ± 4.4	18.0 ± 7.3	12.9 ± 3.6	15.0 ± 5.2	14.3 ± 5.2	10.1 ± 1.2	11.8 ± 3.9	10.9 ± 3.3	11.0 ± 3.3	9.4 ± 2.5	9.4 ± 2.5	9.4 ± 2.5
Fruit abortion [%]	20.5 ± 22.7	6.8 ± 24.7	29.9 ± 37.2	7.7 ± 16.6	32.5 ± 40.2	15.4 ± 20.1	11.1 ± 22.7	7.7 ± 14.6	10.3 ± 21.0	10.3 ± 21.0	8.5 ± 22.8	0 ± 0	0 ± 0	0 ± 0
Rel. dev. growth duration		0.24	0.08	0.24	0.11	0.03	0.01		0.17	0.08	0.09	0.07	0.07	0.07
Rel. dev. fruit abortion		0.67	0.46	0.63	0.58	0.25	0.46		0.33	0.33	0.11	1.00	1.00	1.00
Total relative deviation		0.90	0.54	0.86	0.69	0.28	0.47		0.50	0.41	0.20	1.07	1.07	1.07

In contrast to the R2 canopy, the measured growth durations in the I1 canopy did not show a considerable increase with increasing fruit rank and the standard deviations differed only marginally (Fig. 4.1B). The average growth duration for fruits 7 - 19 was 10.1 days (Table 4.1). The average fruit abortion was 7.7% and on average one event of a younger fruit being harvestable before or simultaneously to a earlier formed fruit occurred per plant. The simulated growth duration increased continuously (Fig. 4.1B). This resulted again in a longer average growth duration of approximately 4 days compared to the measurement (Table 4.1). All fruits on ranks 7 to 19 reached harvest length before the end of the simulation.

Proportional assimilate distribution with abortion

Increasing the value for the fruit abortion threshold increased the rate of aborted fruits (Table 4.1). Changes of the abortion threshold up to 40% clearly affected fruit abortion rates. For thresholds exceeding 40% fruit abortion rates increased only marginally.

Under all tested proportional partitioning simulations with abortion, the parameter set with the A_T = 20% threshold corresponded best to the measurements. The parameter set had the lowest total relative deviations with 1.2 days difference in growth duration and 16.3% mismatch for the abortion rate (Table 4.1). Simulated growth durations and abortion rates could be separated into two phases (Fig. 4.2A): The first phase comprised ranks 7 to 14 in which no fruits were aborted. In this phase the simulated rank growth duration increased constantly with fruit rank from a slight underestimation to a minor overestimation. The second phase from rank 15 to 19 was dominated by the abortion of 95% of all initiated fruits (Fig. 4.2B). The only harvested fruits in this phase were grown at rank 19 and had an appropriate duration.

In the I1 canopy, the increase of the fruit abortion threshold resulted in a decrease of the average growth duration comparable to R2, while at the same time fruit abortion increased with a 10% lower rate compared to R2 (Table 4.1). Similar to the R2 canopy the simulation with A_T = 20% for the I1 canopy had the smallest total relative deviation from the measured results, with a difference of 2.4 days in average growth duration and 2.6% offset in the average fruit abortion rate.

Fig. 4.2 Individual fruit growth duration (A) and fruit abortion rate (B) for a row canopy with two plants m^{-2}. Closed circles and bars represent measurements (n=6) and open circles and bars indicate simulations assuming proportional distribution of assimilates with an abortion threshold A_T of 20% (Eq. 4) (n=9). Error bars indicate standard deviations.

Dominant assimilate distribution with abortion

Based on the results of the simulations with abortion, we used abortion thresholds A_T of 10%, 20% and 30% together with dominance levels of 40%, 60%, 80% and 100% for the further analyses and obtained a linear relation between average abortion rate and average growth duration (Fig. 4.3). The 12 combinations of dominance and abortion thresholds were simulated for both canopies. The 6 closest fits are shown in Table 4.2. Based on the total relative deviation the parameter set with D_T = 80% and A_T = 30% threshold resulted in the best correspondence between measurements and simulations for both canopies (Table 4.2).
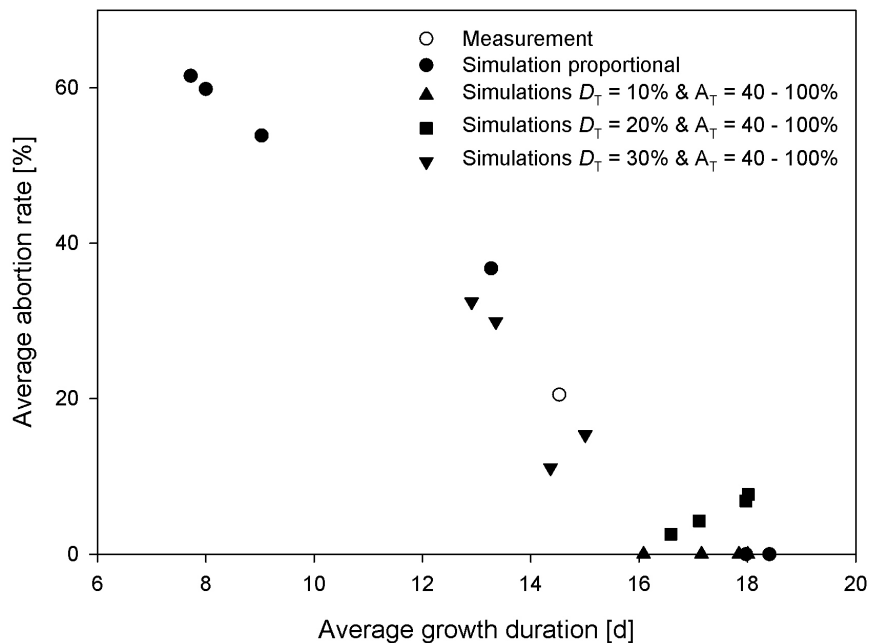
Fig. 4.3 Average fruit abortion rate in relation to average growth duration for rank 7 - 19 for a row canopy with two plants m^{-2}(R2). Measured (open circle), simulated proportional distribution with different abortion thresholds (closed circle), simulated 10% abortion with a set of dominant thresholds (closed triangle up), simulated 20% abortion with a set of dominant thresholds (close square) and simulated 30% abortion with a set of dominant thresholds (closed triangle down). Sets of domination consisted of 40%, 60%, 80% and 100% thresholds. Each symbol represents n=9 for simulations and n=6 for measurements.

In the R2 canopy the simulation underestimated fruit abortion by 5.1% over all ranks and the average growth duration was overestimated by 0.5 days. The simulated growth durations up to rank 15 followed the increasing trend of the measurements with small deviations and the simulated variations ranged in the same order of magnitudes as the measurements (Fig. 4.4A). The simulations overestimated growth duration on fruit ranks 16 – 19 and the standard deviations were slightly higher than in the measurements, too. Measurements and simulations of growth durations differed at the highest ranks, 17 – 19, with a maximum difference of 7.4 days for fruits on rank 18. The simulation results failed to predict the low level of fruit abortion likelihood up to rank 13 (Fig. 4.4B). For ranks 14 - 19 the higher rates of fruit abortion were overall represented by the simulation with a minor underestimation, although for the individual ranks the abortion likelihood differed between measurements and simulations.
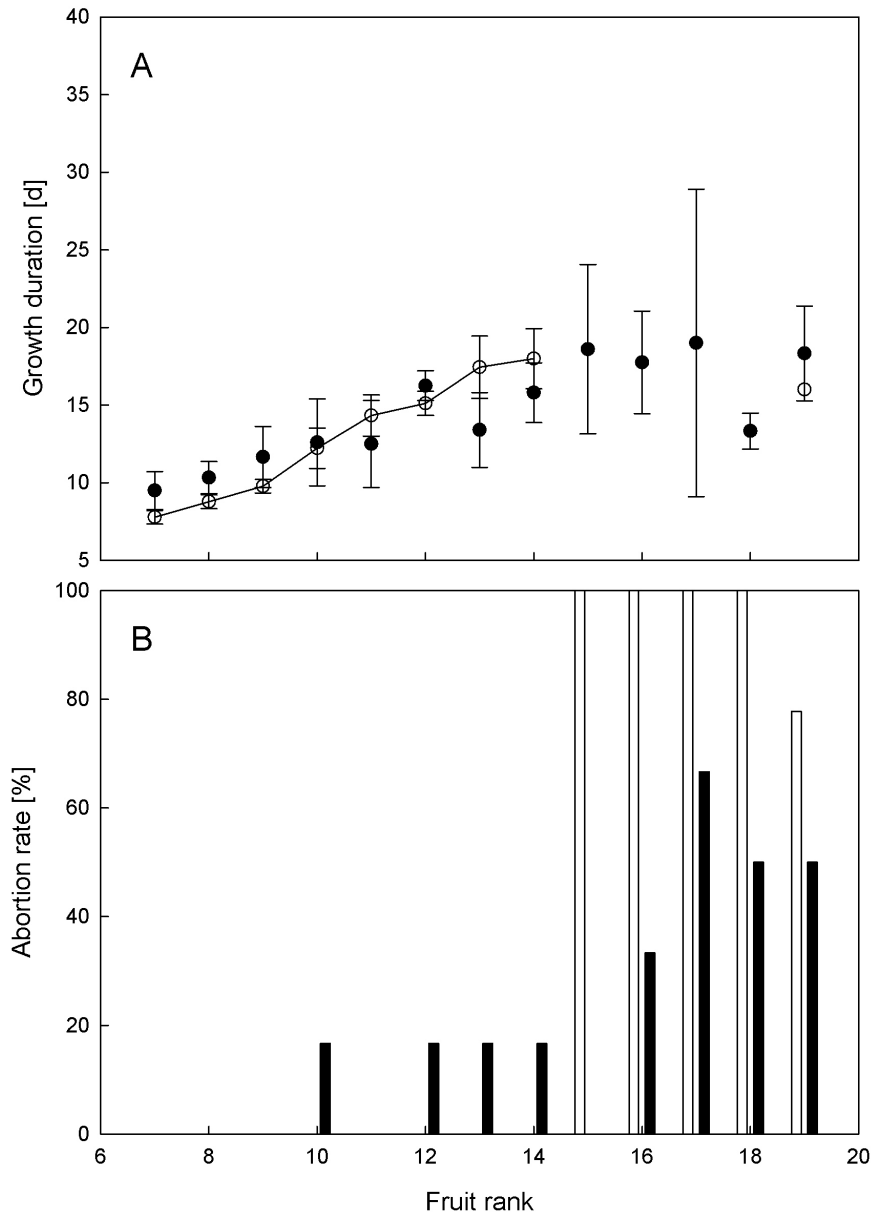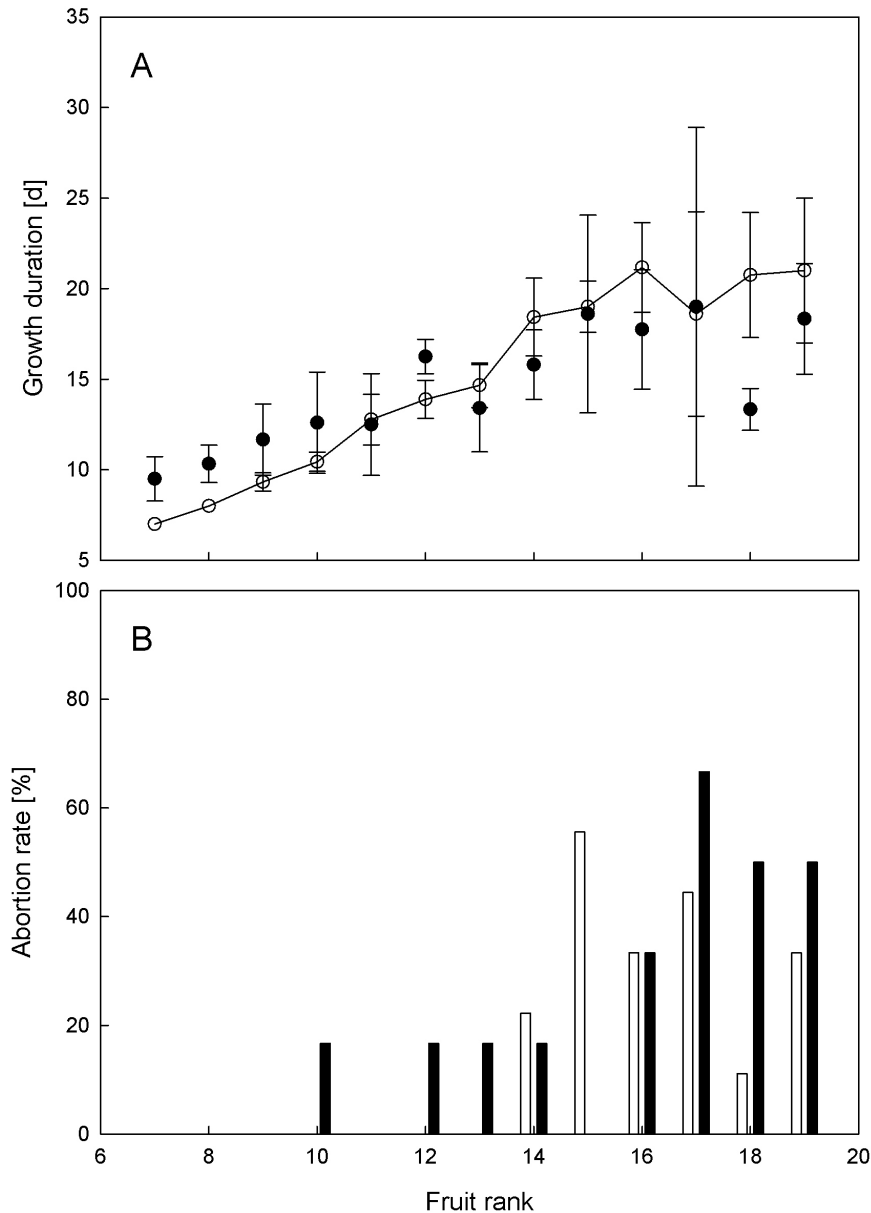
Fig. 4.4 Individual fruit growth duration (A) and fruit abortion rate (B) for a row canopy with two plants m^{-2}. Closed circles and bars represent measurements (n=6) and open circles and bars indicate simulations (n=9) assuming a dominance threshold D_T of 80% and with an abortion threshold A_T of 30% (Eq. 5). Error bars indicate standard deviations.

In the I1 canopy, the average growth durations and fruit abortions were overestimated by 0.9 days and 0.8%, respectively. Simulated growth duration up to rank 15 increased more continuously than the measurements while growth duration differed in most cases by less than one day (Fig. 4.5A). In ranks 16 to 19, the observed reduction of fruit growth duration was not followed by the simulation leading to overestimations of up to 5 days. The variance in simulated growth duration between fruits was small up to rank 15, followed by either pronounced variance, or absence of variation as only one fruit was not aborted. The occurrence of fruit abortion was not correctly estimated as the highest likelihoods were on

rank 9 and 10, whereas the ranks of the second abortion cluster was accounted for correctly but the intensity was overestimated (Fig. 4.5B).
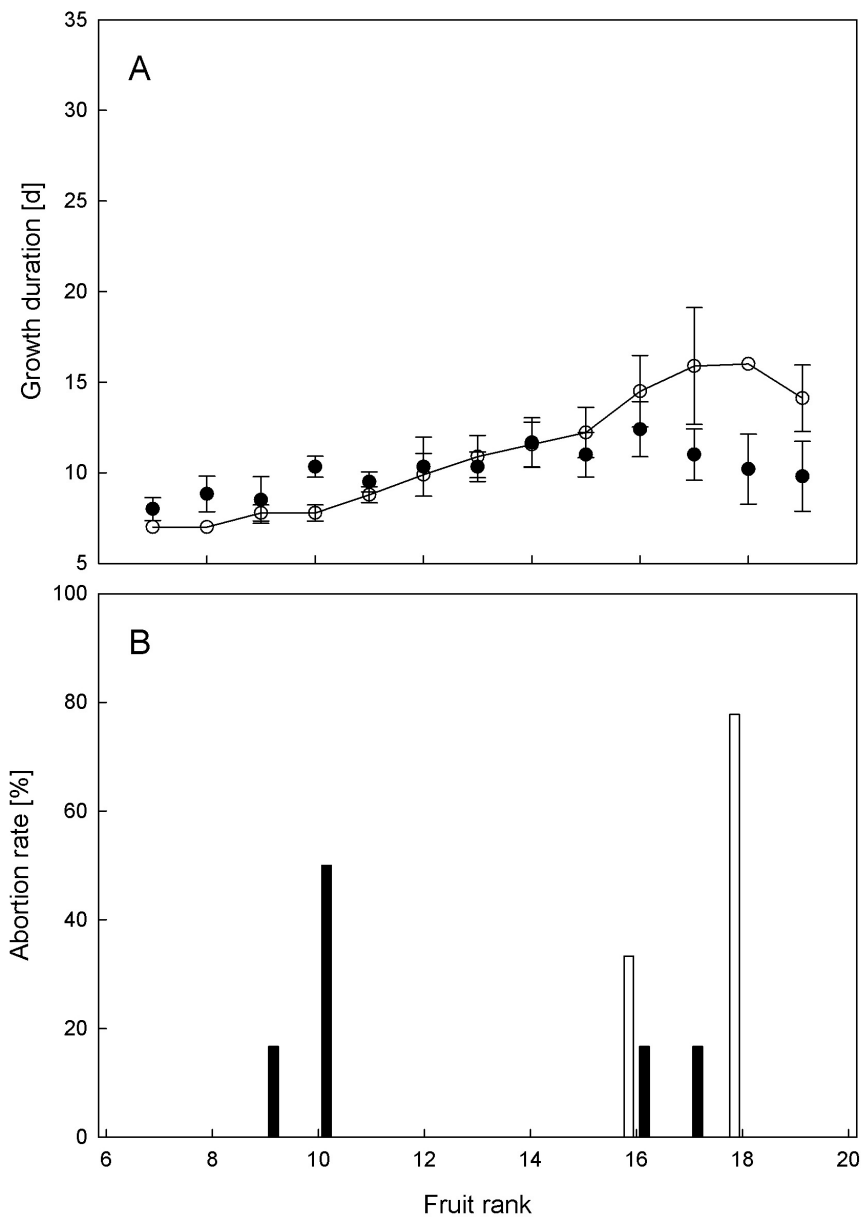
Fig. 4.5 Individual fruit growth duration (A) and fruit abortion rate (B) for an isometric canopy with one plants m^{-2}. Closed circles and bars represent measurements (n=6) and open circles and bars indicate simulations (n=9) assuming a dominance threshold D_T of 80% and with an abortion threshold A_T of 30% (Eq. 5). Error bars indicate standard deviations.

Events of a fruit reaching harvest size before a prior fruit

An example for an event when a fruit was harvestable before or at the same day as a prior formed fruit, as observed in the experiments, is shown in Figure 4.6. All fruits prior to fruit rank 16 reached harvest size with increasing growth durations. Fruits 17 and 18 were aborted allowing fruits on rank 19 and 20 to grow at higher rates. This resulted in a

simultaneous harvest of fruits on rank 16 and 20. The latter fruit took approximately one week less to reach harvest size. The two canopy structures differed in the number of harvestable fruits before a prior fruit reached harvest in the examined fruit ranks. On an average two such events per plant occurred in R2, whereas only one event could be observed in the I1 canopy (Table 4.3). In the R2 canopy the fruit ranks were not clustered, whereas in the I1 canopy these events were observed predominantly on ranks 10 to 13 (data not shown).
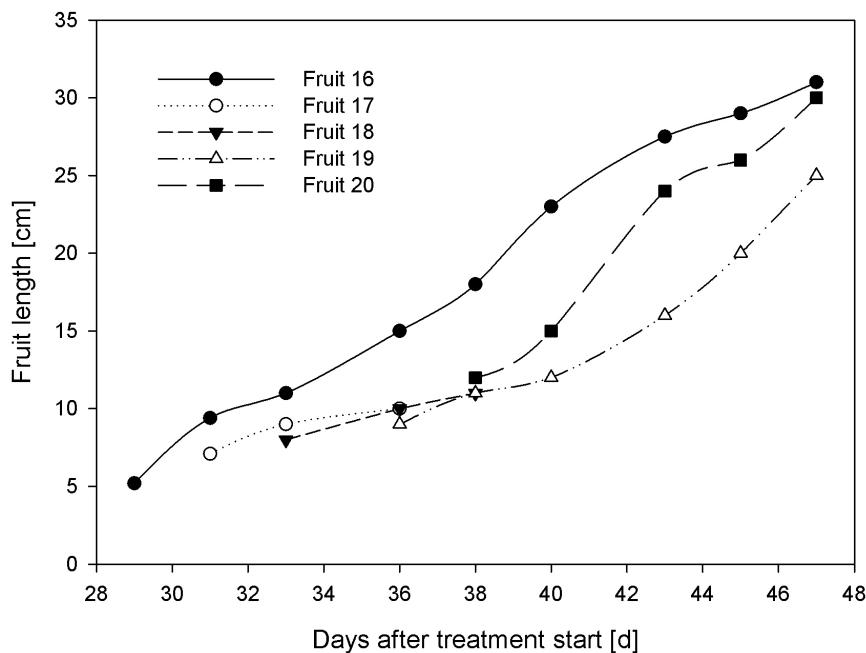
Fig. 4.6 Exemplary measured individual fruit length growth including events that a fruit reached harvest before or simultaneously to a prior fruit in a row canopy with two plants m^{-2} (R2).

Table 4.3 Average number of events that a fruit was harvestable before or simultaneously to a prior fruit for measured and simulated fruit ranks 7-19 in a row canopy with two plants m^{-2} (R2) and an isometric canopy with one plant m^{-2} (I1). Simulations distributed assimilate to the fruits with different dominance and abortion thresholds. Measurements n=6 and simulations n=9.

	R2			I1		
	Measurement	Simulation		Measurement	Simulation	
Dominance [%]		60	80		40	60	80
Abortion [%]		30	30		30	30	30
Harvestable before a prior fruit	2	0.1 ± 0.3	0.1 ± 0.3	1	0.2 ± 0.4	0.6 ± 0.5	0.4 ± 0.5

In the simulations with proportional and proportional with abortion distributions, the abortion threshold did not affect the successive growth of the individual fruits. For both canopies this resulted in an absence of events that a fruit reached harvest size before or

simultaneously to an earlier formed fruit for all parameterisations. The simulations including dominance effects generally underestimated the number of cases in which a fruit was harvestable before or at the same day as a prior fruit. In the simulations of the R2 canopy only the A_T = 30% D_T = 80% and the A_T = 20% D_T = 60% scenarios reproduced harvests of fruits before or simultaneously to an earlier fruit, but not more than one event per plant (Table 4.3). In the I1 canopy, the underestimation of the simulations was less obvious. In the simulations the growth duration for the later initiated fruit was reduced by up to 6 days compared to the prior initiated fruit. In general the harvest fruits before or simultaneous to prior formed fruits concentrated at the highest fruit ranks (data not shown).

Time course of overall dry weight

For the simulation with the smallest total relative deviations of average growth duration and abortion rate, the accumulated dry weight for the vegetative and fruit parts followed closely the data derived from the experiments (Fig. 4.7A, B).

There was a temporal coincidence of plant topping and the approximation of the plateau for the vegetative plant parts around 30 days after transplanting for both, simulations and measurements. The vegetative dry weight at the end of measurements was 85.0 ± 5.8 g plant^{-1} for the R2 and 99.2 ± 4.6 g plant^{-1} for the I1 canopy. Based on the t-test the simulation significantly overestimated the vegetative dry weight for the R2 canopy with 95.8 ± 2.4, whereas for the I1 canopy the simulation did not differ significantly from measured data. For the fruits dry weights of 261.3 ± 39.5 and 334.8 ± 59.9 g plant^{-1} were measured in the R2 and I1 canopies, respectively. The simulation of the fruit dry weights did not differ significantly from measured data.

Discussion

In this study L-Cucumber, a dynamic 3D plant model was used to test hypotheses on dry matter partitioning between individual fruits. Fruit growth duration and abortion were the characteristics used to evaluate the model. Fixed proportions were allocated to roots and vegetative parts as modelling the vegetative growth driven by potential growth driven would have resulted in an increased interaction between vegetative and generative distribution. Furthermore, there are difficulties in determining the potential growth rate of the vegetative

parts (Marcelis 1994).The first hypothesis of proportional assimilate distribution among fruits has been widely used in models of plant growth (e.g. Marcelis, 1993d).
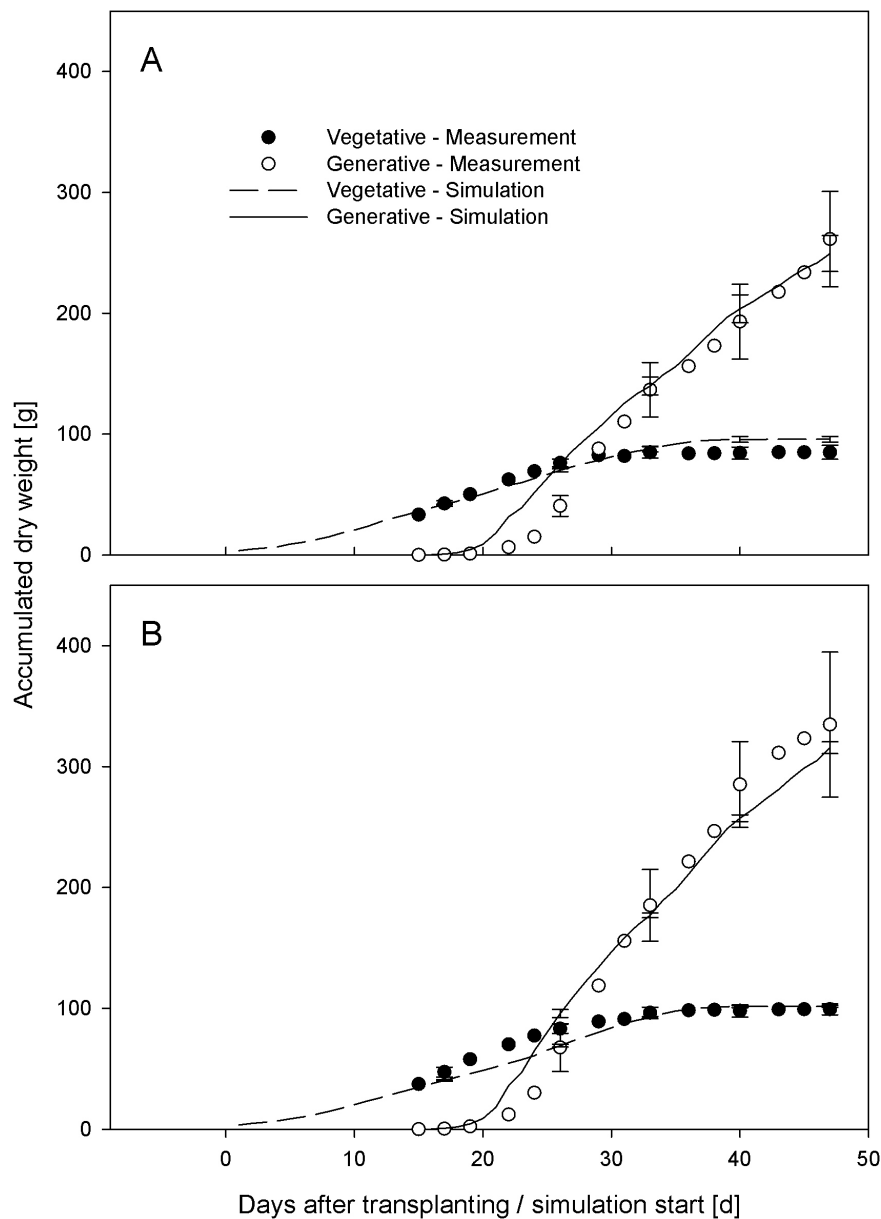
Fig. 4.7 Measured and simulated time course of accumulated vegetative dry weight and accumulated fruit dry weight in a row canopy with two plants m^{-2} (A) and an isometric canopy with one plant m^{-2} (B). Simulations are calculated with proportional 80% D_T threshold with 30% A_T threshold. Measurement (n=6) and simulation (n=9). Error bars represent standard deviations

For both canopies examined, the model overestimated growth durations (Fig. 4.1 A, B), which might be attributed to the fact that no fruits were aborted (Table 4.1). No fruit was simulated to reach harvest size earlier than an older fruit which was due to R_P increasing with increasing fruit size. For the growth of individual fruits in greenhouse cucumber, this was obviously an oversimplification in both canopies.

The second hypothesis assumed fruit abortion to occur when source strength was insufficient. The model approach allowed changing fruit abortion rates by varying the A_T threshold (Table 4.1). The abortion threshold also had an impact on growth duration, as a reduction of the number of growing fruits reduces competition among the remaining fruits, resulting in shorter growth durations. A value of 20% for A_T of resulted in quite good adjustment of the average growth rate (Fig. 4.2). This threshold led, however, to considerable overestimation of the average abortion rate. Recent other approaches to model fruit growth pattern also do not allow for an alternation of the sink strength besides the general age dependency (Mathieu *et al.*, 2008; Wubs *et al.*, 2009b). As a consequence, these approaches mainly control patterns of fruit initialisation and do not account for alternations in the growth phase of individual fruits. In this study, the assimilate distribution based on the second hypothesis allowed for abortion, whereby growth duration was regulated, but the approach failed to reproduce events in which fruits were harvestable before or simultaneously with an prior fruit.

The third hypothesis was tested by choosing a range of A_T thresholds between 10% and 30%, derived from the proportional distribution with abortion, in combination with D_T thresholds between 40% and 100% (Fig. 4.3). The priority function of Marcelis (1994) and our definition of dominance differ: The priority function uses a progressive definition which depends on total potential growth rate whereas the dominance concept is based on a fixed threshold. Furthermore, the dominance threshold was considered constant over time whereas in the priority function the intensity changes over time. In the approach of Marcelis (1994) the priority of an individual fruit influences the allocation of assimilates of all other fruits whereas our approach restricts the influence to the following fruit. The main differences to the dominance approach of Schapendonk & Brouwer (1984) are the discrete consideration of abortion, the analysis of the dominance threshold and a reduced relocation of assimilates under dominance conditions. For existing models including dominance effects among fruits, abortion was one of the weakest features, as a fruit could stop growth at any size (Schapendonk and Brouwer, 1984) or the regulation was assumed to be linearly related to the source : sink ratio (Marcelis, 1994). The model presented here overcame this limitation and the lack of depicting events of fruit harvest before an earlier formed fruit by relating R_P to the organ size. This resulted in non linear changes of the abortion rate for different abortion thresholds (Table 4.1) which were in line with measurements of fruit set under

different ratios of actual to potential growth rate in tomato (Bertin, 1995; their Fig. 11). Comparing the proportional distribution with an A_T = 20% and the corresponding simulations with these A_T and D_T thresholds revealed that the D_T threshold only slightly altered average growth duration but highly affected average abortion rate (Table 4.1, 4.2). This indicated that the model accounts for interactions between dominance and abortion.

The relevance of the A_T = 30% D_T = 80% parameter set was indicated by the smallest total relative deviations for both canopies (Table 4.2), followed in both cases by all sets with D_T = 30% and the occurrence of fruit reaching harvest size before a prior fruit in the simulations with D_T = 30% for both architectures (Table 4.3). The absolute value of events that a fruit was harvestable before or at the same day as an earlier formed fruit was underestimated with all parameter sets. But the occurrence of these events has to be regarded different from the other traits. The occurrence of fruit abortion was controlled by the predefined A_T threshold, which also influenced growth duration. In contrast, there was no explicit influence on the occurrence of fruits reaching harvest size before or simultaneously to an prior fruit by external model parameters. Furthermore, there was also no influence of any intrinsic stochasticity of the model.

By explicitly considering dominance, a good estimate for the growth of the individual fruit was obtained for the fruits up to rank 17 in the R2 and rank 16 in the I1 canopy (Fig. 4.4A, 4.5A). For the uppermost ranks the number of harvested fruits was strongly reduced due the increase of fruit abortion in both architectures (Fig. 4.4B, 4.5B). Averaging of the highly scattering individual growth durations for the low number of remaining fruits per rank increased the uncertainty of the estimates. This might explain the higher differences between measurements and simulations. The less clustered fruit abortion in the simulated R2 canopy gave a more realistic representation than the emphasized abortion event in the I1 canopy. Our intention was to start with the simplest approach and to extend the model stepwise until the measured growth characteristics were accounted for by the model. The first extension of the proportional model, which was able to reproduce all measured growth characteristics, was the combination of an abortion threshold and a dominance threshold affecting the next fruit. Nevertheless, the simulations of both canopies resulted in very precise estimations of accumulated vegetative and fruit dry weights (Fig. 4.7). This indicated that also the timing of fruit and vegetative growth based on the implemented

parameterization was reproduced accurately. In this study the variability in the simulation was introduced by alternating the initial orientation of the simulated plants. Other possibilities to introduce the variability, e.g. variations of source and sink strength have been used to assess model sensitivity (e.g. Wubs *et al.*, 2009b). A third concept used in similar studies is the application of stochastic elements in functional parts of plant models to reproduce the natural variability in plant development (e.g. Barczi *et al.*, 2008). The different concepts have all been capable of simulating variability of resulting growing traits.

In conclusion, the evaluation of the partitioning models showed that the first two hypotheses of proportional growth with and without abortion did not sufficiently describe the dynamics of fruit growth in cucumber. The model based on the third hypothesis using a source strength threshold concept for fruit abortion and accounting for dominance by alternating sink strengths was able to reproduce individual fruit growth of a dense row canopy and a sparse isometric canopy. It allowed for feedback between fruit abortion and the growth of the remaining fruits by adapting of growth duration and accounting for events that a fruit was harvestable before an earlier fruit as well as for influences on the vegetative part. In general, the FSPM was capable of simulating variations in plant architecture on the growth of individual fruits. The high level of detail and the flexibility for the integration of environmental influences indicated the value of the presented model as tool for analysing and improving knowledge about dynamics in assimilates partitioning between vegetative and fruit parts as well as individual among fruits.

General discussion

The previous chapters presented essential aspects of functional sub models of L-Cucumber, a FSPM for the simulation of plant growth and development in greenhouse cucumbers. Here, the relationships between canopy architecture, light interception, photosynthesis and dry matter partitioning are summarized and discussed in context of the findings of the individual previous chapters and possibilities and limitations of the modeling approach are explored.

Starting with a given plant morphology and spatial arrangement of the canopy influencing forthcoming physiological and morphological processes in a dynamically evolving system, allows to stepwise consider the major elements of plant development. Thus, a present canopy architecture is assumed as the basis for the phylloclimate of the existing individual organs, whereas, an individual organ is considered as the target unit of physiological processes. Light is one of the major environmental factors, which have to be considered for a quantitative understanding of yield formation. In greenhouses, light distribution is spatially heterogeneous, caused by the greenhouse construction (Chenu et al., 2008) and by changes of crop plasticity over time (Drouet and Kiniry, 2008).

To gain a more detailed understanding of light distribution in canopies with different spatially discontinuous architectures, a 3D light distribution model in combination with a static 3D reconstruction of the canopy was used in chapter 2 to evaluate the simulations of light distributions on the individual leaf level.

The different shading treatments revealed that the largest share of the standard deviation for a single leaf in a complex light environment could be explained by differences in the 3D plant structure. Plant structure was influenced by plant spacing and morphology as well as the light environment. There was no overall systematic error in the *Caribu* model and the RMSD was considerably smaller than in other studies (Higashide, 2009). Compared to volume based approaches (e.g. Röhrig *et al.*, 1999; Sinoquet *et al.*, 2001; Thornley *et al.*, 1992) the results highlighted that the 3D model approach precisely simulated incident PAR for the individual leaf under a broad range of canopy architectures and shading treatments. Therefore, the combination of a 3D surface based model and 3D light model provides an

accurate estimation for the light component of the phylloclimate, as a major factor of leaf photosynthesis, creating the basis for a precise simulation of plant growth and development.

The production of assimilates is essential for plant growth. Photosynthesis as the source of assimilates in photoautotrophic plants is highly dependent on the availability of light as one of the resource of energy for the assimilation processes (von Caemmerer, 2000). This dependency links the production of dry matter directly to the interrelations of plant morphology, canopy structure and the availability of light as evaluated in chapter 2. To quantify these relations in terms of dry matter production the extended L-Cucumber was used in chapter 3, to simulate plant growth and development in different canopy architectures and environmental conditions.

The Farquhar model (Farquhar *et al.*, 1980) offers the possibility to consider multiple environmental dependencies. Thereby, the model allows accounting for all major environmental factors present in a greenhouse production system. The implemented parameterization for the model of photosynthesis based on the coupled approach of Kim and Lieth (2003) was appropriate to simulate the leaf level photosynthesis of cucumber under greenhouse conditions.

Implementing the model of photosynthesis in L-Cucumber, the extended model approach was capable, by only adapting the spacing of plants and the SLA, to simulate dry matter production realistically in different spatial arrangements. This favored the FSPM approach realized in L-Cucumber in contrast to existing process based model (e.g. Heuvelink, 1999; Marcelis, 1994), which were not designed to account spatial changes of the environment (Vos *et al.*, 2007).

The current implementation of L-Cucumber established the link between biochemical processes of photosynthesis and differences of plant and canopy structures, as a distinct feature of functional-structural plant models, which is not realized by other model approaches. This allowed the extended L-Cucumber to relate variations of productivity in environmental scenarios to properties of the underlying photosynthetic processes. Accounting the high level of interrelation involved in the development of plants also provides the basis for a distinguished simulation of the growth and development of single organs.

The partitioning of dry matter between individual organs was examined for the growth of fruits in chapter 4. Fruits were chosen, as they are the economic target and in the long term the main part of produced dry matter in greenhouse cucumber is partitioned to the generative part (Marcelis, 1992). Furthermore, the yield formation is alternated by the non-uniform growth of individual fruits (Marcelis, 1992; Schapendonk and Brouwer, 1984) and influenced by plant arrangement and plant density (Kahlen, 2007). In existing models for the prediction of fruit growth, the simulation of fruit abortion was one the weakest features (Schapendonk and Brouwer, 1984). Additionally, due to a common definition of the potential growth rate as a peak function of organ age, fruits could stop growth even close before harvest (Marcelis, 1992; Schapendonk and Brouwer, 1984).

To be able to describe the occurring dynamics of fruit growth in cucumbers a potential growth rate related to the organ size was combined with a source strength related threshold concept to simulate fruit abortion and dominance threshold alternating the individual sink strengths. In contrast to existing models (Heuvelink, 1996; Marcelis, 1992; Schapendonk and Brouwer, 1984; Wubs *et al.*, 2009b), the implementation of the partitioning model into L-Cucumber permitted to relate variations in plant architecture on the growth of individual fruits and even accounted for events that a fruit was harvestable before an earlier fruit.

The dry matter production in the current implementation of L-Cucumber focuses on the precise production of assimilates based on the simulation of light interception, photosynthesis and partitioning of assimilates among the vegetative and generative plant organs with special consideration of the growth of individual fruits. Effects of respiration, originating from growth processes are simplified and effects of maintenance respiration were not accounted for by the model. For cucumber fruits it was shown that temperature has no effect grow respiration, but affects the maintenance respiration (Marcelis and Baan Hofman-Eijer, 1995). As no spatial gradient for the temperature was assumed and the average day temperature in the experiments was only fluctuating with ±2°C, possible deviations should be rather small. For a more precise estimation of fruit growth under different temperatures these temperature effects should be accounted.

The simulation of the canopies including the calculation of incident light at the organ level requires considerable computational power and simulation time. Strategies to reduce the computational demands by downsizing the number of plants assembling the canopy could

provoke border effects. Under greenhouse conditions also excising repetitive concepts (Chelle *et al.*, 1998), which define continuous canopies, are not appropriate. However, a reduction of the resolution of the light model or the level of detail representing the individual organs (Wiechers, 2004) is possible to a certain degree, but this procedure generally contradicts the approach of a high spatial resolution. Optimized algorithms and the proceeding development of computational power is expected to help to reducing these limitations. This would allow improving the model with a detailed incorporation of the greenhouse structure and by mapping the diversity of the anisotropic light distribution due to clouds.

Future research needs

The current implementation of L-Cucumber contains a distribution system for assimilates which is based on a common assimilate pool. The growing knowledge about the distribution of assimilates in plants from e.g. isotope carbon studies (Minchin and Thorpe, 2003) provides the basis for more mechanistic models transport-resistance models (Minchin and Lacointe, 2005). With L-Peach, a FSPM for a tree was developed which used a concept of resistances for the transport of carbohydrates (Allen *et al.*, 2005). Besides the consideration of the transport of assimilates also the distribution of water, nutrients and hormones can be essential to answer specific research questions. Especially for the simulation of hormonal interactions efficient and robust mathematical solutions are necessary (Hemmerling *et al.*, 2010; Prusinkiewicz *et al.*, 2009). An accurate simulation of the transport and distribution of nitrogen would also allow introducing a sensitivity of photosynthesis to nitrogen (Niinemets, 2007). With LEAFC3-N the necessary integration of the response of photosynthesis to nitrogen as an extension of the widely used model of photosynthesis by Farquhar and coworkers (1980) has been developed (Müller *et al.*, 2005). As the allocation of nitrogen is closely related to the photosynthetic capacity and leaf senescence (Niinemets, 2007), a direct consideration of nitrogen would also allow to introduce a more mechanistic description of the changes in photosynthesis over time. Furthermore, there are interactions between the availability of light and the acceleration of aging (Niinemets, 2007). Thus, the given possibilities to precisely estimate the radiation transfer could be used in combination with a detailed simulation of nitrogen turnover (Bertheloot *et al.*, 2008), allowing to analyze strategies towards improving the distribution of natural and assimilation light in order to either save energy or increase productivity. As the simulation of the light environment is not

limited to the total spectral range of PAR, the influences of special wave bands on the morphology and physiology of the plants could be modeled. In greenhouse production systems the possibilities of manipulating the spectral composition of light within the canopy is given, as light emitting diodes (LED) are a possible replacement for existing assimilation lighting. The use of LED offers the possibility to specifically adapt the spectral composition locally as they emit only very small wave bands and their small form factor allows placing them within the canopy (Trouwborst *et al.*, 2010). Experimental results from cucumbers grown with red and blue LEDs given between rows showed that morphological adaptations (Trouwborst *et al.*, 2010) can reduce positive effects of an adaptation of the spectral composition on photosynthesis (Hogewoning *et al.*, 2010). To evaluate the interactions of plant physiological and morphological responses, reliable models to estimate the light environment are a valuable tool for a quantitative understanding of the light propagation in canopies, since direct measurements of the radiation regime under canopy conditions are complicated and laborious (Chenu *et al.*, 2008). To optimize production processes analyzing and comparing different control strategies is essential. As L-Cucumber is not limited to the environmental influences and spatial resolutions of light, it could be an appropriate approach to simulate the impact of the precise spatial and temporal control of e.g. CO_2 or water vapor or the effect of pruning on productivity. Extended with an explicit mockup of the greenhouse the model could be used to analyze effects of the greenhouse design on the crop.

Concluding, the current implementation of L-Cucumber was capable of simulating variations in plant architecture on the growth of individual fruits. The results of the individual studies of this thesis highlighted key points for the influence of light interception and canopy architecture for a precise simulation of yield formation of greenhouse cucumber. The high level of detail and the flexibility for the integration of environmental influences indicated the value of the presented model as tool for analysing and improving knowledge about the dynamics in assimilates partitioning between vegetative and fruit parts as well as individual fruits.

References

Aikman DP. 1989. Potential Increase in Photosynthetic Efficiency from the Redistribution of Solar Radiation in a Crop. *Journal of Experimental Botany*, **40:** 855-864.

Allen MT, Prusinkiewicz P, DeJong TM. 2005. Using L-systems for modeling source-sink interactions, architecture and physiology of growing trees: the L-PEACH model. *New Phytologist*, **166:** 869-880.

Ball JT, Woodrow IE, Berry JA. 1987. A model predicting stomatal conductance and its contribution to the control of photosynthesis under different environmental conditions. *Progress in Photosynthesis Research,* **4**: 221-224.

Ballare CL, Scopel AL. 1997. Phytochrome Signalling in Plant Canopies: Testing Its Population-Level Implications with Photoreceptors Mutants of Arabidopsis. *Functional Ecology,* **11**: 441-450.

Bangerth F, Li CJ, Gruber J. 2000. Mutual interaction of auxin and cytokinins in regulating correlative dominance. *Plant Growth Regulation,* **32**: 205-217.

Barczi JF, Rey H, Caraglio Y, De Reffye P, Barthelemy D, Dong QX, Fourcaud T. 2008. AmapSim: A structural whole-plant simulator based on botanical knowledge and designed to host external functional models. *Annals of Botany,* **101**: 1125-1138.

Bernacchi CJ, Pimentel C, Long SP. 2003. In vivo temperature response functions of parameters required to model RuBP-limited photosynthesis. *Plant, Cell & Environment,* **26**: 1419-1430.

Bernacchi CJ, Portis AR, Nakano H, von Caemmerer S, Long SP. 2002. Temperature response of mesophyll conductance. Implications for the determination of Rubisco enzyme kinetics and for limitations to photosynthesis in vivo. *Plant Physiology,* **130**: 1992-1998.

Bertheloot J, Andrieu B, Fournier C, Martre P. 2008. A process-based model to simulate nitrogen distribution in wheat (Triticum aestivum) during grain-filling. *Functional Plant Biology,* **35**: 781-796.

Bertin N. 1995. Competition for assimilates and fruit position affect fruit set in indeterminate greenhouse tomato. *Annals of Botany,* **75**: 55-65.

Bird RE. 1984. A simple, solar spectral model for direct-normal and diffuse horizontal irradiance. *Solar Energy*, **32:** 461-471.

Chelle M, Andrieu B. 1998. The nested radiosity model for the distribution of light within plant canopies. *Ecological Modelling*, **111:** 75-91.

Chelle M, Andrieu B, Bouatouch K. 1998. Nested radiosity for plant canopies. *The Visual Computer*, **14:** 109-125.

Chelle M. 2005. Phylloclimate or the climate perceived by individual plant organs: What is it? How to model it? What for? *New Phytologist*, **166:** 781-790.

Chelle M. 2006. Could plant leaves be treated as Lambertian surfaces in dense crop canopies to estimate light absorption? *Ecological Modelling*, **198:** 219-228.

Chelle M, Evers JB, Combes D, Varlet-Grancher C, Vos J, Andrieu B. 2007. Simulation of the three-dimensional distribution of the red:far-red ratio within crop canopies. *New Phytologist*, **176:** 223-234.

Chenu K, Franck N, Dauzat J, Barczi JF, Rey H, Lecoeur J. 2005. Integrated responses of rosette organogenesis, morphogenesis and architecture to reduced incident light in *Arabidopsis thaliana* results in higher efficiency of light interception. *Functional Plant Biology*, **32:** 1123-1134.

Chenu K, Rey H, Dauzat J, Lydie G, Lecoeur J. 2008. Estimation of light interception in research environments: a joint approach using directional light sensors and 3D virtual plants applied to sunflower (*Helianthus annuus*) and *Arabidopsis thaliana* in natural and artificial conditions. *Functional Plant Biology*, **35:** 850-866.

Cieslak M, Lemieux C, Hanan J, Prusinkiewicz P. 2008. Quasi-Monte Carlo simulation of the light environment of plants. *Functional Plant Biology*, **35:** 837-849.

Cieslak M, Seleznyova AN, Hanan J. 2010. A functional-structural kiwifruit vine model integrating architecture, carbon dynamics and effects of the environment. *Annals of Botany,* **107:** 747-764.

Combes D, Chelle M, Sinoquet H, Varlet-Grancher C. 2008. Evaluation of a turbid medium model to simulate light interception by walnut trees (hybrid NG38 x RA and *Juglans regia*) and sorghum canopies (*Sorghum bicolor*) at three spatial scales. *Functional Plant Biology*, **35:** 823-836.

Damour G, Simonneau T, Cochard H, Urban L. 2010. An overview of models of stomatal conductance at the leaf level. *Plant, Cell & Environment,* **33**: 1419-1438.

Daughtry CST, Ranson KJ, Biehl LL. 1989. A New Technique to Measure the Spectral Properties of Conifer Needles. *Remote Sensing of Environment*, **27:** 81-91.

de Koning ANM. 1989. The effect of temperature on fruit growth and fruit load of tomato. *Acta Horticulturae,* **248**: 329-336.

De Pury DGG, Farquhar GD. 1997. Simple scaling of photosynthesis from leaves to canopies without the errors of big-leaf models. *Plant, Cell and Environment,* **20**: 537-557.

de Reffye P, Blaise F, Houllier F. 1998. Modelling plant growth and architecture: some recent advances and applications to agronomy and forestry. In: Marcelis LFM ed. *Proceedings of the second International Symposium on Models for Plant Growth, Environmental Control and Farm Management in Protected Cultivation. Acta Horticulturae*, **456:** 105-116

Disney M, Lewis P, Saich P. 2006. 3D modelling of forest canopy structure for remote sensing simulations in the optical and microwave domains. *Remote Sensing of Environment,* **100**: 114-132.

Drouet JL, Kiniry JR. 2008. Does spatial arrangement of 3D plants affect light transmission and extinction coefficient within maize crops? *Field Crops Research*, **107:** 62-69.

Dubois JJB, Fiscus EL, Booker FL, Flowers MD, Reid CD. 2007. Optimizing the statistical estimation of the parameters of the Farquhar-von Caemmerer-Berry model of photosynthesis. *New Phytologist,* **176**: 402-414.

Escobar-Gutiérrez AJ, Combes D, Rakocevic M, de Berranger C, Eprinchard-Ciesla A, Sinoquet H, Varlet-Grancher C. 2009. Functional relationships to estimate Morphogenetically Active Radiation (MAR) from PAR and solar broadband irradiance measurements: The case of a sorghum crop. *Agricultural and Forest Meteorology*, **149:** 1244-1253.

Evers JB, Vos J, Yin X, Romero P, van der Putten PEL, Struik PC. 2010. Simulation of wheat growth and development based on organ-level photosynthesis and assimilate allocation. *Journal of Experimental Botany,* **61**: 2203-2216.

Farquhar GD, von Caemmerer S, Berry JA. 1980. A biochemical model of photosynthetic CO_2 assimilation in leaves of C_3 species. *Planta,* **149**: 78-90.

Fourcaud T, Zhang X, Stokes A, Lambers H, Körner C. 2008. Plant Growth Modelling and Applications: The Increasing Importance of Plant Architecture in Growth Models. *Annals of Botany,* **101**: 1053-1063.

Hao X, Papadopoulos AP. 1999. Effects of supplemental lighting and cover materials on growth, photosynthesis, biomass partitioning, early yield and quality of greenhouse cucumber. *Scientia Horticulturae,* **80**: 1-18.

Hemmerling R, Smolenova K, Kurth W. 2010. A programming language tailored to the specification and solution of differential equations describing processes on networks. *Lecture Notes in Computer Science,* **6031:** 297-308.

Heuvelink E. 1996. Dry matter partitioning in tomato: validation of a dynamic simulation model. *Annals of Botany,* **77**: 71-80.

Heuvelink E. 1999. Evaluation of a dynamic simulation model for tomato crop growth and development. *Annals of Botany,* **83**: 413-422.

Higashide T. 2009. Light interception by tomato plants (*Solanum lycopersicum*) grown on a sloped field. *Agricultural and Forest Meteorology*, **149:** 756-762.

Hogewoning SW, Trouwborst G, Maljaars H, Poorter H, van Ieperen W, Harbinson J. 2010.
Blue light dose-responses of leaf photosynthesis, morphology, and chemical
composition of Cucumis sativus grown under different combinations of red and blue
light. *Journal of Experimental Botany,* **61**: 3107-3117.

Hovi-Pekkanen T, Tahvonen R. 2008. Effects of interlighting on yield and external fruit
quality in year-round cultivated cucumber. *Scientia Horticulturae*, **116:** 152-161.

Kahlen K. 2007. Towards functional-structural modelling of greenhouse cucumber In: J. Vos,
L.F.M. Marcelis, P.H.B.d. Visser, P.C. Struik and J.B. Evers (Editors), Functional-
Structural Plant Modelling in Crop Production. pp. 209-217, Wageningen UR Frontis
Series. Springer, Dordrecht, The Netherlands.

Kahlen K, Stützel H. **2007.** Estimation of Geometric Attributes and Masses of Individual
Cucumber Organs Using Three-dimensional Digitizing and Allometric Relationships.
Journal of the American Society for Horticultural Science, **132:** 439-446.

Kahlen K, Wiechers D, Stützel H. 2007. Model leaf phototropism in a cucumber canopy. In:
Prusinkiewicz P, Hanan J, Lane B eds. *5th International Workshop on Functional-
Structural Plant Models.* Napier, HortResearch, New Zealand.

Kahlen K, Wiechers D, Stützel, H. 2008. Modelling leaf phototropism in a cucumber canopy.
Functional Plant Biology, **35:** 876-884.

Kahlen K, Stützel H. 2011. Modelling photo-modulated internode elongation in growing
glasshouse cucumber canopies. *New Phytologist,* **190**: 697-708.

Kharkina TG, Ottosen CO, Rosenqvist E. 1999. Effects of root restriction on the growth and
physiology of cucumber plants. *Physiologia Plantarum,* **105**: 434-441.

Kim SH, Lieth JH. 2003. A coupled model of photosynthesis, stomatal conductance and
transpiration for a rose leaf (*Rosa hybrida* L.). *Annals of Botany,* **91**: 771-781.

Kläring HP, Hauschild C, Heißner A, Bar-Yosef B. 2007. Model-based control of CO_2
concentration in greenhouses at ambient levels increases cucumber yield.
Agricultural and Forest Meteorology, **143**: 208-216.

Klieber A, Lin WC, Jolliffe PA, Hall JW. **1993.** Training Systems Affect Canopy Light Exposure and Shelf Life of Long English Cucumber. *Journal of the American Society for Horticultural Science*, **118:** 786-790.

Kniemeyer O, Kurth W. 2008. The modelling platform GroIMP and the programming language XL. *Lecture Notes in Computer Science,* **5088:** 570-572.

Kobayashi K, and Salam MU. **2000.** Comparing simulated and measured values using mean squared deviation and its components. *Agronomy Journal*, **92:** 345-352.

Kubo T, Kobayashi T, Kato K, Nishimura S, Uemura S, Ono K, Sumida A, Hara T. 2008. Estimating the three-dimensional structure of canopy foliage based on the light measurements in a *Betula ermanii* stand. *Agricultural and Forest Meteorology*, **148:** 1293-1304.

Kuwar G. 2007. *Modelling dry matter partitioning in greenhouse cucumber,* Msc Thesis, Leibniz Universität Hannover, Germany.

Liu Z, Zhang Z, Wang Z, Shu Q. 2008. Measuring and modeling stomatal conductance of cucumber crop in solar greenhouse in Northeast China. *Scientia Horticulturae,* **117**: 103-108.

Loreto F, Harley PC, Marco GD, Sharkey TD. 1992. Estimation of mesophyll conductance to CO_2 flux by three different methods. *Plant Physiology,* **98**: 1437-1443.

Louarn G, Lecoeur J, Lebon E. 2008. A Three-dimensional Statistical Reconstruction Model of Grapevine (*Vitis vinifera*) Simulating Canopy Structure Variability within and between Cultivar/Training System Pairs. *Annals of Botany*, **101:** 1167-1184.

Ma YT, Wubs AM, Mathieu A, Heuvelink E, Zhu JY, Hu BG, Courède PH, de Reffye P. 2011. Simulation of fruit-set and trophic competition and optimization of yield advantages in six Capsicum cultivars using functional-structural plant modelling. *Annals of Botany*. doi: 10.1093/aob/mcq223.

Marcelis LFM. 1991. Effects of Sink Demand on Photosynthesis in Cucumber. *Journal of Experimental Botany,* **42**: 1387-1392.

Marcelis LFM. 1992. The dynamics of growth and dry-matter distribution in cucumber. *Annals of Botany,* **69**: 487-492.

Marcelis LFM. 1993a. Effect of assimilate supply on the growth of individual cucumber fruits. *Physiologia Plantarum,* **87**: 313-320.

Marcelis LFM. 1993b. Fruit growth and biomass allocation to the fruits in cucumber. 1. Effect of fruit load and temperature. *Scientia Horticulturae,* **54**: 107-121.

Marcelis LFM. 1993c. Fruit growth and biomass allocation to the fruits in cucumber. 2. Effect of irradiance. *Scientia Horticulturae,* **54**: 123-130.

Marcelis LFM. 1993d. Simulation of biomass allocation in greenhouse crops - a review. *Acta Horticulturae,* **328**: 49-68.

Marcelis LFM. 1994. A simulation model for dry matter partitioning in cucumber. *Annals of Botany,* **74**: 43-52.

Marcelis LFM, Baan Hofman-Eijer LR. 1995. Growth and maintenance respiratory costs of cucumber fruits as affected by temperature, and ontogeny and size of the fruits. *Physiologia Plantarum,* **93**: 484-492.

Marcelis LFM, Heuvelink E, Goudriaan J. 1998. Modelling biomass production and yield of horticultural crops: a review. *Scientia Horticulturae,* **74**: 83-111.

Marcelis LFM, Heuvelink E, Baan Hofman-Eijer LR, Den Bakker J, Xue LB. 2004. Flower and fruit abortion in sweet pepper in relation to source and sink strength. *Journal of Experimental Botany,* **55**: 2261-2268.

Mathieu A, Cournede PH, Barthelemy D, De Reffye P. 2008. Rhythms and alternating patterns in plants as emergent properties of a model of interaction between development and functioning. *Annals of Botany,* **101**: 1233-1242.

Mech R, Prusinkiewicz P. 1996. Visual models of plants interacting with their environment, Proceedings of the 23rd annual conference on Computer graphics and interactive techniques. pp. 397-410, ACM Press, New York, USA.

Mech R. 2004. CPFG Version 4.0 User's Manual. www.algorithmicbotany.org/lstudio/CPFGman.pdf, accessed 2011-04-25.

Minchin PEH, Lacointe A. 2005. New understanding on phloem physiology and possible consequences for modelling long-distance carbon transport. *New Phytologist,* **166**: 771-779.

Minchin PEH, Thorpe MR. 2003. Using the short-lived isotope C-11 in mechanistic studies of photosynthate transport. *Functional plant biology,* **30**: 831-841.

Monsi M, Saeki T. 2005. On the factor light in plant communities and its importance for matter production. *Annals of Botany*, **95:** 549-567.

Monteith JL, Moss CJ. 1977. Climate and the Efficiency of Crop Production in Britain [and Discussion]. *Philosophical Transactions of the Royal Society of London. B, Biological Sciences,* **281**: 277-294.

Monteith J, Unsworth M. 1990. Principles of Environmental Physics. Edward Arnold, London. United Kingdom.

Müller J, Wernecke P, Diepenbrock W. 2005. LEAFC3-N: a nitrogen-sensitive extension of the CO_2 and H_2O gas exchange model LEAFC3 parameterised and tested for winter wheat (Triticum aestivum L.). *Ecological Modelling,* **183**: 183-210.

Nederhoff EM. 1994. *Effects of CO2 Concentration on Photosynthesis, Transpiration and Production of Greenhouse Fruit Vegetable Crops.,* Phd, Wageningen University, Wageningen. The Netherlands

Niinemets Ü. 2007. Photosynthesis and resource distribution through plant canopies. *Plant, Cell & Environment,* **30**: 1052-1071.

Papadakis. G, Briassoulis D, Scarascia Mugnozza G, Vox G, Feuilloley P, Stoffers JA. 2000. Review Paper: Radiometric and Thermal Properties of, and Testing Methods for, Greenhouse Covering Materials. *Journal of Agricultural Engineering Research*, **77:** 7-38.

Papadopoulos AP, Ormrod DP. 1988. Plant Spacing Effects on Light Interception by Greenhouse Tomatoes. *Canadian Journal of Plant Science*, **68:** 1197-1208.

Peil RM, Gonzalez-Real MM, Lopez-Galvez J. 2002. Light interception of a Greenhouse cucumber crop: Measurements and modeling results. In: S. Nishimura, H. Ezura, T. Matsuda and A. Tazuke (Editors), Proceedings of the second International Symposium on Cucurbits. *Acta Horticulturae*, **588:** 81-87.

Pettersen RI, Torre S, Gislerød HR. 2010. Effects of leaf aging and light duration on photosynthetic characteristics in a cucumber canopy. *Scientia Horticulturae,* **125**: 82-87.

Pradal C, Dufour-Kowalski S, Boudon F, Fournier C, Godin C, 2008. OpenAlea: a visual programming and component-based software platform for plant modelling. *Functional Plant Biology*, **35:** 751-760.

Prusinkiewicz P, Hammel M, Hanan J, Mech R. 1997. *L-systems: From the theory to visual models of plants*, In M. T. Michalewicz, *Proceedings of the 2nd CSIRO Symposium on Computational Challanges in Life Sciences* CSIRO Publishing, Collingwood, Australia.

Prusinkiewicz P, Crawford S, Smith RS, Ljung K, Bennett T, Ongaro V, Leyser O. 2009. Control of bud activation by an auxin transport switch. *Proceedings of the National Academy of Sciences,* **106**: 17431-17436.

Retuerto R, Rochefort L, Woodward FI. 1996. The influence of plant density on the responses of Sinapis alba to CO2 and windspeed. *Oecologia,* **108**: 241-251.

Roden JS. 2003. Modeling the light interception and carbon gain of individual fluttering aspen (*Populus tremuloides* Michx) leaves. *Trees-Structure and Function*, **17:** 117-126.

Röhrig M, Stützel H, Alt C. 1999. A three-dimensional approach to modeling light interception in heterogeneous canopies. *Agronomy Journal*, **91:** 1024-1032.

Rosati A, Badeck FW, DeJong TM. 2001. Estimating canopy light interception and absorption using leaf mass per unit leaf area in *Solanum melongena. Annals of Botany*, **88:** 101-109.

Sánchez-Guerrero MC, Lorenzo P, Medrano E, Castilla N, Soriano T, Baille A. 2005. Effect of variable CO2 enrichment on greenhouse production in mild winter climates. *Agricultural and Forest Meteorology,* **132**: 244-252.

Schapendonk AHCM, Brouwer P. 1984. Fruit growth of cucumber in relation to assimilate supply and sink activity. *Scientia Horticulturae,* **23**: 21-33.

Sharkey TD, Bernacchi CJ, Farquhar GD, Singsaas EL. 2007. Fitting photosynthetic carbon dioxide response curves for C3 leaves. *Plant, Cell & Environment,* **30**: 1035-1040.

Sinoquet H, Le Roux X, Adam B, Ameglio T, Daudet FA. 2001. RATP: A model for simulating the spatial distribution of radiation absorption, transpiration and photosynthesis within canopies: Application to an isolated tree crown. *Plant, Cell and Environment,* **24:** 395-406.

Spitters CJT, Toussaint HAJM, Goudriaan J. 1986. Separating the diffuse and direct component of global radiation and its implications for modeling canopy photosynthesis Part I. Components of incoming radiation. *Agricultural and Forest Meteorology,* **38:** 217-229.

Thornley JHM, Hand DW, Warren Wilson J. 1992. Modeling light-absorption and canopy net photosynthesis of glasshouse row crops and application to cucumber. *Journal of Experimental Botany,* **43:** 383-391.

Trouwborst G, Oosterkamp J, Hogewoning SW, Harbinson J, Van Ieperen W. 2010. The responses of light interception, photosynthesis and fruit yield of cucumber to LED-lighting within the canopy. *Physiologia Plantarum,* **138:** 289-300.

Uchijima Z, Inoue K, and Kimura S. 1976. The climate in growth chamber: (6). Diffuse radiation environment in vinylhouses. *Journal of Agricultural Meteorology,* **32:** 117-125.

von Caemmerer S, Farquhar G. 1981. Some relationships between the biochemistry of photosynthesis and the gas exchange of leaves. *Planta,* **153**: 376-387.

von Caemmerer S. 2000. Biochemical models of leaf photosynthesis, CSIRO Publishing Collingwood, Australia.

Vos J, Heuvelink E. 2007. Concepts to model growth and development of plants. *Proceedings Pma 2006: Second International Symposium on Plant Growth Modeling, Simulation, Visualization and Applications,* pp. 3-10, IEEE Computer Society, Washington, USA.

Vos J, Marcelis LFM, Evers JB. 2007. Functional-Structural plant modelling in crop production: adding a dimension. In: J. Vos, L.F.M. Marcelis, P.H.B.d. Visser, P.C. Struik and J.B. Evers (Editors), Functional-Structural Plant Modelling in Crop Production. pp. 1-12, Springer, Dordrecht, The Netherlands.

Vos J, Evers JB, Buck-Sorlin GH, Andrieu B, Chelle M, and de Visser PHB. 2010. Functional-structural plant modelling: a new versatile tool in crop science. *Journal of Experimental Botany*, **61:** 2101-2115.

Warren CR. 2008. Stand aside stomata, another actor deserves centre stage: the forgotten role of the internal conductance to CO2 transfer. *Journal of Experimental Botany,* **59**: 1475-1487.

Warren Wilson J, Hand DW, Hannah MA. 1992. Light interception and photosynthetic efficiency in some glasshouse crops. *Journal of Experimental Botany*, **43:** 363-373.

Wayne PM, Carnelli AL, Connolly J, Bazzaz FA. 1999. The density dependence of plant responses to elevated CO2. *Journal of Ecology,* **87**: 183-192.

Wiechers D. 2004. *Non-destructive estimation of area and light interception of cucumber leaves in situ using 3D digitizing,* Diploma thesis, Insitut für Gemüse und Obstbau, Universität Hannover, Germany.

Wiechers D, Kahlen K, Stützel H. 2006. A method to analyse the radiation transfer within a greenhouse cucumber canopy (*Cucumis sativus* L.). *Acta Horticulturae*, **718:** 75-80.

Wiechers D, Kahlen K, Stützel H. 2011a. Dry matter partitioning models for the simulation of individual fruit growth in greenhouse cucumber canopies. *Annals of Botany,* **in press**.

Wiechers D, Kahlen K, Stützel H. 2011b. Evaluation of a radiosity based light model for greenhouse cucumber canopies. *Agricultural and Forest Meteorology,* **151:** 906-915.

Wubs AM, Heuvelink E, Marcelis LFM. 2009a. Abortion of reproductive organs in sweet pepper (Capsicum annuum L.): a review. *Journal of Horticultural Science & Biotechnology,* **84**: 467-475.

Wubs AM, Ma Y, Heuvelink E, Marcelis LFM. 2009b. Genetic differences in fruit-set patterns are determined by differences in fruit sink strength and a source : sink threshold for fruit set. *Annals of Botany,* **104**: 957-964.

Xu L, Henke M, Zhu J, Kurth W, Buck-Sorlin G. 2011. A functional-structural model of rice linking quantitative genetic information with morphological development and physiological processes. *Annals of Botany*, doi: 10.1093/aob/mcq264.

Yan HP, Kang MZ, De Reffye P, Dingkuhn M. 2004. A Dynamic, Architectural Plant Model Simulating Resource-dependent Growth. *Annals of Botany,* **93**: 591-602.

Danksagung

An dieser Stelle möchte ich mich bei allen bedanken, die mich während meiner Promotion unterstützt haben:

Herrn Prof. Hartmut Stützel für die Überlassung des Themas, das entgegengebrachte Vertrauen und die kritische und konstruktive Zusammenarbeit.

Frau Dr. Katrin Kahlen für die Betreuung und Unterstützung während der Promotion.

Herrn Prof. Henning Kage für die Übernahme des Korrefferats.

Herrn Prof. Bernhard Hau für die Übernahme des Prüfungsvorsitzes.

Allen Mitarbeitern des Fachgebietes für ihre Hilfe bei meinen Versuchen und das gute Miteinander.

Karin die hilfreiche Unterstützung und ihr Vertrauen.

Meinem Bruder Lutz für das brüderliche Verständnis.

Meinem Eltern für ihre Unterstützung und das Sie immer an mich geglaubt haben.

Curriculum Vitae

Name: Dirk Wiechers

Date and place of birth: May 28, 1978, Hannover

Nationality: German

1/2005 – present   **Phd Candidate**

                               Institute of Biological Production Systems

                               Vegetable Systems Modelling

                               Leibniz Universität Hannover, Hannover

9/1998 – 12/2004   **Horticultural Science – Dipl.-Ing. agr.**

                               Leibniz Universität Hannover, Hannover

                               Diploma thesis:

                               Non-destructive estimation of area

                               and light interception of cucumber

                               leaves *in situ* using 3-D digitizing

                               Institute of Biological Production Systems

                               Vegetable Systems Modelling

8/1997 – 9/1998   **Civilian service**

                               Jugendpflege Hemmingen

6/1997   **High school Diploma (Abitur)**

                               Carl-Friedrich Gauß Schule

                               Hemmingen

Veröffentlichungen

Wiechers D, Kahlen K, Stützel H. (2011): Dry matter partitioning models for the simulation of individual fruit growth in greenhouse cucumber canopies, Annals of Botany, doi:10.1093/aob/mcr150

Wiechers D, Kahlen K, Stützel H. (2011): Evaluation of a radiosity based light model for greenhouse cucumber canopies, Agricultural and Forest Meteorology, 151, 906-915

Kahlen K, Wiechers D, Stützel H. (2008): Modelling leaf phototropism in a cucumber canopy, Functional Plant Biology, 35, 876-884

Wiechers D, Kahlen K, Stützel H. (2006): A method to analyse the radiation transfer within a greenhouse cucumber canopy (*Cucumis   sativus* L.), Acta Horticulturae, 718, 75-80.

Erklärung zur Dissertation

gemäß §6(1) der Promotionsordnung der Naturwissenschaftlichen Fakultät der Gottfried Wilhelm Leibniz Universität Hannover

für die Promotion zum Dr. rer. hort.

Hierdurch erkläre ich, dass ich meine Dissertation mit dem Titel:

Influence of canopy structure on light interception and productivity of greenhouse cucumber

selbständig verfasst und die benutzten Hilfsmittel und Quellen sowie gegebenenfalls die zu Hilfeleistungen herangezogenen Institutionen vollständig angegeben habe.

Die Dissertation wurde nicht schon als Masterarbeit, Diplomarbeit oder andere Prüfungsarbeit verwendet.

_____

(Unterschrift)

Dirk Wiechers